MARINE RECORDS OF RIVERINE WATER AND SEDIMENT DISCHARGE IN FJORDS OF NUNATSIAVUT

ELISABETH KAHLMEYER

MARINE RECORDS OF RIVERINE WATER AND SEDIMENT DISCHARGE IN FJORDS OF NUNATSIAVUT

by

© Elisabeth Kahlmeyer

A thesis submitted to the School of Graduate Studies

in partial fulfilment of the requirements for the degree of Master of Science

Department of Earth Sciences

Memorial University of Newfoundland

September 2011

St. John's Newfoundland

ABSTRACT

This thesis focuses on the understanding of patterns and variability of sediment and fresh water delivery from land to sea, and sediment dispersal in the marine basins of two fjords in Northern Labrador. Multibeam and sub-bottom acoustic data and sediment cores were collected in Nachvak and Saglek fjords. Sediment cores were sub-sampled for X-radiography, grain size, and radiochemical analysis (based on the particle-bound radioisotopes ^{210}Pb and ^{137}Cs,), to study sedimentary structures and determine sediment accumulation rates. Results show that the sediments are generally mottled and fine grained. Sediment accumulation rates are on average 0.21 cm/y in Nachvak fjord and 0.26 cm/y in Saglek Fjord with temporal resolutions ranging from 15 – 68 years in Nachvak Fjord and 12 – 49 years in Saglek Fjord. Mass accumulation rate values suggest that the majority of the sediment is accumulating in the center of the basins. Further analyses suggest that: postglacial sedimentation was on average constant in Nachvak Fjord; in Saglek Fjord sediment accumulation was more rapid during the last ~100 y as compared to post-glacial times; the main sediment source in Saglek fjord is from rivers with extensive catchments that lack glaciers, and in Nachvak fjord from smaller rivers with steep, small and presently glaciated catchments as well as from additional sources such as from the erosion of glaci-marine terraces.

ACKNOWLEDGMENTS

I would like to thank my supervisor Dr. Sam Bentley for his guidance, patience and support. Moreover, I would like to thank him for giving me the chance to travel some of the most spectacular places on Earth, and to meet, befriend and learn from some very special persons, such as Joey, Leo and Dorothy Angnatok, and Elias Obed. I would also like to thank Dr. Trevor Bell for his scientific advice. Special thanks to Dr. Elliott Burden for serving on my supervisory committee.

Further, I would like to thank the captain and crew of the *What's Happening* for their help in the field in 2008 and 2009, and Parks Canada, the Nunatsiavut Government and the Environmental Science Group for establishing the kANGIDLUASUk base camp and for giving students like me the invaluable opportunity to experience the beautiful nature of Labrador and the friendliness of its people. Many thanks to Tanya Brown, Mallory Carpenter, Tom Sheldon, Dave Cote and Angus Simpson for their help in the field and for their help with field work logistics and accommodation in Nain. I would also like to thank Jodie Chadbourn for help with information on the glacier extend in the study area.
Inside Memorial University I would especially like to thank Kerry Hiscock for his patience and readiness to help with any laboratory and field work related problem and Michelle Miskell for her organizational and mental support throughout my time as a student at MUN. I would also like to thank the ISA for their help with information on study and work permits.

Finally, I would like to thank my family, my father Norbert Kahlmeyer, my mother Ilse Kahlmeyer, and my sister Veronika Kahlmeyer for their financial support and for their perpetual mental support and guidance in life. More than anyone else, I would like to thank Peter Huelse for his scientific advice, his help and advice on fieldwork and in the laboratory, and his unceasing mental support and patience. Without him and my family I could never have undertaken this project.

TABLE OF CONTENTS

LIST OF TABLES

Chapter 2

LIST OF FIGURES

Chapter 1

Chapter 2

LIST OF APPENDICES

CO-AUTHORSHIP STATEMENT

The following thesis chapters are presented in manuscript format. Chapter 2 has been developed in collaboration between myself (the author of this thesis) and others. For the manuscript contained here within I outline the work personally done and the contributions made by my co-authors in the following paragraph. As the author of this thesis, the work is predominantly my own, with guidance from my supervisor and co-author Dr. Sam Bentley.

Chapter 2 evaluates recent marine records of fluvial sediment supply to two sub-arctic fjords in northern Labrador as part of a baseline ecosystem study of Torngat Mountains National Park. Field work to collect sediment cores consisted of two field seasons (two weeks in August 2008, and two weeks in August 2009). It was undertaken by myself and my supervisor Dr. Samuel Bentley, with help from Peter Huelse during the field season in 2009. All of the authors were involved in the logistics and planning of the field season. I preformed all data collection and analytical work for this project. I am the primary author on this manuscript with my supervisor Dr. Samuel Bentley providing guidance and editorial comments. Funding for this work was provided in the form of a grant from ArcticNet, a Network of Centres of Excellence of Canada, to Dr. Samuel Bentley.

Chapter 1

Introduction

This thesis is organized into three separate chapters as stand-alone papers. Chapter one gives an overview on the research up to date in Northern Labrador and summarizes the basics of sedimentary delivery to the coastal ocean and fjord processes. Chapter two presents the research done for this MSc thesis, including an introduction to the regional setting, a description of the methods used, a description of the results with a subsequent discussion, and conclusions. Chapter three summarizes the research results and conclusions, points out the significance of the research and mentions future studies to which this thesis may contribute to.

Project Overview

Research in Northern Labrador – Overview and Incentive

This Master's Thesis is part of a baseline ecosystem study of the Torngat Mountains National Park sponsored by ArcticNet, a Network of Centres of Excellence of Canada (NCE). The government of Canada together with The Canadian Institutes for Health Research (CIHR), the Natural Sciences and Engineering Research Council (NSERC) and the Social Sciences and Humanities Research Council (SSHRC) administer the Networks of Centres of Excellence in partnership with Industry Canada (www.nce-rce.gc.ca, retrieved 2010). The NCE aims to support talented researchers and improve the ability to transform their research into products and services beneficial to Canadians. It links

academia, industry, government and non-profit organizations to ensure Canada's global economic competitiveness. ArcticNet, as one of Canada's NCE's, supports scientists studying the impacts of climate change in the coastal Canadian Arctic by linking natural, human health and social sciences with their partners from Inuit organizations, northern communities, federal and provincial agencies and the private sector. ArcticNet's motivation is driven by the fact that climate warming is causing changes in the environment and social life in Canada, and especially in the Arctic communities and territories (ArcticNet Rationale, 2008). Impacts of a warming climate in the Canadian Arctic include changes to Inuit hunting traditions, modifications to habitats of Arctic fauna, increased vigilance on Canadian sovereignty and security as international shipping ways through the Canadian Arctic open, and re-engineered transportation and infrastructure on thawing permafrost. For ArcticNet the collaboration between Inuit organizations, northern communities, universities, research institutes, industry, government and international agencies is very important to ensure adaptation strategies are formulated in mutual agreement.

Phase 2 of ArcticNet's compendium contains numerous projects, such as projects on coastal marine ecosystems, coastal terrestrial ecosystems, Inuit health and adaptation, and industrial development in the North (ArcticNet Projects, 2008). These projects are grouped into four Integrated Regional Impact Studies (IRIS) according to a geographical area in Canada. This MSc Project is part of *IRIS 4*. *IRIS 4* is focused on Canada's Eastern sub-Arctic including the Inuit territories of Nunavik (northern Quebec) and Nunatsiavut (northern Labrador). Geographically *IRIS 4* is bound by Hudson Bay to the west, Hudson

Strait and Ungava Bay to the north, and the Labrador Sea to the east. The climate of this area is continental with high precipitation (mainly snow). It is expected to warm by 3-4 °C and have precipitation increase by 10 to 25% by the middle of the century (ArcticNet Projects, 2008). One study evaluating adaptation in this area is the project "*Nunatsiavut Nuluak*", of which this MSc Thesis is a part. *Nunatsiavut Nuluak* is concerned with understanding and responding to the effects of climate change and modernization in Nunatsiavut. It is led by the Nunatsiavut Government (NG) through Marina Biasutti-Brown, and the Environmental Science Group (ESG) of the Royal Military College through Ken Reimer. Parks Canada, the Department of National Defence, Vale Inco (Voisey's Bay Nickel Company), Sikumiut Environmental Management Ltd., the Canadian Wildlife Service, and the Department of Fisheries and Oceans work together as partners to provide the area with insights into the health of the marine ecosystem in Northern Larbrador and how residents can adapt. For all members of this research project it is important to know that Inuit and Inuit knowledge are closely involved in all processes. This helps to ensure that regional communities understand the importance of baseline data and trends and that formulated strategies are relevant and meaningful to the future of the people of Northern Labrador.

To implement research in Northern Labrador, Parks Canada and the Nunatsiavut Government have established a base camp located in kANGIDLUASUk (Inuktituk for St. John's Harbour) in Saglek Fiord, 200 km north of Nain in Nunatsiavut and 100 km from Kangiqsualujjuaq in Nunavik (http://kangidluasuk.com, retrieved 2010). The base camp was established for the first time in the summer of 2006, and is run and managed by Inuit.

The basecamp's philosophy is to re-connect Inuit to their land; to give Inuit from Nunavik and Nunatsiavut the chance to meet old friends, to share memories of their childhood in the Torngat Mountains, and to teach the Inuit youth about their land; to give scientists and Inuit the chance to connect, share, teach and learn together, and very importantly for us, it is a science basecamp.

Research to date in Nachvak and Saglek Fjord

To promote the maintenance of ecological integrity of the Torngat Mountains, Parks Canada has started a baseline ecosystem study of the Torngat Mountains National Park, assisted by ArcticNet and the International Polar Year program (http://kangidluasuk.com, retrieved 2010). Projects include the assessment of marine ecosystem recovery from PCB contaminations in Saglek Bay and interactions with ringed seal, paleoceanographic and paleolimnologic studies in fiords and lakes, monitoring for ecological integrity, glacier observations, marine food web models and habitat mapping, the effects of climate change on Arctic char, the assessment of stream ecosystem structure and function, as well as the impacts of climate change on the vegetation in the Torngat Mountains (http://kangidluasuk.com, retrieved 2010, and Brown et al., 2010; Brown et al., 2009; Carpenter et al., 2009; King et al., 2009; Richerol et al., 2009).

Projects to which this thesis might contribute, include:

- Benthic habitat mapping and community inventory of Saglek and Nachvak Fjord, aiming to provide detailed maps of seabed morphology and substrate

type, as well as an inventory of the of benthic biota present in the fjords and the distribution of their habitats (Annual Report of Research and Monitoring in Torngat Mountains National Park Reserve, 2007).

- Establishing monitoring measures for marine ecological integrity in both fjords, evaluating the impact of climate change, industrialization, and contaminants to the marine environment (Annual Report of Research and Monitoring in Torngat Mountains National Park Reserve, 2007).
- Assessment of potentially contaminated sites in Torngat Mountains National Park, studying if hazardous material (such as from fuel drums or plane wrecks) is migrating into the environment (Annual Report of Research and Monitoring in Torngat Mountains National Park, 2009).
- Reduction of PCB contamination in an Arctic Coastal Environment, assessing ecosystem recovery (Brown et al., 2009).

General Research Background

This project provides a baseline assessment for environmental processes, hydrologic processes as well as seabed characteristics in the fjords of northern Labrador. It will be useful as some of the first such measurements in Canadian northern coastal waters. Our research focuses on understanding patterns and variability of sediment and fresh water delivery from the land to the sea, and specifically, sediment dispersal in the marine basins of Nachvak and Saglek Fjord. Studying sediment delivery and dispersal is important because freshwater and fluvial sediment carry nutrients to the coastal ocean where they influence both the terrestrial and marine ecosystems.

Sedimentary Delivery to the Coastal Ocean – Processes and Applications

For this thesis the focus is on the riverine delivery of sediment from the land to the ocean. The key factor in the accumulation of riverine sediment on the continental shelf is the availability of accommodation space, the amount of space available for sediment to accumulate and fill up between the seafloor and the sea surface (Posamentier and Vail, 1988). Marine accommodation space is created when the coastal plain is flooded and it is reduced or removed through filling with sediment. Controlling factors include relative sea-level rises, subsidence, and sediment aggradation. In general, deltas form where the available accommodation space is filled, while estuaries form in regions where accommodation space is created faster than the rate of fluvial sediment supply and accumulation (Boyd et al., 1992). Once sediment is delivered to the ocean there are static

as well as dynamic processes that control the trapping efficiency of the sediment (Sommerfield et al., 2007). Topography and morphology (i.e. canyons, banks, coastline orientation) of the marine basin define the static trapping factor and influence sediment trapping on a wide range of time-scales. Dynamic trapping, on the other hand, is controlled by properties of the water column and processes therein, such as density stratification, hydrodynamics, and particle flocculation. This is usually happening on shorter time-scales, ranging from minutes to days. Currents in the water column transport sediment, while energetic wave processes can resuspend sediment (Ogston et al., 2004).

Marine sediment can be characterized as three gradational layers beneath the sediment-water interface: a resuspension layer, a zone of bioturbation, and a zone of preservation (Sommerfield et al., 2007). Factors controlling particle transport, settling, deposition, resuspension and preservation are current velocity, suspended-sediment concentration, particle-settling velocity, biological mixing, deposition rate, and accumulation rate. Sediment accumulation links sediment supply and dispersal in a temporal and special reference frame. Most scientists who study sediment flux transform sediment accumulation rates into mass accumulation rates expressing the mass of sediment buried per unit area per unit time (e.g. g cm^{-2} yr^{-1}).

A common method to estimate sediment accumulation rates is the use of natural and anthropogenic radioisotopes, such as ^{137}Cs, $^{239,240}Pu$, ^{210}Pb, ^{7}Be, and ^{234}Th (Turekian and Cochran, 1978). These radioisotopes are scavenged by fine-grained particles in the water column and thus delivered to the seabed and buried. Once they are removed from their source their concentration decreases through radioactive decay as a function of the

isotope's half life. Therefore, activities of the radioisotope decrease with depth in the seabed due to the law of radioactive decay, and can be used to determine sediment accumulation rates. This method has been applied in fjord settings by other scientists such as Jaeger et al. (1999).

The radioisotope ^{210}Pb occurs naturally as a member of the ^{238}U decay series, where in sediments it is generally characterized as one of two categories: supported and unsupported (Noller, 2000). Unsupported (or excess) ^{210}Pb is produced in the atmosphere as an unsupported daughter product of the gas ^{222}Rn, an element produced from ^{226}Ra decay, and which quickly escapes to the atmosphere to decay. Unsupported ^{210}Pb settles out of the atmosphere or is scavenged by rain, deposited on land or in the ocean, and scavenged by fine-grained particles. By leaving the atmosphere, it is in disequilibrium with its parent ^{222}Rn. This means that once unsupported ^{210}Pb is deposited it will decay and decrease in concentration. Supported ^{210}Pb is produced by *in situ* decay of ^{226}Ra within mineral grains, and ^{222}Rn rising from sediments and rocks at depth. In sediment cores total concentrations and activities of ^{210}Pb can be measured and separated into supported and unsupported concentrations and activities. The decrease in unsupported activity with core depth due to radioactive decay can then be used as a method to calculate sediment accumulation rates. The following assumptions have to be made in order to successfully apply this method in continental-margin sedimentology: a) ^{210}Pb is quickly removed from the atmosphere and streams and sequestered in soils and sediments, b) ^{210}Pb is immobile once it is deposited, c) Unsupported ^{210}Pb is independent

of depth and does not migrate down in sedimentary column, and d) Supported ^{210}Pb is in secular equilibrium with its grandparent ^{226}Ra.

The radioisotope ^{137}Cs has been introduced into the atmosphere from nuclear testing or from release from nuclear reactors. It was first released by early nuclear tests in 1945 (Carter and Moghissi, 1977), becoming widespread globally in November 1952 (Perkins and Thomas, 1980). It is detectable in sediments formed around 1952 ± 2 yr (Robbins et al., 1978), and peaks in weapons tests in 1963 (Ritchie and McHenry, 1990). Maximum penetration depth and peaks in the activity-depth profile are commonly used to date sediment and estimate sediment accumulation rates. It is a second approach to validate results from other radiotracers (i.e. ^{210}Pb) (Ritchie and McHenry, 1990).

To study the dispersal of fluvial sediment on the continental shelf it is useful to compile a sediment budget to quantify the relations between sediment production, transport, storage and burial (Sommerfield et al., 2007). To do this one needs to quantify source and sink terms for sediment. River discharge is a crucial factor in delivering fine-grained sediment to the coastal ocean. Today, many rivers worldwide are gauged, which makes it easy to define an accurate source term in these regions. However, many smaller rivers, especially at high latitudes and in remote places are under-gauged or ungauged. Fortunately, there has been great progress in developing models to estimate fluvial sediment discharge by using other simple environmental factors. To determine a value for a sediment sink for a region of interest, there are mainly two ways: a) measure sub-bottom profiles (graphic method) or b) measure sediment accumulation rates (burial flux method). The graphic method uses sub-bottom profiles to measure the thickness and

extent of sediment of a known age and density (Grützner and Meinert, 1999). The burial flux method is based on sediment accumulation rate measurements from several stations distributed within the dispersal system (Nittrouer and Sternberg, 1981).

Fjord Processes

Modern fjords, the products of the advance and retreat of glacial ice and relative sea level fluctuations (Syvitski et al., 1995), occur in the mid to high latitudes of both hemispheres and form so-called fjord belts (Howe et al., 2010). They can be classified as polar, subpolar, and temperate fjords according to their climate regime. They are immature, non-steady state systems, formed by post-glacial erosion of coastal valleys, evolving and changing over relatively short time scales of centuries to millennia (Syvitski et al., 1995). In appearance, they are long, narrow, deep and steep-sided valleys that may remain connected to the sea (Syvitski, 1987). They can be branched, but also may be remarkably straight where ice followed fault lines (Syvitski et al., 1995). They often contain one or more submarine sills created from bedrock, moraines or other glaciomarine deposits (Fig.1). This often leads to poorly coupled ocean circulation above and below the sill height and pronounced vertical hydrographic gradients in water properties. The restricted deep water circulation and resulting low currents, reduced oxygen, and reduced bioturbation make silled basins in fjords excellent natural sediment traps. Fjords are often viewed as proxy miniature ocean basins with unique hydrography, fauna, biogeochemistry, and sedimentation, and are interesting to study (Syvitski et al. 1987). Fjord research is not only scientifically important, but also important from a

historical and social point of view (Howe et al., 2010). For at least 9.5 ka, fjords have been a place for communities. Easily accessed, sheltered and fertile, they are often used for farming and fishing. This also applies to fjords on the Labrador Coast as Historic Inuit, Thule and Dorset have used and occupied the area for centuries (http://kangidluasuk.com, retrieved 2010). Thus, it is important to scientists as well as local communities to understand the fate of a fjord's ecosystem in a changing environment.

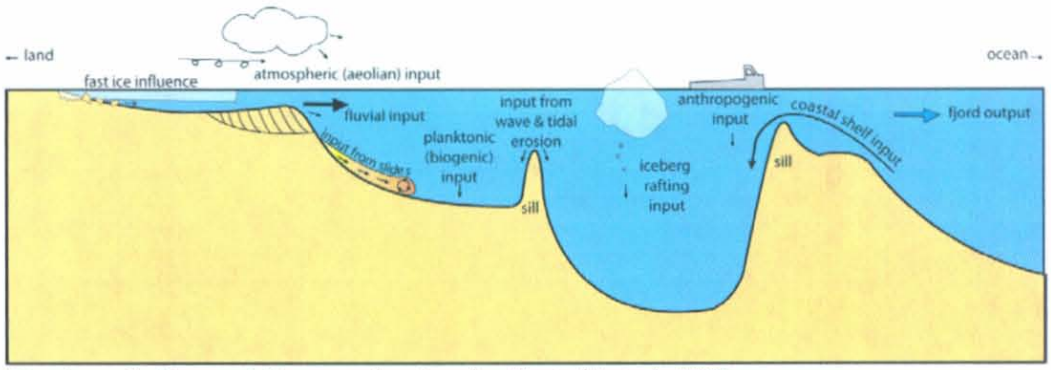

Fig. 1: Sediment delivery to fjords, after Syvitski et al. 1995

Fjord dynamics include sedimentary (suspended-sediment deposition, gravity currents), oceanographic (wave, tidal, estuarine), and glacial processes (meltwater discharge, ice rafting), which work in concert to produce sedimentary strata at a number of time scales (minutes to centuries) (Fig. 1) (Jaeger et al., 1999). The fluvial input of river-influenced fjords mainly consists of erosional products from weathering, reworked glaciogenic and raised marine deposits, as well as freshly produced glacial flour (Syvitski et al., 1995). Areas with vegetation can contribute terrestrial organic matter (pollen, leaves, twigs, humic substances) transported from land to the fjord basin. Oceanographic and meteorological processes also exert strong control on the discharge, transport, and

deposition of sediment in fjords (Jaeger et al., 1999). Freshwater input at the fjord head creates a buoyancy gradient, which leads to a surface flow down fjord and the establishment of estuarine circulation. This two-layer flow, with an outward flowing surface layer and an inward-moving compensating current, is influenced by the Coriolis effect (which forces flow to the right in the northern hemisphere), the centrifugal force, bathymetry, pressure gradients developed from meteorological conditions (wind structure, freshwater discharge), and by surface mixing from strong winds (Syvitski et al., 1995). Estuarine circulation in high-latitude fjords is also strongly influenced by sea ice, icebergs and tidewater glaciers (Fig. 1) (Syvitski, 1987). Sea ice may stimulate circulation by rejecting brine on freezing or it may limit circulation as it prevents wind waves and currents, dampens tides and tidal currents, and enhances stratification by production of meltwater (Gilbert et al., 1983).

The fluvial sediment entering the fjord separates into two components seaward of the river mouth: the bedload and the suspended load (Syvitski et al., 1995). Stream discharge, hydraulic slope, bottom roughness, bed compaction, and grain properties control bed-load transport. The bed load is of coarser grain size than the suspended load and, therefore, settles quickly onto delta foreset beds once the velocity of a stream falls below a threshold value for deposition of a particular grain diameter. The fine-grained suspended sediment load is carried seaward within the river plume and its concentration increases exponentially with increasing stream discharge. Thus, a change in river runoff will be reflected in the sediments deposited. The river plume is created by low-density freshwater which enters the fjord and spreads and thins over more dense saline water of the fjord.

As the river plume mixes with saline water, flocculation can occur. Dyer (1995) describes flocculation as a result of the total surface ionic charge on the particles and the enveloping electrical double layer. He states that there is an overall attraction when the particles are in close proximity which leads to the formation of aggregates of particles, or flocs. As a result the grain size of the flocs is greater than that of their individual components and their settling velocity is increased over that of parent grains (Syvitski et al., 1995). Human activities, such as land use and deforestation, can increase river run-off and thus the supply of fluvial sediment to the fjord (Howe et al., 2010).

Apart from the major fluvial input other sediment sources include aeolian terrestrial sources, anthropogenic sources, continental shelf sources (via estuarine circulation), input from wave and tidal erosion, input from landslides, biogenic input as well as input from icebergs or land-fast ice (Syvitski et al., 1995). The study of the glacial sediments introduced into ocean basins has become of interest in the last decade as ice sheets are important contributors to deep-sea sediment budgets, and interpretations of marine cores are used as indicators of abrupt climate change (Andrews et al., 2002). Ice cover of a fjord also has an influence on the sedimentation within the fjord. Sediment can accumulate on or within the ice by wind action, stream discharge, rock fall, seafloor erosion, wave and current wash-over or bottom freezing (Syvitski et al., 1995). Drift ice can become land-fast ice if it freezes to sediment near shore. Land-fast ice can release sediments from the ground, transport it within the fjord and deposit it somewhere in the fjord basin. The presence of coarser-grained sediment in an otherwise fine-grained matrix is often evident in studies of fjord sediment and is often interpreted as an indicator for ice-rafted and aeolian material or sediment deposited by glaciers, such as in Ameralik Fjord,

SW Greenland (Møller et al., 2006), Joseph Fjord, East Greenland (Evans et. al., 2002), Icy Bay, Alaska (Jaeger et al., 1999), and others. A study by Yoon et al. (1998) in Maxwell Bay, Antarctica shows the influence of glaciers on sedimentation. The distribution of suspended particulate matter in the waters of Maxwell Bay indicates that the glaciofluvial discharges from glaciers which end on land introduce more suspended sediment than the fjord-head trunk glacier.

Most sediment delivered to the fjords is closely tied to processes on land. Therefore, fjord sediment deposits retain high quality records of terrestrial processes, while also recording the influence of marine processes (Howe et al., 2010). Fjords often have the advantage of reflecting a continuous sedimentary record throughout the Holocene that can be correlated with terrestrial climate records such as tree-rings and lake varves (Cage and Austin 2010). Because fjords provide such high-resolution insights in previous climatic changes, they are a valuable predictive tool.

Even though fjords are such a valuable predictive tool, there have been only few truly integrated quantitative studies of sediment budgets in cold environments (Beylich et al., 2009). A few studies on sediment budgets in fjords include fjords on Greenland and Iceland, and in Canada, Alaska, Norway, Scotland and Antarctica (i.e. Jaeger et al., 1999; Yoon et al., 1998; Møller et al., 2006; Paetzel et al., 1994 and 2010; Beylich et al., 2009; Seidenkrantz et al., 2007; Evans et al., 2002; Barrie, 1983; Rosen, 1980; Hass et al., 2010; Forwick et al., 2010; Dallimore and Jmieff, 2010; Mcintyre and Howe, 2010). Comparing the findings in these studies suggests that the sediment budget depends on each fjord's individual geometry and environmental conditions rather than following a geographical

trend. Some fjords govern permanent or periodically anoxic conditions, such as the Barsnesfjord and the Nordåsvannet fjord in western Norway (Paetzel et al., 1994 and 2010) and several fjords on Vancouver Island, Canada (Dallimore and Jmieff, 2010). The distribution of oxygen depends on factors such as sill depth, photosynthetic production, and the level of oxygen consumption (Dallimore and Jmieff, 2010). For example, in the inlets of Vancouver Island the water column is usually highly stratified due to high rainfall, shallow sills, weak freshwater recharge, and the interrupted inflow of marine water, leading to dysoxic or anoxic bottom waters and restricted bioturbation. In these basins annually laminated sediments can be preserved. Although both Barsnesfjord and Nordåsvannet fjord are in geographical proximity and have much in common (i. e. shallow sills, anoxic conditions) the rates of sedimentation are very different (0.85 cm/y in Barsnesfjord and 0.4 mm/y in Nordåsvannet fjord) due to differences in fjord geometry and drainage basins. Fjords with less restricted water circulation govern oxic conditions and usually homogenous sediments with indications for bioturbation, such as Ameralik Fjord in SW Greenland (Seidenkrantz et al., 2007).

Dallimore and Jmieff (2010) summarize Canadian west coast fjord environments and characterize two types of fjords: a) areas where rivers drain high mountains and ice fields and most of the sediment input to the fjords is from snowmelt and glacier runoff in spring and summer with high sediment accumulation rates (i. e. 30 cm/y in Bute Inlet), such as fjords on the mainland in British Columbia, and b) fjords located in a milder marine climate which receive most of the sediment during heavy rains in autumn and

winter and lower sediment accumulation rates (i. e. 0.25 cm/y in Effingham Inlet), such as the inlets on Vancouver Island.

The fjords studied in this paper are located in northern Labrador and are both uninhabited and pristine (Bentley and Kahlmeyer, 2008). Both Nachvak and Saglek fjord apparently receive most of their sediment from river catchments (1 – 77 km^2, 2 – 809 km^2 in size, respectively), draining through relatively high mountains (up to 1400 m high). Rivers entering Nachvak fjord drain from snow and ice fields and small glaciers, while the drainage basins of rivers entering Saglek fjord do not contain glaciers. Maximum water depths in the marine basins are 180 meters in Nachvak fjord and 300 meters in Saglek fjord. Sediments are fine-grained with admixtures of ice rafted debris. Sediment accumulation rates are on the order of several millimeters per year. The sedimentary texture is comparable to sediments in other fjords, such as Makkovik Bay, Labrador (Barrie, 1983); and Ameralik Fjord, SW Greenland (Seidenkrantz et al., 2007); and sediment accumulation rates (0.12 – 0.52 cm/y in Nachvak fjord and 0.08 – 0.36 cm/y in Saglek Fjord) are comparable to fjords such as Icy Bay, Alaska (Jaeger et al., 1999); Ameralik Fjord, SW Greenland (Møller et al., 2006); Sogndalsfjord, western Norway (Paetzel et al., 2010); and inlets on Vancouver Island (Dallimore and Jmieff, 2010).

REFERENCES

Andrews, J.T., and Principato, S.M., 2002. Grain-size characteristics and provenance of ice-proximal glacial marine sediments. Geological Society, London, Special Publications v. 203, p. 305-324.

ArcticNet home page. Retrieved December 17, 2010, from ArcticNet Web site: http://www.arcticnet.ulaval.ca/index.php

ArcticNet Rational (2008). Retrieved October 8, 2008, from ArcticNet Web site: http://www.arcticnet.ulaval.ca/index.php?fa=ArcticNet.aboutUs

Barrie, C.Q., 1983. Late Glacial and contemporary deposition of clay-size minerals in Makkovik Bay, Labrador. Marine Geology, v. 53, p. 199-209.

Bentley, S.J., and Kahlmeyer, E., 2008. Marine records of sediment flux from glaciated and unglaciated catchments, Torngat Mountains, Canada. Arctic Change 2008, Conference Programme and Abstracts, p. 184-185.

Beylich, A.A., and Kneisel, C., 2009. Sediment Budget and Relief Development in Hrafndalur, Subarctic Oceanic Eastern Iceland. Arctic, Antarctic, and Alpine Research, v. 41, no. 1, p. 3-17.

Boyd, R., Dalrymple, R. and Zaitlin, B.A., 1992. Classification of clastic coastal depositional environments. Sediment. Geology, v. 80, p. 139–150.

Brown, T.M., Sheldon, T.A., Burgess, N.M. and Reimer, K.J., 2009. Reduction of PCB Contamination in an Arctic Coastal Environment: A First Step in Assessing Ecosystem Recovery after the Removal of a Point Source. Environmental Science & Technology, v.43, no.20, p. 7635-7642.

Brown, T.M., Sheldon, T.A., Luque, S.P., A.T. Fisk, Iverson, S.J. and Reimer, K.J., 2010. Use of chemical tracers and satellite telemetry to assess diet, foraging patterns and contaminant exposure in northern Labrador ringed seals (Phoca

hispida). Contaminants in Freezing Ground 7th International Conference, Proceedings (talk).

Cage, A. G.and Austin, W. E. N. 2010. Marine climate variability during the last millennium: the Loch Sunart record, Scotland, UK. Quaternary Science Reviews.

Carpenter, M., Brown, T., Bell, T. and Edinger, E., 2009. Benthic Habitat Mapping in shallow environments of Nachvak and Saglek Fjords, Labrador. 2009 ArcticNet Annual Conference Proceedings.

Carter, M.W., and Moghissi, A.A., 1977. Three decades of nuclear testing. Health Phys. v. 33, p. 55-71.

Dallimore, A., and Jmieff, D.G., 2010. Canadian west coast fjords and inlets of the NE Pacific Ocean as depositional archives. Geological Society, London, Special Publications, v. 344, p. 143-162.

Dyer, K.R., 1995. Sediment transport processes in estuaries. Geomorphology and Sedimentology of Estuaries (Ed. G.M.E. Perillo), p. 423–449.

Evans, J., Dowdeswell, J.A., Grobe, H., Niessen, F., Stein, R., Hubberten, H.-W., and Whittington, R.J., 2002. Late Quaternary sedimentation in Keijser Franz Joseph Fjord and the continental margin of East Greenland. Geological Society, London, Special Publications, v. 203, p. 149-179.

Forwick, M., Vorren, T.O., Hald, M., Korsun, S., Roh, Y., Vogt, C., and Yoo, K.-C., 2010. Spatial and temporal influence of glaciers and rivers on the sedimentary environment in Sassenfjorden and Tempelfjorden, Spitsbergen. Geological Society, London, Special Publications, v. 344, p. 163-193.

Gilbert, R., 1983. Sedimentary Processes of Canadian Arctic Fjords. Sedimentary Geology v. 36, p. 147-175.

Grützner, J. and Meinert, J., 1999. Lateral changes ofmass accumulation rates derived from seismic reflection profiles: an example from the Western Atlantic. GeoRes. Forum, v. 5, p. 87–108.

Hass, H.C., Kuhn, G., Monien, P., Brumsack, H.-J., and Forwick, M., 2010. Climate fluctuations during the past two millennia as recorded in sediments from Maxwell Bay, South Shetland Islands, West Antarctica. Geological Society, London, Special Publications, v. 344, p. 243-260.

Howe, J. A., Austin, E. N., Forwick, M., Paetzel, M., Harland, R., and Cage, A.G., 2010. Fjord systems and archives: a review. Geological Society, London, Special Publications 2010, v. 344, p. 5-15.

Jaeger, J.M., and Nittrouer, C.A., 1999. Sediment Deposition in an Alaskan-Fjord: Controls on the Formation and Preservation of sedimentary structures in Icy Bay. Journal of Sedimentary Research, v. 69, no. 5, p. 1011-1026.

kANGIDLUASUk home page. Retrieved December 17, 2010 from web site: http://kangidluasuk.com

King, J.R., Bell, T., Barrand, N.E., and Sharp, M., 2009. Measuring and modeling glacier change in the Torngat Mountains, northern Labrador. 2009 ArcticNet Annual Conference Proceedings.

Mcintyre, K.L., and Howe, J.A., 2010. Scottish west coast fjords since the last glaciations: a review. Geological Society, London, Special Publications, v. 344, p. 305-329.

Møller, H.S., Jensen, K.G., Kuijpers, A., Aagaard-Sørensen, S., Seidenkrantz, M.-S., Prins, M., Endler, R., and Mikkelsen, N., 2006. Late-Holocene environment and climatic changes in Ameralik Fjord, southwest Greenland: evidence from the sedimentary record. The Holocene, v. 16, no. 5, p. 685-695.

Networks of Centres of Excellence of Canada, Government of Canada homepage. Retrieved December 17, 2010 from web site: www.nce-rce.gc.ca

Nittrouer, C.A., and Sternberg, R.W., 1981. The formation of sedimentary strata in an allochthonous shelf environment: the Washington continental shelf. Marine Geology, v. 42, p. 201-232.

Noller, J.S., 2000. Lead-210 Geochronology. Quaternary Geochronology: Methods and Applications, p. 115-120.

Ogston, A.S., Guerra, J.V. and Sternberg, R.W., 2004. Interannual variability of nearbed sediment flux on the Eel River shelf, northern California. Continental Shelf Research, v. 24, p. 117–136.

Parks Canada, 2007. 2007 Annual Report of Research and Monitoring in Torngat Mountains National Park Reserve.

Parks Canada, 2009. 2009 Annual Report of Research and Monitoring in Torngat Mountains National Park.

Paetzel, M., Schrader, H., and Croudace, I., 1994. Sewage history in the anoxic sediments of the fjord Nordåsvannet, western Norway: (I) dating and trace-metal accumulation. The Holocene, v. 4, no. 3, p. 290-298.

Paetzel, M., and Dale, T., 2010. Climate proxies for recent fjord sediments in the inner Sognefjord region, western Norway. Geological Society, London, Special Publications, v. 344, p. 271-288.

Perkins, R.W., and Thomas, C.W., 1980. Worldwide fallout. In W.C. Hanson (ed.) Transuranic elements in the environmet. USDOE/TIC-22800. US DOE, Washington, DC, p. 53-82.

Posamentier, H.W. and Vail, P.R., 1988. Eustatic controls on clastic deposition II-sequence and systems tract models. In: Sea-level Changes; an Integrated Approach (Eds C.K. Wilgus, B.S. Hastings, C.A. Ross, et al.), p. 125–154. Special

Publication 42, Society of Economic Paleontologists and Mineralogists, Tulsa, OK.

Richerol, T., Pienitz, R. and Rochon, A., 2009. Paleoceanographic conditions in three Labrador fjord ecosystems (Canada): Preliminary results. Arctic Frontier 2009 Congress, Tromsø (Norway).

Ritchie, J.C., and McHenry, J.R., 1990. Application of Radioactive Fallout Cesium-137 for Measuring Soil Erosion and Sediment Accumulation Rates and Patterns: A Review. Journal of Environmental Quality, v. 19, p. 215-233.

Robbins, J.A., 1978. Geochemical and geophysical applications of radioactive lead. In J.O. Nriagu (ed.) The biochemistry of lead in the environment. Elsevier/North Holland Biomedical Press, p. 285-393.

Rosen, P.S., 1980. Coastal Environments of the Makkovik Region, Labrador. in The Coastline of Canada, S.B. McCann, editor; Geological Survey of Canada, Paper 80-10, p. 267-280.

Seidenkrantz, M.-S., Aagaard-Sørensen, S., Sulsbrück, H., Kuijpers, A., Jensen, K.G., and Kunzendorf, H., 2007. Hydrography and climate of the last 4400 years in a SW Greenland fjord: implications for Labrador Sea palaeoceanography. The Holocene, v. 17, no. 3, p. 387-401.

Sommerfield, C. K., Ogston, A. S., Mullenbach, B. L., Drake, D.E., Alexander, C. R., Nittrouer, C. A., Borgeld, J. C., Wheatcroft, R. A., and Leithold, E. L., 2007. Oceanic dispersal and accumulation of river sediment. Continental-Margin Sedimentation: Transport to Sequence. Blackwell Publishing.

Syvitski, J. P. M., Burrell, D. C. and Skei, J. M. 1987. Fjords – Processes and Products. Springer, New York.

Syvitski, J.P.M., and Shaw, J., 1995. Sedimentology and Geomorphology of Fjords. Geomorphology and Sedimentology of Esutaries. Developments in Sedimentology v. 53, p. 113-178.

Turekian, K.K. and Cochran, J.K., 1978. Determination of marine chronologies using natural radionuclides. Chemical Oceanography, v. 7, p. 313–360.

Yoon, H.I., Park, B.-K., Domack, E.W., and Kim, Y., 1998. Distribution and dispersal pattern of suspended particulate matter in Maxwell Bay and its tributary, Marian Cove, in the South Shetland Islands, West Antarctica. Marine Geology, v. 152, p. 261-275.

Chapter 2

Dispersal of fluvial sediment in two sub-arctic fjords on the Labrador Coast: Nachvak Fjord and Saglek Fjord, Canada

Abstract

Recent marine records of fluvial sediment supply to two sub-arctic fjords in northern Labrador (Eastern Canada) have been studied in order to determine fluvial transfer of terrestrial material to the fjords, and to develop baseline knowledge for future studies. Multibeam and sub-bottom acoustic data and sediment cores were collected in Nachvak and Saglek fjords in Northern Labrador, within Canada's Torngat Mountains National Park, as part of the most extensive study of the park's marine resources to date. In order to assess sediment discharge and the fjord's sediment dispersal system, data collection was concentrated on marine basins fed by the largest fluvial catchments associated with each fjord. Each core was sub-sampled for X-radiography, grain size, and radiochemical analysis, and was analyzed for sedimentary structures and sediment accumulation rates. Radiochemical analysis is based on the particle-bound radioisotopes ^{210}Pb and ^{137}Cs, which have been used to determine sediment accumulation rates (SAR), and ^{210}Pb inventories and flux over decadal to centennial time scales. Sediment thickness and extent in the fjord basins were studied from sub-bottom profiles and bathymetry data. Results show that in both fjords sediment is accumulating in depocentres in the centre of each basin. In Nachvak Fjord, which is fed primarily by small rivers with very steep, small,

presently glaciated catchments, the thickness of postglacial sediment observed in sub-bottom profiles compares well with thicknesses projected from recent sediment accumulation rates and implies that postglacial sedimentation was on average constant. In Saglek Fjord, which is fed by larger rivers with more extensive catchments that lack glaciers, postglacial sediment thickness is on average 40 % less than that projected from recent sediment accumulation rates, suggesting more rapid sediment accumulation for the past ~100 y than for that averaged over post-glacial time. Present mass accumulation rates for the Nachvak fjord basin are on average 39,000 t/y for the entire basin, and for Saglek 43,000 t y^{-1} for the entire basin. Comparison between MAR values and results from a previously published statistical model estimating fluvial sediment supply from catchment properties support the hypothesis that the marine basins of both fjords are excellent natural sediment traps with the capacity to trap the modeled sediment load entirely. Results for Nachvak Fjord suggest a high sediment yield of the river catchments draining into the fjord and/or a significant supply of sediment from sources additional to rivers.

1. Introduction

The goal of this study is to evaluate recent marine records of fluvial sediment supply to two sub-arctic fjords in northern Labrador as part of a baseline ecosystem study of Torngat Mountains National Park. Sediments delivered by rivers to the fjords play an important role in the transport of nutrients from land to the ocean. Terrestrial animals such as bears feed on marine life, and migratory fish, such as char, inhabit both ocean and rivers. So fluvial-marine interactions influence both terrestrial and marine ecosystems. River runoff links processes in the atmosphere, the land surface, and the oceans and is controlled by climate-sensitive factors such as air temperatures, precipitation, snowcover, or permafrost (Déry et al., 2005). Thus, changes in river runoff are sensitive indicators for changes in climate and are reflected in the fluvial sediment accumulated in marine basins (Syvitski et al., 1995). Resulting observations of this study will provide information about environmental processes, hydrologic processes as well as seabed characteristics in the fjords of northern Labrador and will be useful as some of the first such measurements in northern Labrador.

This study is part of a larger project called "Nunatsiavut Nuluak", directed at understanding and responding to the effects of climate change and modernization in Nunatsiavut, and lead and sponsored by Arctic Net (Reimer et al., 2008). ArcticNet is a research network concerned with creating links among natural, human health and social sciences, regarding climate change in the coastal Canadian Arctic (ArcticNet Rational, 2008). This project in particular is concerned with the impacts of climate change, modernization and contaminants on the health of communities and the marine ecosystem

in northern Labrador (ArcticNet Projects, 2008). Inuit are closely involved in the research to ensure that adaptation strategies are relevant for the communities (ArcticNet Projects, 2008).

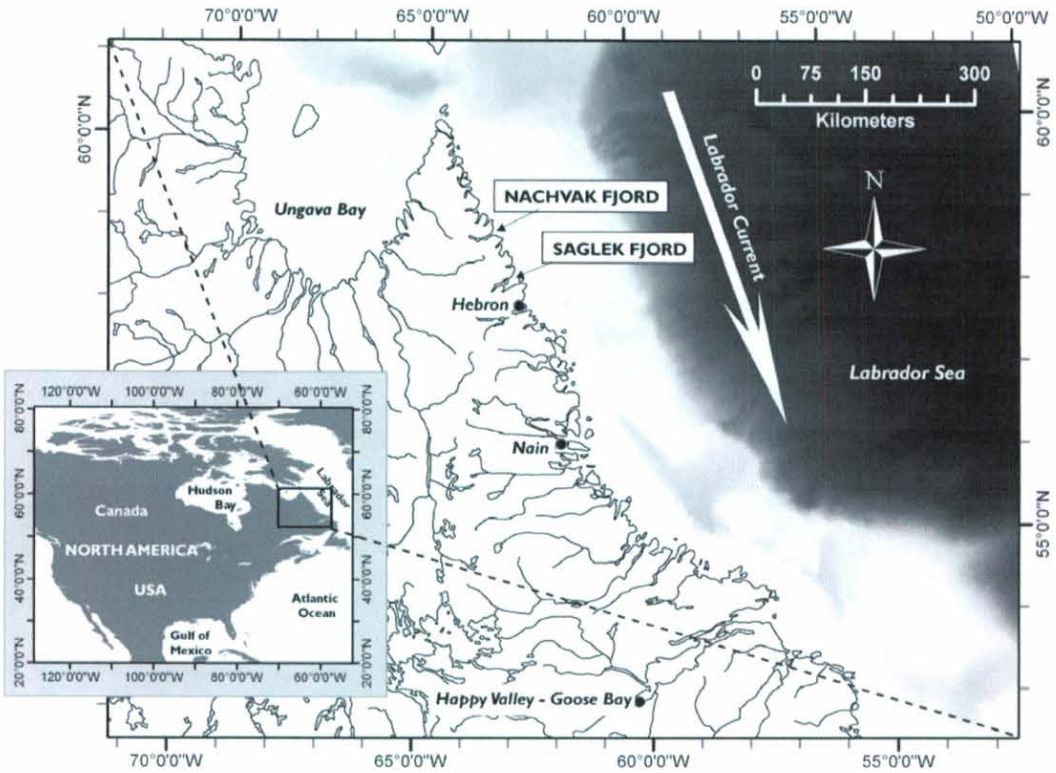

Fig. 1 Map of study area showing locations of Nachvak and Saglek Fjord

The study areas are two subarctic fjords on the Nunatsiavut/Labrador coast (Canada), Nachvak Fjord and Saglek Fjord (Fig.1). Sediment cores were collected in the main basin of each fjord and have been analyzed for sedimentary structures and sediment accumulation rates (Fig. 2 and 3). These results have been compared for each basin and used to describe how sediment is dispersed within the basin. Sediment accumulation rates (SAR) have been used to estimate an average sediment discharge, assuming rivers to be

the only sediment source. These results have been compared to modeled sediment discharge and used to draw conclusions on sediment sources and dispersal of fluvial sediment. Basic observations of seasonal stream flow have been conducted to get an idea of prevailing flow conditions in the two rivers under study. Sub-bottom profiles and bathymetry data collected in the fjords have been used to describe sediment thickness and extent in the fjord basins.

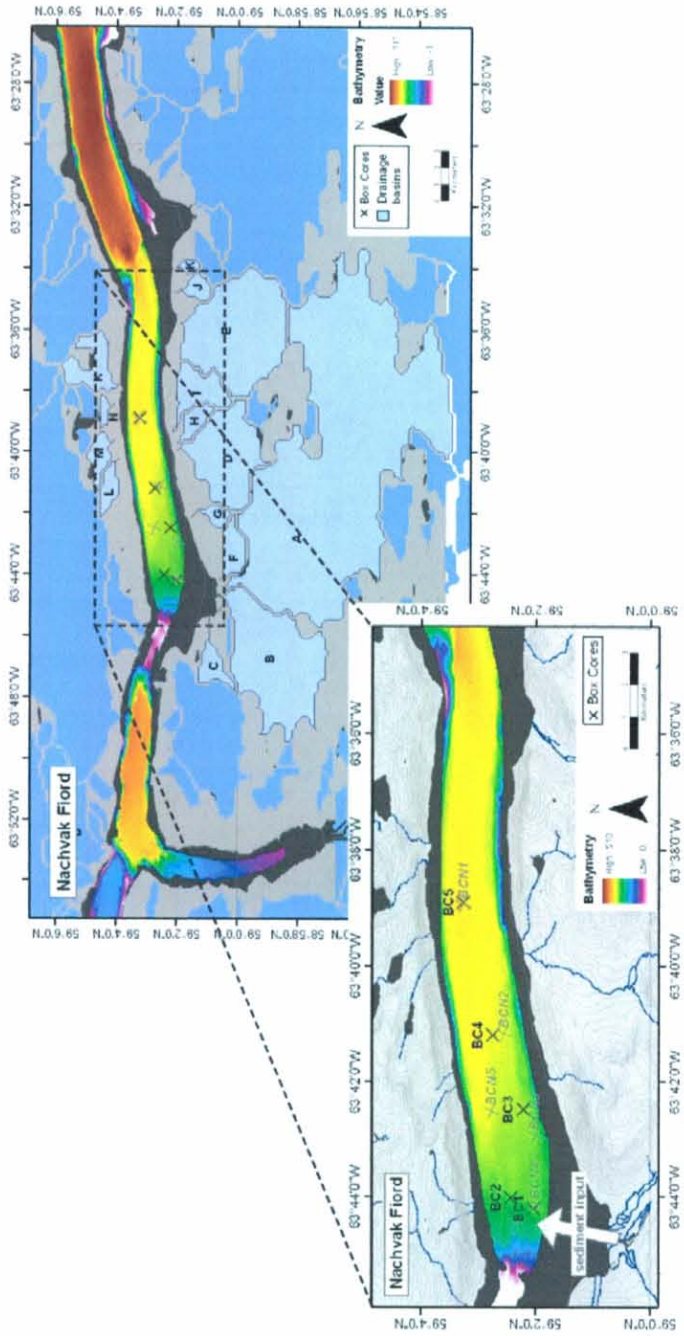

Fig. 2 Map of Nachvak Fjord showing bathymetry, drainage basins (blue shaded, bright blue shaded are drainage basin of interest for this study) and core locations.

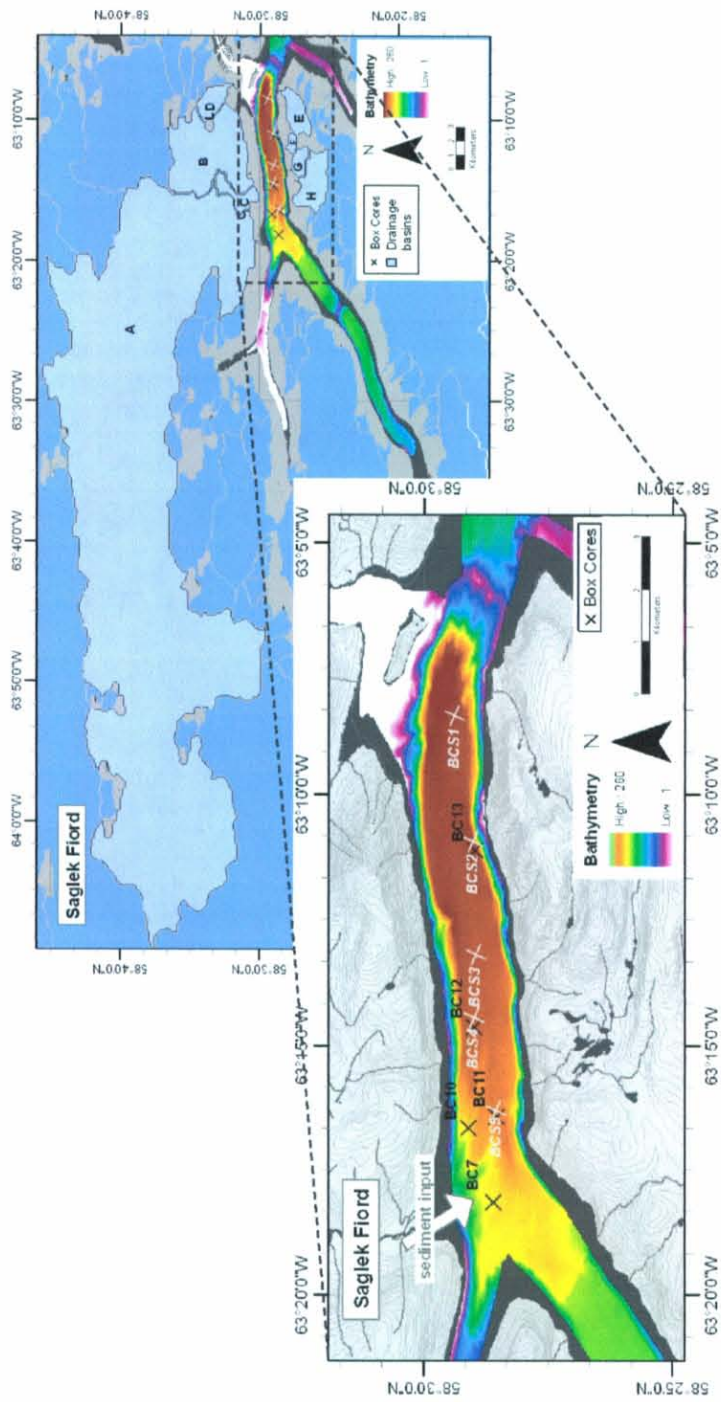

Fig. 3 Map of Saglek Fjord showing bathymetry, drainage basins (blue shaded, bright blue shaded are drainage basin of interest for this study) and core locations.

2 *Fjord processes*

Fjords are a product of glacial erosion and can be found along glaciated belts at mid to high latitudes in both hemispheres (Howe, 2010). Depending on climate, glaciogene regimes and environmental factors, fjords can be classified as polar fjords (narrow bays permanently covered with sea ice, with a resident headwater glacier, and major sediment supply from glacial processes), subpolar fjords (seasonally open narrow bays with summer mean air temperatures above 0 °C, common icebergs, some hinterland rivers, and major sediment supply from subglacial meltwater) and temperate fjords (narrow, formerly glacial bays with sediment from hinterland rivers, and sea ice generally absent). Fjords are geomorphological features that represent the transition from the terrestrial to the marine environment. They typically have entrance sills restricting water circulation, making fjords ideal depositional environments for preserving high-resolution environmental changes. Sills can be created from bedrock, moraines or other glaciomarine deposits (Syvitski et al., 1995). Fjord processes are controlled by sedimentological (suspended-sediment deposition, gravity currents), oceanographic (wave, tidal, estuarine), and glacial processes (meltwater discharge, ice rafting), which work in concert to produce sedimentary strata at a number of time scales (minutes to centuries) (Jaeger et al., 1999). During the Early/Mid-Holocene, the disappearance of ice, crustal unloading and associated isostatic sea level changes led to the reactivation of faults, increased sub-aerial and submarine landslides, rockfalls, and increased sedimentation (ForwickandVorren 2002 and Bøe et al. 2003). Sediment in polar fjords is typically glacier-derived; in temperate fjords it is river-derived (Howe, 2010).

Bathymetry, depth, and the hydrographic regime steer the distribution of the sediment. Deposition in form of sediment creep, slides, debris flows and turbidity flows are common in fjords due to high sediment supply on steep slopes (Syvitski et al. 1987). Sediment accumulation rates are typically on the order of millimeters to centimeters per year (Howe, 2010).

In non-glaciated fjords the main sediment supply is from terrestrial rivers, especially if the fjord basin is protected from coastal processes by a sill. Processes associated with the deposition of fine-grained fluvial sediment include density currents, flocculation and turbulence (Relling and Nordseth, 1979). Density currents carry sediment in suspension, which is then deposited by settling out of the water column. Flocculation causes the formation of aggregates and an increase in grain size leading to more rapid deposition of the sediment. Turbulence causes erosion of deposited sediment and resuspension. In the fjords of this study the main sediment input is thought to be from rivers and mainly consisting of erosional products from weathering, reworked glaciogenic and raised marine deposits, and some freshly produced glacial flour. The river plume carries the fine-grained suspended sediment load (sand to clay) seaward and its concentration increases exponentially with increasing stream discharge (Syvitski et al., 1995).

Apart from the major fluvial input other sediment sources include wind-transported terrestrial sources, anthropogenic sources, continental shelf sources (via estuarine circulation), input from wave and tidal erosion, input from landslides, biogenic input as well as input from icebergs or land-fast ice (Syvitski et al., 1995). Ice cover of a fjord also

has an influence on the sedimentation within the fjord. Sediment can accumulate on or within the ice by wind action, stream discharge, rock fall, seafloor erosion, wave and current wash-over or bottom freezing. Drift-ice can become sediment laden land-fast ice as it freezes near shore. Land-fast ice returning to drift ice can transport sediment from the shore and distribute it in the basin. Most sediments delivered to fjords are closely tied to processes on land. Therefore, sediment deposits in fjords retain high quality records of terrestrial processes, while also recording local marine processes and conditions.

Kahlmeyer (2008) provides first basic data on sediment delivery in Nachvak, Saglek, and Anaktalak fjords. Sediment accumulation rates in this area range between 0.18 cm/y and 0.33 cm/y, and estimated sediment discharge range between 32,000 ± 30,000 t/y and 580,000 ± 330,000 t/y (Kahlmeyer, 2008). However, for this 2008 study only one to two box cores per fjord were analyzed. A greater number of cores have now been analyzed, covering an area from the river mouth to the centre of the basin, to improve interpretations for the mode and dispersal of sediment and to improve estimations for sediment discharge.

The specific objectives of this paper are, to determine:

1. dispersal patterns of fluvial sediment in one major basin for each fjord
2. the mode of sediment delivery from land to ocean
3. the thickness, extent, and age of sediment deposits of fluvial origin in marine basins
4. a temporal resolution for palaeoenvironmental marine records in this area

2. Regional Setting

Study Area

The two fjords in this study (Nachvak Fjord and Saglek Fjord) are located in the northern part of Labrador (Fig. 1, 2 and 3). Nachvak Fjord, the northernmost fjord, is a pristine, uninhabited fjord (Bentley and Kahlmeyer, 2008) and receives most of its sediment from river catchments such as the glacierized McCornick River catchment. Nachvak Fjord consists of three marine basins with water depths near 180 meters. Nachvak Fjord offers the opportunity to study natural environmental conditions in the fjords in northern Labrador. In contrast, Saglek fjord sediments have been influenced by human activities (Richerol et al., 2007). A major source of sediment to Saglek fjord is Nakvak Brook (a non-glacierized catchment). Sediments in Saglek fjord have been affected by produced wastes of a former military site and have been contaminated with PCB's (Richerol et al., 2007). Maximum water depth in Saglek fjord is near 300 m.

The inner shelf of northern Labrador is covered by land-fast sea ice for several months each year and, farther offshore, drifting pack ice covers the shelf for 6-11 months each year (Hall et al., 1999). Large numbers of icebergs, from western and north-western Greenland, and from the Canadian High Arctic, cause iceberg scouring as they drift southward along the shelf in the Labrador Current (Hall et al., 1999), and are a possible source for ice-rafted debris deposited in fjords in Labrador. The glacial landscape of Labrador is a result of the action and retreat of the Laurentide Ice Sheet. In the sedimentary record of a small lake (Square Lake) in the catchment of Nakvak Brook Clark et al. (1989) detected a distinct shift in the depositional environment accompanied

by an increase in organic matter around 8 ka BP, indicating ice retreat from the Saglek Moraine. Remains of this ice retreat and the accompanying isostatic uplift have exposed deposits of thick till and glaciomarine sediments along the fjord coast (Syvitski et al., 1997). Climate model simulations show that the Labrador sector of the Laurentide Ice Sheet was particularly sensitive to the abrupt changes in North Atlantic sea-surface temperatures that characterized the last deglaciation (Fawcett et al., 1997; Hostetler et al., 1999). This suggests that this area may show an equally strong sensitivity to climatic changes at the present. Therefore, the lakes and fjords offer excellent opportunities for studies related to climate change.

Geology

Northeastern Labrador consists of the Archean Nain Province craton, an ancient crustal mass > 600km long and ≤ 100 km wide (Wilton, 1996). The Nain Province has been intruded by the Nain Plutonic Suite and separated into two parts: the Saglek Block to the North and the Hopedale Block to the South. The Saglek Block is complex high-grade gneisses unconformably overlain by sedimentary and metasedimentary strata of the Ramah Group, the rocks which form the landscape of Nachvak and Saglek Fjord. Ramah strata consist of 1.7 km thick deposits of shallow-water siliciclastics overlain by deep-water shales, carbonates and sandstones deformed into a north-trending fold belt (Wardle 1983).

3. Methods

Sample collection

Marine geological surveys and sampling were conducted from the M/V *What's Happening* in the summers of 2008 and 2009. Sediment samples include five box cores in each fjord in 2008 and five box cores in each fjord in 2009. Box cores were subsampled on board for X-radiography, grain size analysis, and radioisotope geochronology. In summer 2008 sub-bottom profiles and sidescan sonar data were collected by using a 100/500 Hz sidescan sonar (Edgetech 4100p) and a 2-16 kHz Chirp system (Edgetech 3200XS). Multibeam bathymetry data were collected and initially processed by the University of New Brunswick Ocean Mapping Group, with final compilation by Bell et al. (2009). On land, stream flow measurements have been conducted in the two major rivers (McCornick River and Nakvak Brook) using a hand held accoustic doppler velocimeter. Stream stage was measured by using HOBO water level loggers that were deployed in each stream for one year. Soil cores were collected close to river banks to estimate the supply of ^{210}Pb to the land surface.

Radiogeochemistry (^{210}Pb, ^{137}Cs)

For radiogeochemistry measurements the cores were extruded in 1 – 2 cm intervals on board the ship and packed in air tight plastic bags for transport to St John's. In the laboratory at MUN, samples were dried in an oven at around 90 °C, and then ground and sealed in petri dishes. Water content and porosity were measured by weight loss in

drying. To measure the activity of ^{210}Pb and ^{137}Cs, dried samples were counted for 24 hours on Canberra low-background planar gamma detectors. The natural radioisotope ^{210}Pb is product of the U-series decay and has a half-life of 22 years (Nittrouer and Sternberg, 1979), while ^{137}Cs, a product of nuclear fission in nuclear reactors and bombs, has been dispersed globally in the environment since 1952 (Perkins and Thomas, 1980). Its half-life is 30.7 years. Correction for self-adsorption of ^{210}Pb was done using the method of Cutshall et al. (1983). Total ^{210}Pb was determined by measurement of the 46.5 keV gamma peak. Supported ^{210}Pb (from decay of ^{226}Ra within the seabed) was determined by measurement of the granddaughters of ^{226}Ra: ^{214}Pb (295 and 352 keV) and ^{214}Bi (609 keV). The unsupported ^{210}Pb (excess ^{210}Pb) was determined by subtracting the supported ^{210}Pb from the total ^{210}Pb. ^{137}Cs activities were determined by measuring the 662 keV peak directly.

Apparent sediment accumulation rates (S, cm y^{-1}) were calculated, assuming no bioturbation below the observed bioturbation depth. Bioturbation depths were determined by inflection points in ^{210}Pb profiles, and by measuring depths of burrows visible in x-radiographs of the cores. If accumulation is the dominant process and steady-state conditions are assumed (e.g., Nittrouer and Sternberg, 1981), mixing can be ignored and accumulation rates (S, cm y^{-1}) can be estimated by a least squares fit to:

$$A(z) = A(0)e^{\left(\frac{-S}{\lambda z}\right)} \qquad \text{Eq. 1}$$

where λ is the decay constant for the radionuclide of interest (year^{-1}) and A is excess activity (dpm g^{-1}) at depth z (Nittrouer et al., 1984).

Anthropogenic ^{137}Cs can be used as a second approach to calculating accumulation rates and thus validate the $^{210}Pb_{xs}$ results. The sediment accumulation rate can be calculated from:

$$S = (z_p - z_b)/t_0 - t_i \qquad \text{Eq. 2}$$

where z_p is the maximum penetration depth of ^{137}Cs, z_b is the bioturbation depth, t_0 is the year of sample collection and t_i is the year ^{137}Cs was introduced into the atmosphere (Nittrouer et al., 1984).

The temporal resolution (T_r) of the core's sedimentary record is controlled by bioturbation rate, SAR, and depth of bioturbation. It can be estimated from the residence time for a parcel of sediments within the region of the seabed influenced by bioturbation:

$$T_r = L_b/S \qquad \text{Eq. 3}$$

where L_b is the depth of bioturbation, estimated from x-ray images and $^{210}Pb_{xs}$ profiles, and S is the sedimentation rate (Wheatcroft et al., 2006).

Sedimentological analyses

For X-radiographic sampling of box cores, a three-sided Plexiglas tray (2. 5 cm thick x 16 cm wide) was inserted vertically into the sediment and a fourth side was then inserted into machined grooves with great care not to disturb the sedimentary fabric. The trays were sealed air tight with rubber and electrical tape for shipment. Slabs for X-radiography were returned to the laboratory at Memorial University, and imaged using a

Thales Flashscan 35 digital X-ray detector panel, illuminated with a Medison Acoma PX15HF X-ray generator. X-ray images were used to study sedimentary structures, which is useful for interpretation of and correlation with radioisotope profiles (Bentley and Nittrouer, 2003). Granulometric measurements were done with a HORIBA Partica LA-950, using a laser scattering method where the instrument correlates the intensity and the angle of light scattered from a particle (Horiba, 2006).

Fluvial measurements

For basic stream flow measurements two pressure sensors (HOBO U20 Water Level Logger) were deployed in the streams, one in Nakvak Brook and one in McCornick River. They were programmed to measure pressure and temperature in 30-minute intervals and were recovered one year after deployment. Another HOBO U20 Water Level Logger was deployed on land in St. John's Harbour in Saglek Fjord to measure air temperature and atmospheric pressure. The Onset HOBOware Software Barometric Compensation Assistant was used to create a water level/sensor depth series by combining the barometric datasets from the HOBO U20 Water Level loggers in the streams and on land.

Additionally, stream discharge and velocity profiles were conducted in the summer in both streams by using the SonTek Handheld Acoustic Doppler Velocimeter FlowTracker. The FlowTracker measures the change in frequency of sound reflected off particles in the water and uses the Doppler principle to determine stream velocity. Measuring stream depth and velocity at different locations along a profile across the river

perpendicular to its stream flow allows measurements of stream discharge. Discharge is computed by using the Mid Section Equation based on ISO/USGS procedures (SonTek/YSI FlowTracker Handheld ADV Technical Manual, 2009).

Estimations of fluvial sediment load

A digital elevation model for land surrounding each fjord was extracted from Space Shuttle Topography Mission data (USGS, 2008). The DEM was then processed using RiverTools and GIS Modeling software to outline terrestrial river drainage basins. These data were then loaded into ArcGIS for analysis. These data were then used to estimate fluvial sediment discharge, using the model of Syvitski and Milliman (2007) for areas where basin-averaged temperature of the drainage basin is below 2℃:

$$Q_s = 2\,\omega\,B\,Q^{0.31}A^{0.5}\,R \qquad \text{Eq. 4}$$

where Q_s is the long-term sediment load (kg/s), Q is freshwater discharge (km^3/y), R is maximum relief from sea level to mountain-top (km), A is basin area (km^2), ω is 0.02 and B is an environmental factor accounting for important geological and human factors (Syvitski and Milliman, 2007). Freshwater discharge Q is defined as (Syvitski and Milliman, 2007):

$$Q = 0.075\,A^{0.8} \qquad \text{Eq. 5}$$

And the environmental factor B is defined as (Syvitski and Milliman, 2007):

$$B = I\,L\,(1 - T_E)\,E_h \qquad \text{Eq. 6}$$

where I is a glacier erosion factor, L is an average basin-wide lithology factor, T_E is the trapping efficiency of lakes and man-made reservoirs so that $(1\text{-}T_E) \leq 1$, and E_h is a human-influenced soil erosion factor (Syvitski and Milliman, 2007). For the lithology factor L we use a value of 0.5 as assigned by Syvitski and Milliman (2007) for basins composed principally of hard, acid plutonic and/or high-grade metamorphic rocks. The sediment trapping term $(1\text{-}T_E)$ is designed to vary between 0.1 for basins with high quantity of man-made reservoirs and 1 for basins with no sediment trapping (Syvitski and Milliman, 2007). We use the average value in the database of Syvitski and Milliman (2007) of 0.8 for the term $(1\text{-}T_E)$. This reflects the lack of man-made reservoirs in the study area but allows for natural sediment trapping (i. e. by lakes). For E_h we use the value 1 as assigned by Syvitski and Milliman (2007) for basins with low human footprint. The glacier erosion factor I is defined as:

$$I = 1 + 0.09A_g \qquad \text{Eq. 7}$$

where A_g is the surface area of glaciers as a percentage of the drainage basin area (Syvitski and Milliman, 2007).

Estimation of ^{210}Pb supply to land surface

Soil cores were collected near river banks by using a hand auger of 10 cm diameter with an approximate core depth of 60 cm. These cores were subsampled for radiochemical analysis to determine long-term average ^{210}Pb supply to the land surface. The cores were sliced in the Laboratory at MUN, dried, ground and sealed in petri dishes.

Activities of ^{210}Pb have been measured by counting the intervals for 24 hours on Canberra low-background planar gamma detectors as above.

4. Results

Profiles of ^{210}Pb and ^{137}Cs geochronology (SAR)

^{210}Pb and ^{137}Cs activities are shown in figures 4-6. ^{210}Pb activity profiles of both fjords show a characteristic shape with an inflection point at the base of a mixed surface layer due to bioturbation and a logarithmic decrease in activities below this point. Sediment accumulation rates (SAR) were calculated using Eqs. 1 and 2 as described in 3.2 for activities below the inflection point. ^{137}Cs was used as a complementary tool for ^{210}Pb geochronology, using Eq. 2 to estimate SAR. Temporal resolution was calculated for each fjord by using Eq. 3. In Nachvak Fjord SAR derived from ^{210}Pb (Eq. 1) range from 0.12 cm/y (WH0809 BCN1) to 0.52 cm/y (WH0809 BCN5). In the profile of WH0808 BC3 (Fig. 4) a single inflection point cannot be determined. In this core activities decrease downward in a step-like manner. Bioturbation depths in Nachvak Fjord range from 4 cm (WH0808 BC4, Fig. 4) to 9 cm (WH0809 BCN1, Fig. 6). Temporal resolution ranges between 15 years (WH0808 BC4, Fig. 4) and 68 years (WH0809 BCN5, Fig. 6). Where the maximum penetration depth of ^{137}Cs was detectable, ^{137}Cs SAR is equal to or less than the ^{210}Pb SAR.

In Saglek Fjord SAR derived from ^{210}Pb activities range from 0.08 cm/y (WH0808 BC10, Fig. 5) and 0.36 cm/y (WH0808 BC12, Fig. 5). Bioturbation depth ranges from 3 cm (WH0809 BCS2, Fig. 7) to 9 cm (WH0808 BC11, Fig. 5). Temporal resolution ranges from 12 years (WH0809 BCS2, Fig. 7) to 49 years (WH0808 BC10, Fig. 5). Maximum

penetration depth of ^{137}Cs was detectable in all cores from Saglek Fjord with SAR (^{137}Cs) $\leq$ SAR (^{210}Pb).

Fig.4a

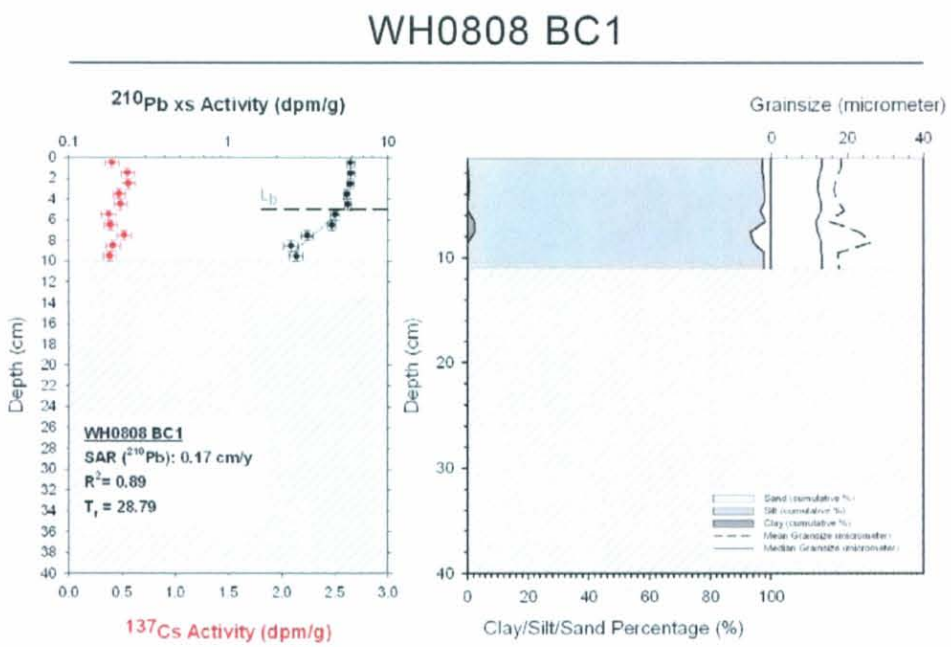
WH0808 BC1
210Pb xs Activity (dpm/g)
Grainsize (micrometer)
Depth (cm)
WH0808 BC1
SAR (210Pb): 0.17 cm/y
R2= 0.89
T, = 28.79
137Cs Activity (dpm/g)
Clay/Silt/Sand Percentage (%)

Fig. 4b

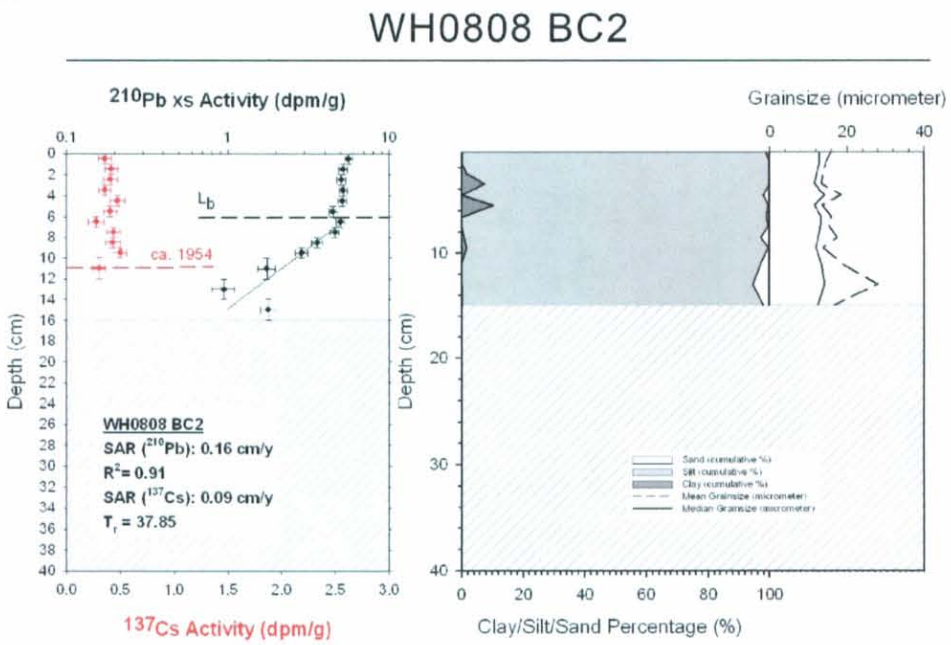
WH0808 BC2
210Pb xs Activity (dpm/g)
Grainsize (micrometer)
ca. 1954
Depth (cm)
WH0808 BC2
SAR (210Pb): 0.16 cm/y
R2= 0.91
SAR (137Cs): 0.09 cm/y
T, = 37.85
137Cs Activity (dpm/g)
Clay/Silt/Sand Percentage (%)

Fig. 4c

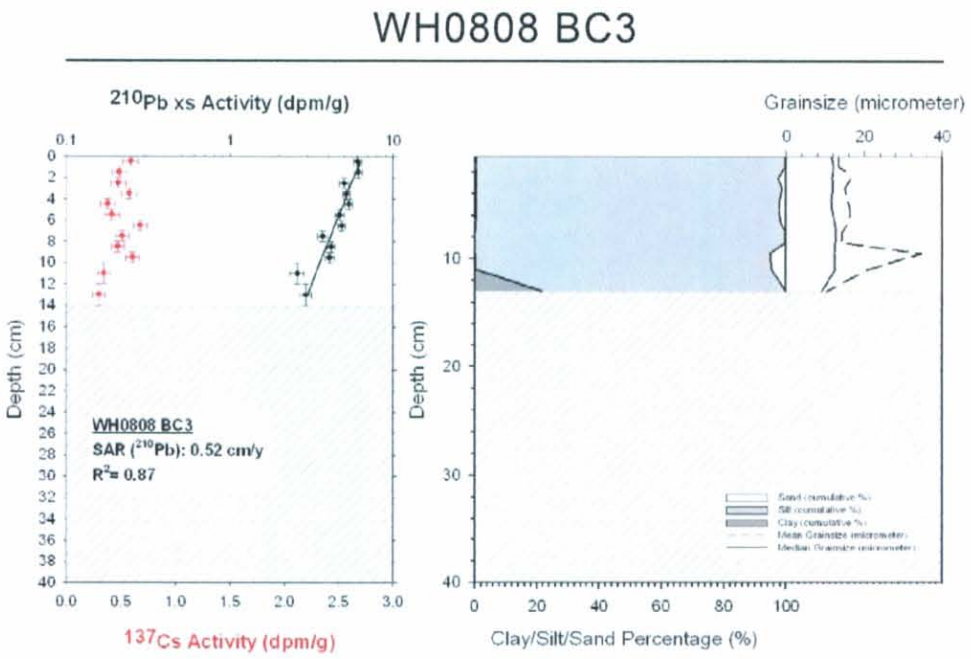
WH0808 BC3
210Pb xs Activity (dpm/g)
Grainsize (micrometer)
Depth (cm)
WH0808 BC3
SAR (210Pb): 0.52 cm/y
R2= 0.87
137Cs Activity (dpm/g)
Clay/Silt/Sand Percentage (%)

Fig. 4d

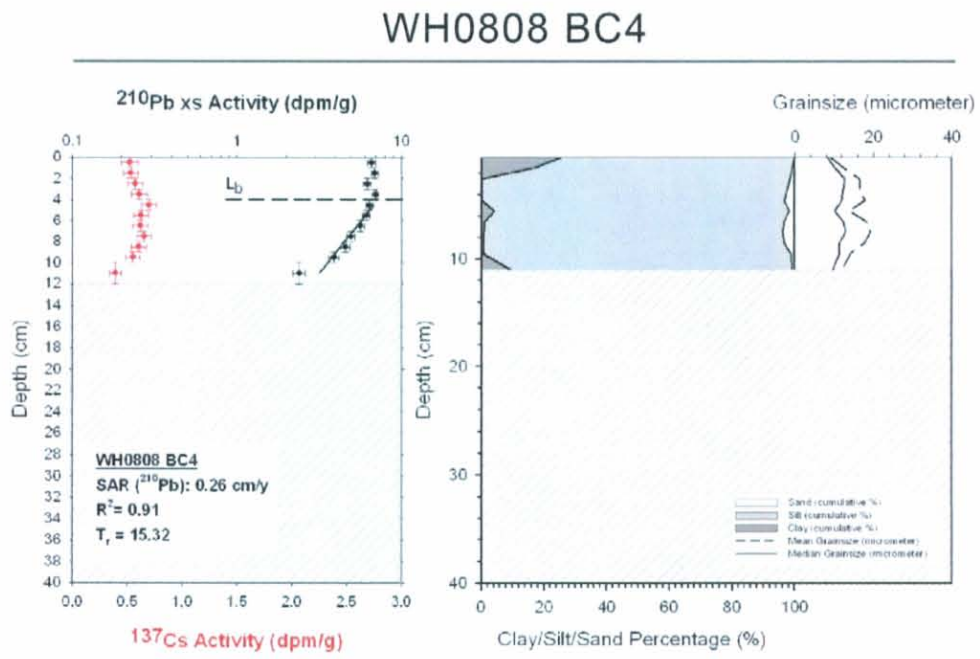
WH0808 BC4
210Pb xs Activity (dpm/g)
Grainsize (micrometer)
Lb
Depth (cm)
WH0808 BC4
SAR (210Pb): 0.26 cm/y
R2= 0.91
Tr = 15.32
137Cs Activity (dpm/g)
Clay/Silt/Sand Percentage (%)

Fig. 4e

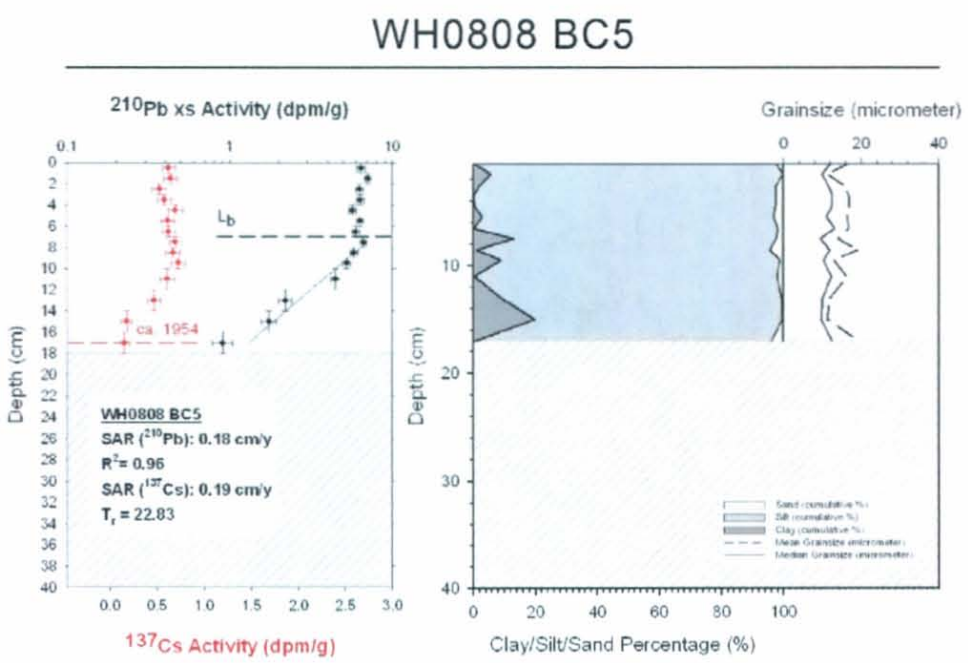

Fig. 4 Radio isotope and grain size plots of cores from Nachvak fjord, collected in 2008. Core locations can be seen in Fig. 2. ^{137}Cs activities are plotted in red, ^{210}Pb activity are plotted in black. Trend lines in the ^{210}Pb activities show the result of the least square fit to Eq. 1, used to calculate SARs. SARs derived from ^{210}Pb and ^{137}Cs data and temporal resolutions are shown in boxes in the radioisotope activity graphs. The grain size graphs are divided into an area plot, where the dark grey is the clay fraction in the core, light grey is silt and white is sand, and a line plot, where the dashed line shows the mean grain size in the core and the continuous line shows median grain size.

Fig. 5a

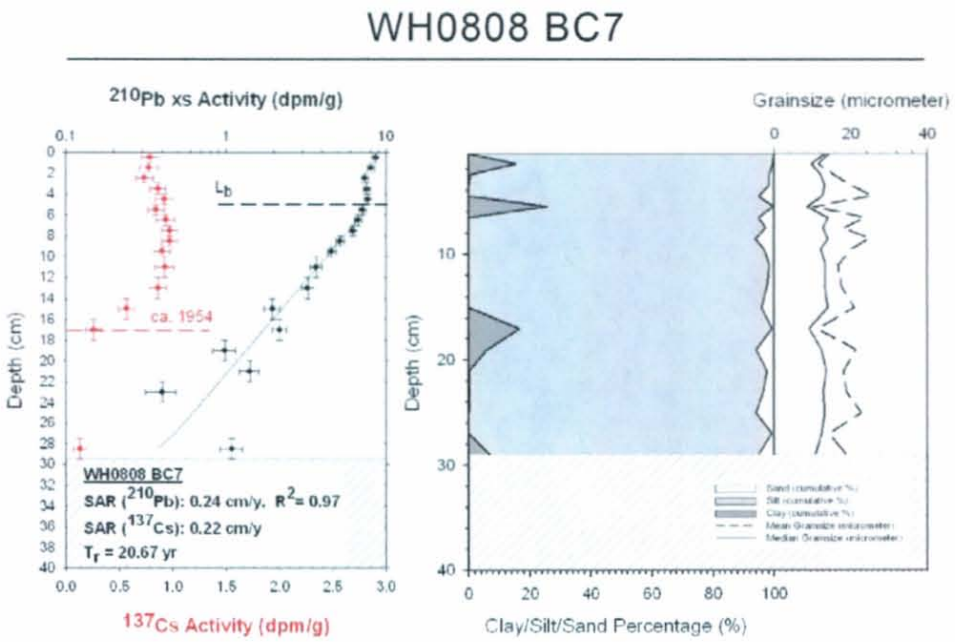
WH0808 BC7
210Pb xs Activity (dpm/g)
Grainsize (micrometer)
Depth (cm)
Lb
ca. 1954
WH0808 BC7
SAR (210Pb): 0.24 cm/y. R2= 0.97
SAR (137Cs): 0.22 cm/y
Tf = 20.67 yr
137Cs Activity (dpm/g)
Clay/Silt/Sand Percentage (%)

Fig. 5b

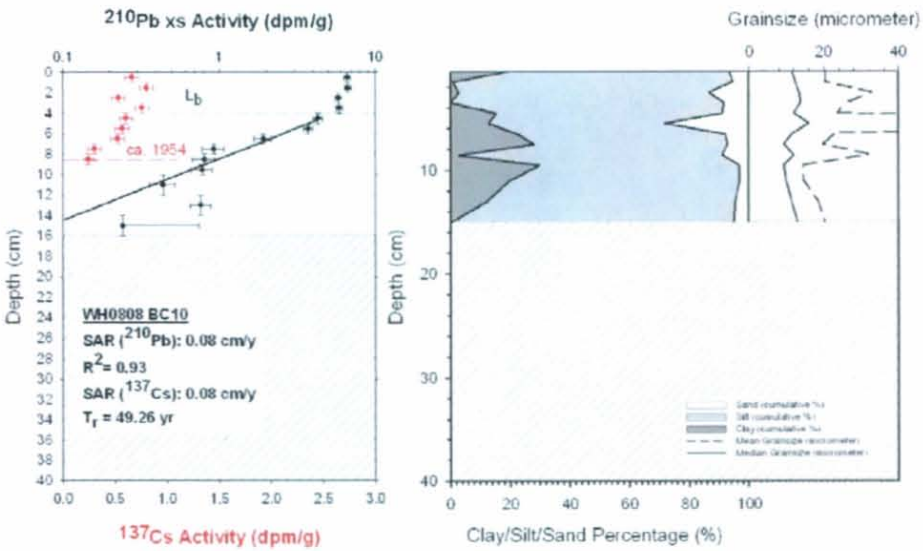
WH0808 BC10
210Pb xs Activity (dpm/g)
Grainsize (micrometer)
Depth (cm)
Lb
ca. 1954
WH0808 BC10
SAR (210Pb): 0.08 cm/y
R2= 0.93
SAR (137Cs): 0.08 cm/y
Tf = 49.26 yr
137Cs Activity (dpm/g)
Clay/Silt/Sand Percentage (%)

Fig. 5c

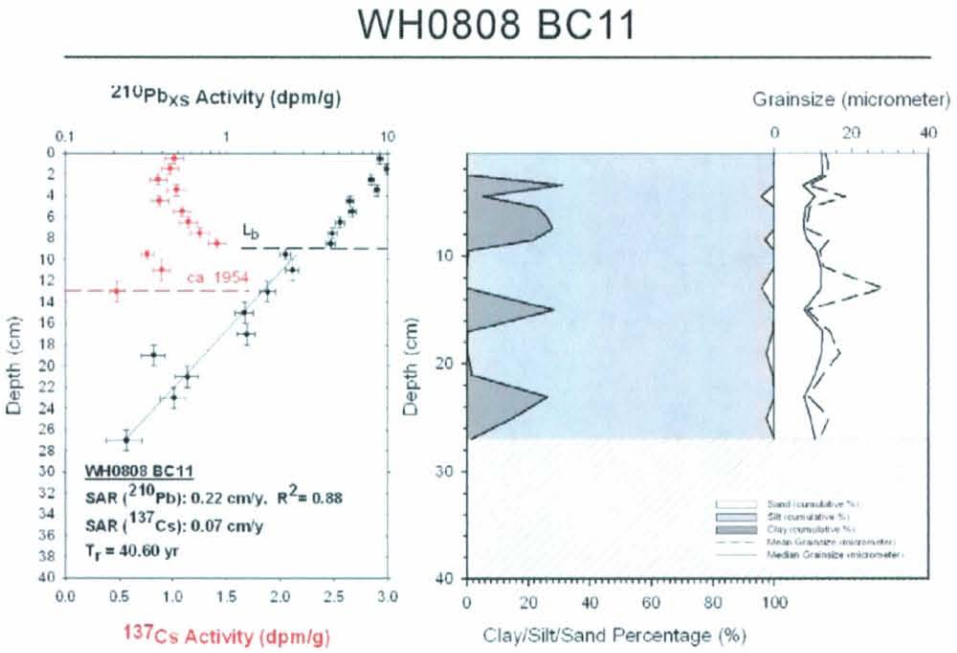
WH0808 BC11
210Pbxs Activity (dpm/g)
Grainsize (micrometer)
Depth (cm)
Lb
ca. 1954
WH0808 BC11
SAR (210Pb): 0.22 cm/y. R2= 0.88
SAR (137Cs): 0.07 cm/y
Tf = 40.60 yr
137Cs Activity (dpm/g)
Clay/Silt/Sand Percentage (%)

Fig. 5d

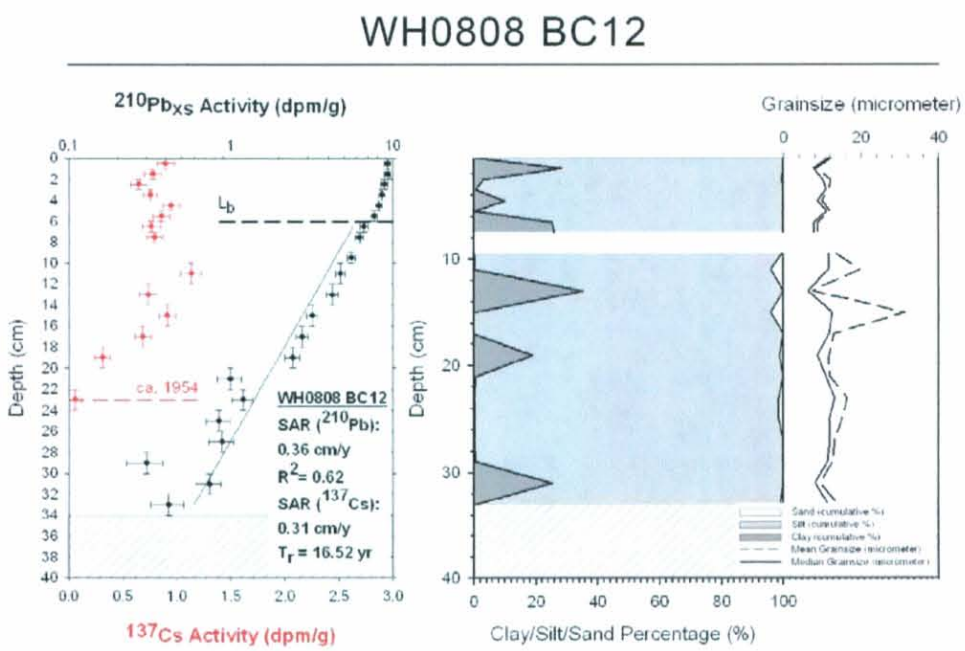
WH0808 BC12
210Pbxs Activity (dpm/g)
Grainsize (micrometer)
Depth (cm)
Lb
ca. 1954
WH0808 BC12
SAR (210Pb):
0.36 cm/y
R2= 0.62
SAR (137Cs):
0.31 cm/y
Tf = 16.52 yr
137Cs Activity (dpm/g)
Clay/Silt/Sand Percentage (%)

Fig. 5e

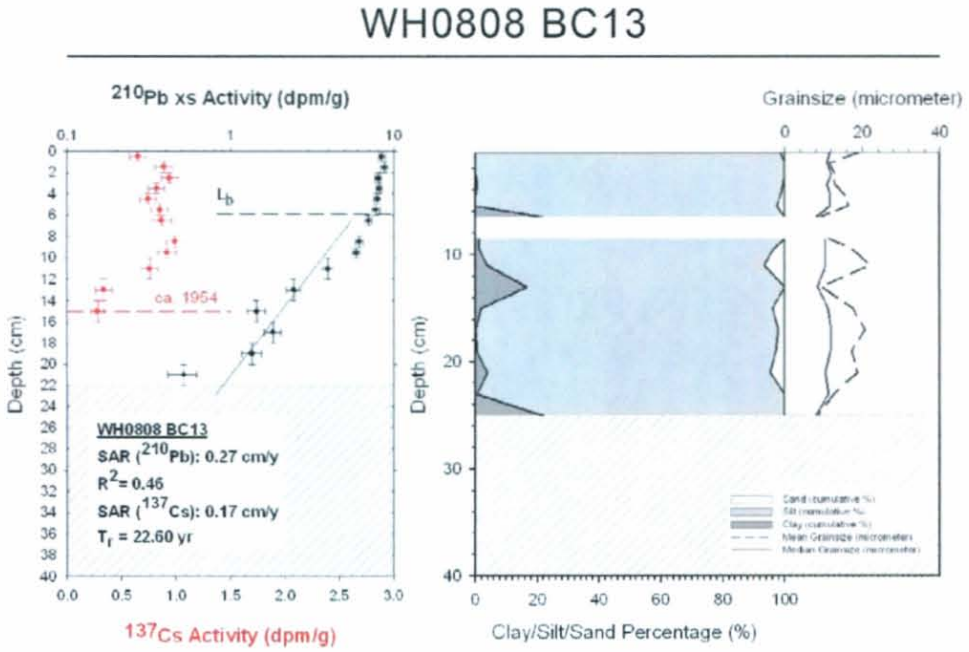

Fig. 5 Radio isotope and grain size plots of cores from Saglek fjord, collected in 2008. Core locations can be seen in Fig. 2. ^{137}Cs activities are plotted in red, ^{210}Pb activity are plotted in black. Trend lines in the ^{210}Pb activities show the result of the least square fit to Eq. 1, used to calculate SARs. SARs derived from ^{210}Pb and ^{137}Cs data and temporal resolutions are shown in boxes in the radioisotope activity graphs. The grain size graphs are divided into an area plot, where the dark grey is the clay fraction in the core, light grey is silt and white is sand, and a line plot, where the dashed line shows the mean grain size in the core and the continuous line shows median grain size.

Fig. 6a

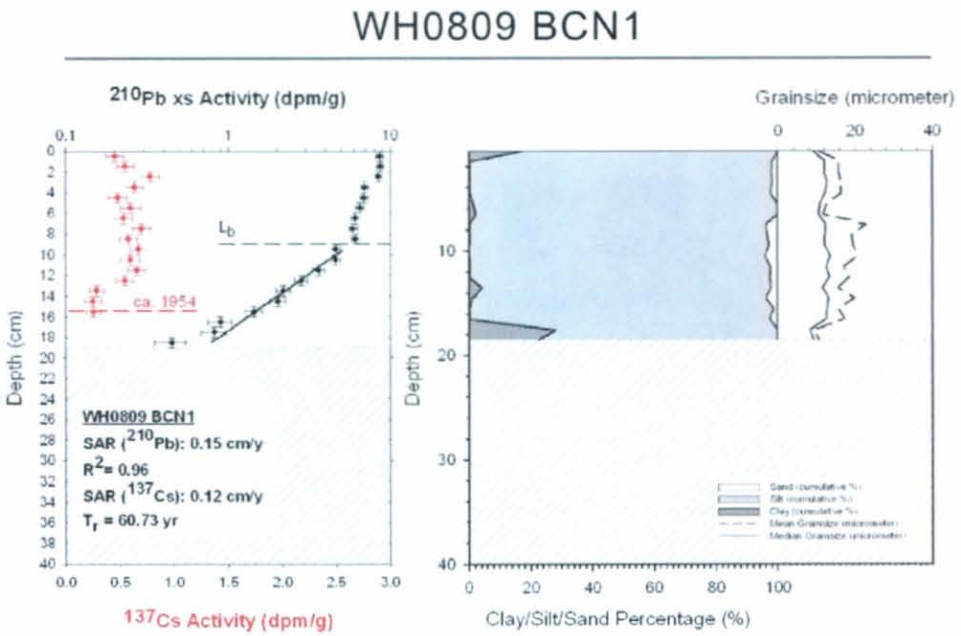
WH0809 BCN1
210Pb xs Activity (dpm/g)
Grainsize (micrometer)
Depth (cm)
Lb
ca. 1954
WH0809 BCN1
SAR (210Pb): 0.15 cm/y
R2= 0.96
SAR (137Cs): 0.12 cm/y
Tr = 60.73 yr
137Cs Activity (dpm/g)
Clay/Silt/Sand Percentage (%)

Fig. 6b

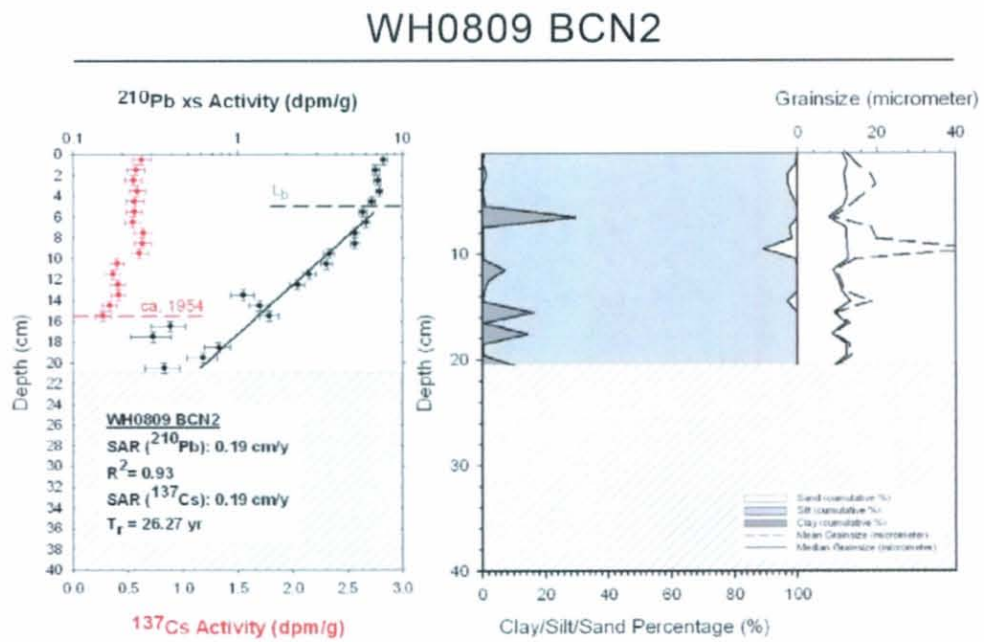
WH0809 BCN2
210Pb xs Activity (dpm/g)
Grainsize (micrometer)
Depth (cm)
Lb
ca. 1954
WH0809 BCN2
SAR (210Pb): 0.19 cm/y
R2= 0.93
SAR (137Cs): 0.19 cm/y
Tr = 26.27 yr
137Cs Activity (dpm/g)
Clay/Silt/Sand Percentage (%)

Fig. 6c

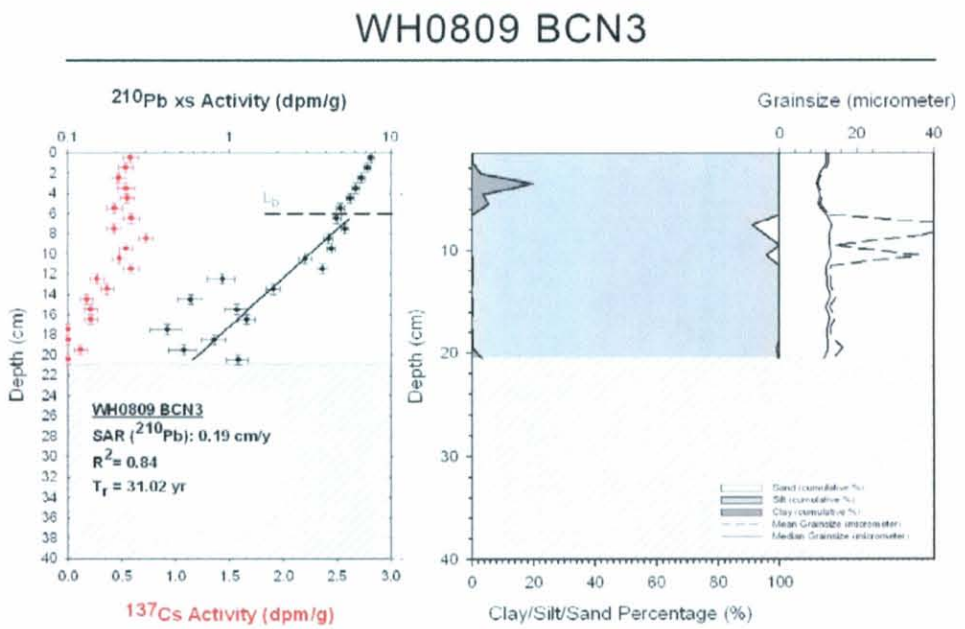
WH0809 BCN3
210Pb xs Activity (dpm/g)
Grainsize (micrometer)
Depth (cm)
WH0809 BCN3
SAR (210Pb): 0.19 cm/y
R2= 0.84
Tf = 31.02 yr
137Cs Activity (dpm/g)
Clay/Silt/Sand Percentage (%)

Fig. 6d

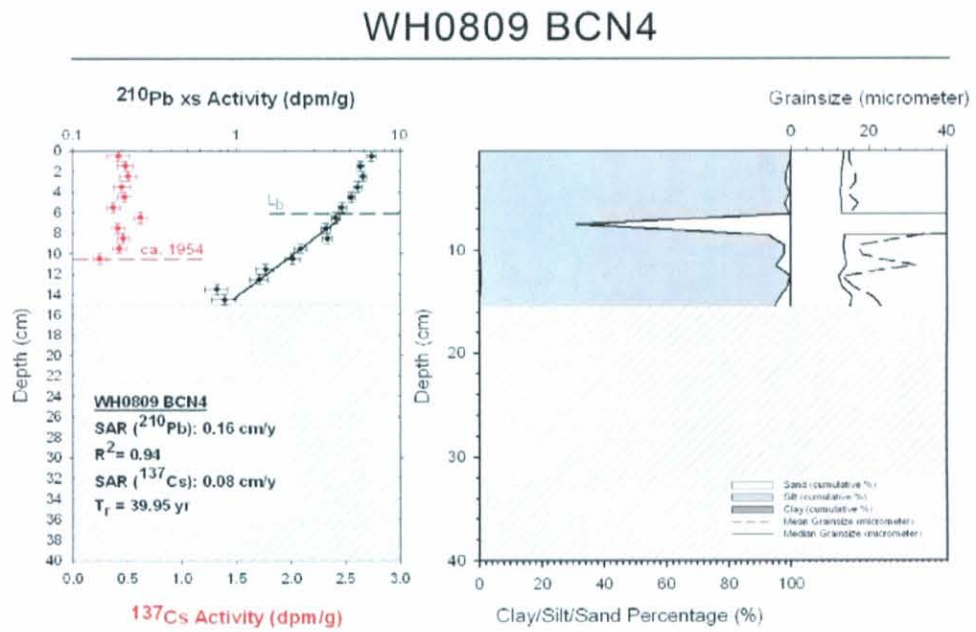
WH0809 BCN4
210Pb xs Activity (dpm/g)
Grainsize (micrometer)
ca. 1954
Depth (cm)
WH0809 BCN4
SAR (210Pb): 0.16 cm/y
R2= 0.94
SAR (137Cs): 0.08 cm/y
Tf = 39.95 yr
137Cs Activity (dpm/g)
Clay/Silt/Sand Percentage (%)

Fig. 6e

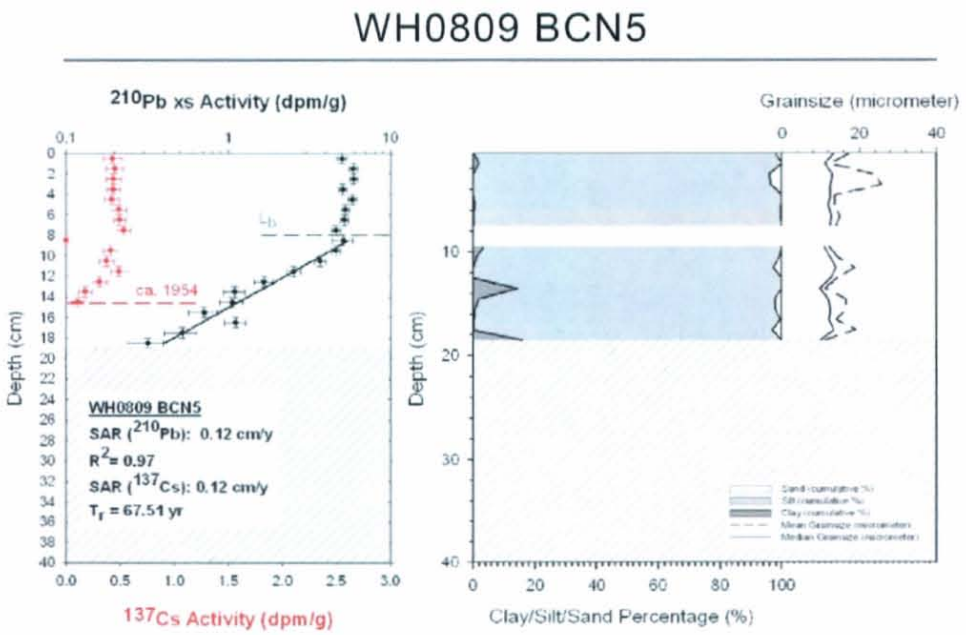

Fig .6 Radio isotope and grain size plots of cores from Nachvak fjord, collected in 2009. Core locations can be seen in Fig. 2. ^{137}Cs activities are plotted in red, ^{210}Pb activity are plotted in black. Trend lines in the ^{210}Pb activities show the result of the least square fit to Eq. 1, used to calculate SARs. SARs derived from ^{210}Pb and ^{137}Cs data and temporal resolutions are shown in boxes in the radioisotope activity graphs. The grain size graphs are divided into an area plot, where the dark grey is the clay fraction in the core, light grey is silt and white is sand, and a line plot, where the dashed line shows the mean grain size in the core and the continuous line shows median grain size.

Fig. 7a

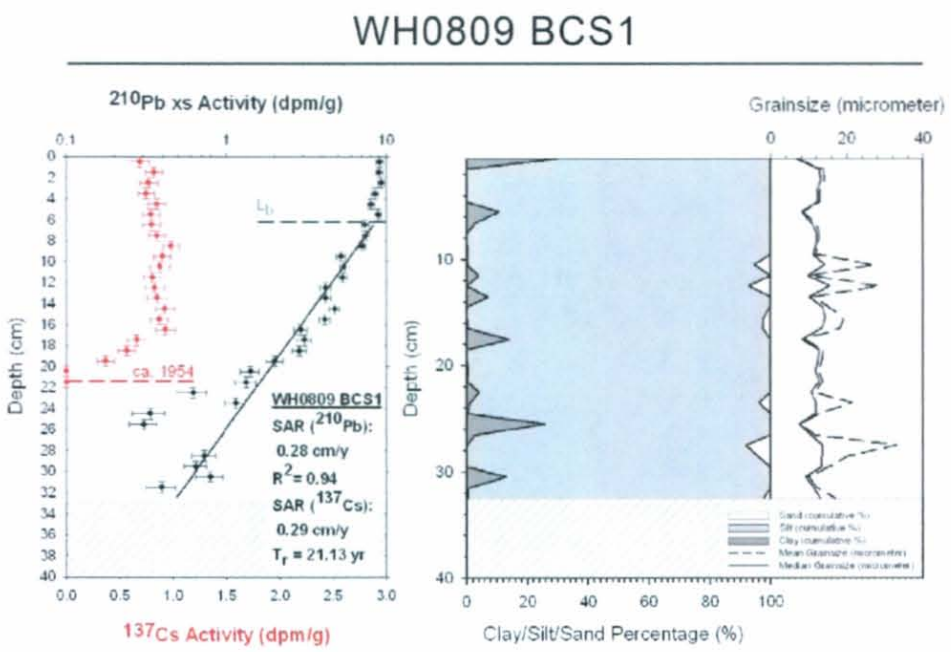
WH0809 BCS1
210Pb xs Activity (dpm/g)
Grainsize (micrometer)
Depth (cm)
ca. 1954
WH0809 BCS1
SAR (210Pb):
0.28 cm/y
R2= 0.94
SAR (137Cs):
0.29 cm/y
Tf = 21.13 yr
137Cs Activity (dpm/g)
Clay/Silt/Sand Percentage (%)

Fig. 7b

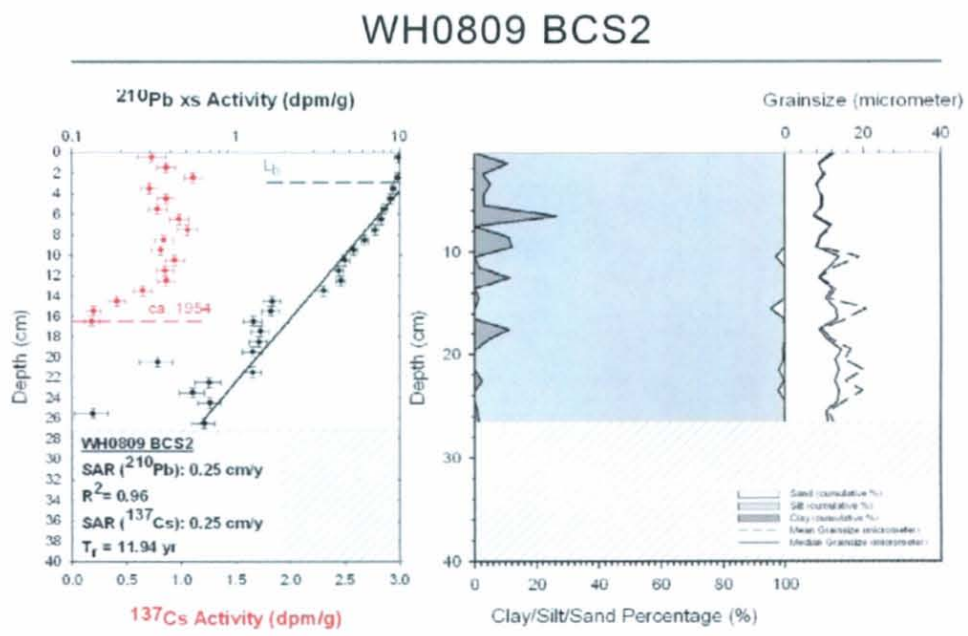
WH0809 BCS2
210Pb xs Activity (dpm/g)
Grainsize (micrometer)
Depth (cm)
ca. 1954
WH0809 BCS2
SAR (210Pb): 0.25 cm/y
R2= 0.96
SAR (137Cs): 0.25 cm/y
Tf = 11.94 yr
137Cs Activity (dpm/g)
Clay/Silt/Sand Percentage (%)

Fig. 7c

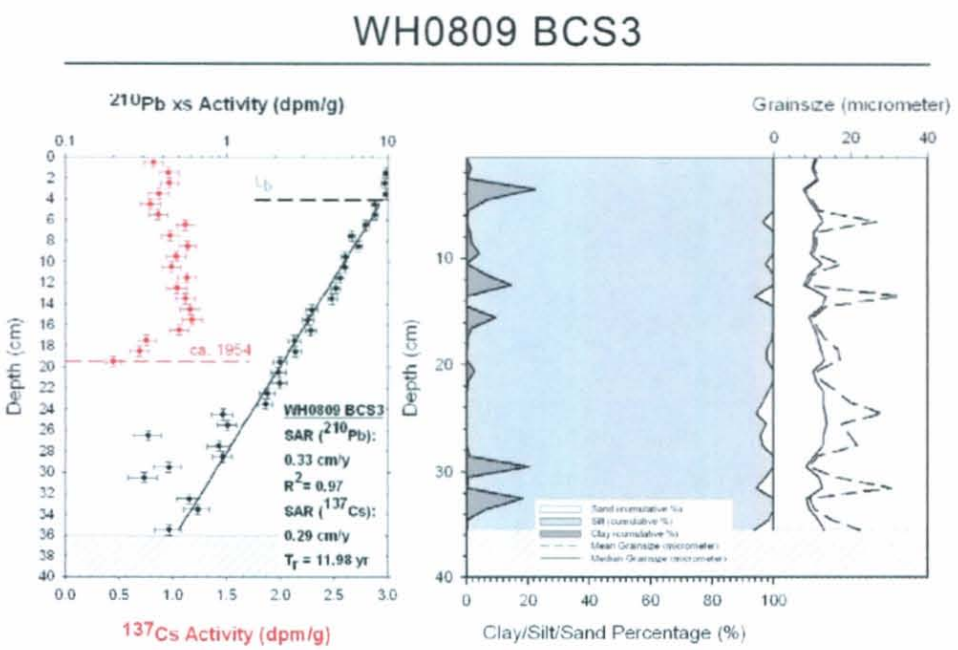
WH0809 BCS3
210Pb xs Activity (dpm/g)
Grainsize (micrometer)
Depth (cm)
ca. 1954
WH0809 BCS3
SAR (210Pb):
0.33 cm/y
R2= 0.97
SAR (137Cs):
0.29 cm/y
Tf = 11.98 yr
137Cs Activity (dpm/g)
Clay/Silt/Sand Percentage (%)

Fig. 7d

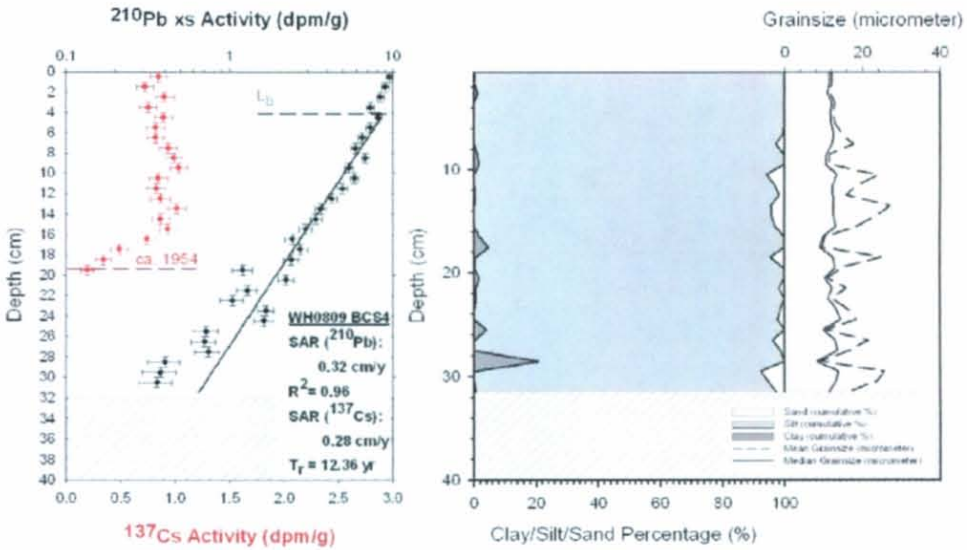
WH0809 BCS4
210Pb xs Activity (dpm/g)
Grainsize (micrometer)
Depth (cm)
ca. 1954
WH0809 BCS4
SAR (210Pb):
0.32 cm/y
R2= 0.96
SAR (137Cs):
0.28 cm/y
Tf = 12.36 yr
137Cs Activity (dpm/g)
Clay/Silt/Sand Percentage (%)

Fig. 7e

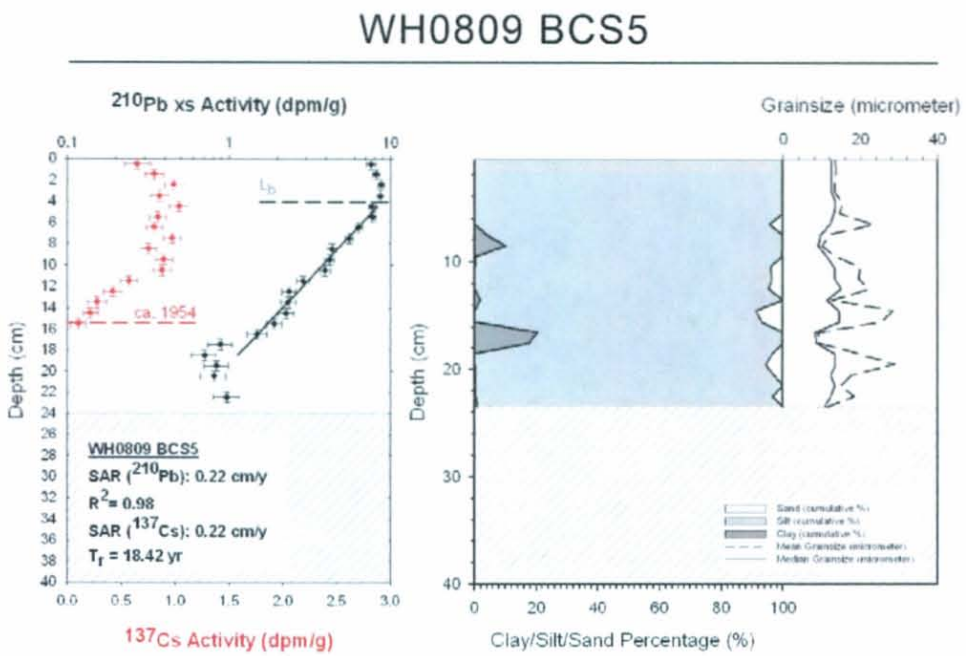

Fig. 7 Radio isotope and grain size plots of cores from Saglek fjord, collected in 2009. Core locations can be seen in Fig. 2. ^{137}Cs activities are plotted in red, ^{210}Pb activity are plotted in black. Trend lines in the ^{210}Pb activities show the result of the least square fit to Eq. 1, used to calculate SARs. SARs derived from ^{210}Pb and ^{137}Cs data and temporal resolutions are shown in boxes in the radioisotope activity graphs. The grain size graphs are divided into an area plot, where the dark grey is the clay fraction in the core, light grey is silt and white is sand, and a line plot, where the dashed line shows the mean grain size in the core and the continuous line shows median grain size.

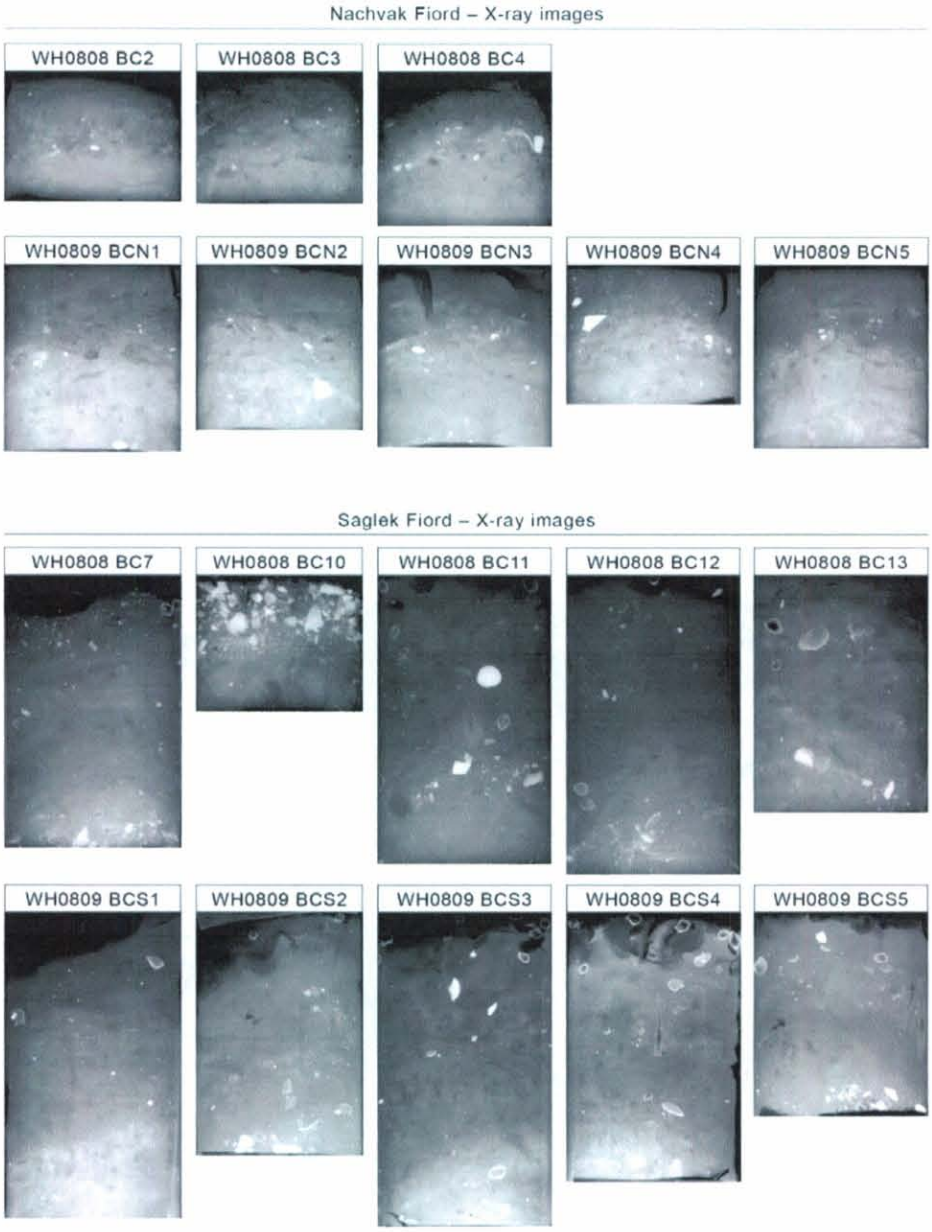

Fig. 8 X-radiograph images of all box cores. The darker colour sediments are less dense. Overall the cores show mottled sediment with ice rafted debris (rocks), shells and polychaetes tubes. Remnant bedding is visible in core WH0808 BC7 and ice rafted debris is particularly abundant in core WH0808 BC10.

Granulometry

Sediments of all cores are generally fine grained with silt as the dominant size fraction (Fig. 4, 5, 6, 7). In Nachvak Fjord mean grain sizes range between 8 and 40 microns and in Saglek Fjord between 8 and 36 microns. The mean grain size for the marine basin in Nachvak Fjord is around 17 microns, with 19 microns close to the mouth of McCornick River and 15 microns in the centre of the marine basin. In the marine basin of Saglek Fjord the mean grainsize is around 16 microns, with 22 microns close to the mouth of Nakvak Brook and 15 microns in the core at greatest distance from the river mouth.

X-Radiographs

X-radiographs of all cores show generally mottled sediments containing varying quantities of shells and shell fragments, polychaetes tubes, and ice rafted debris (IRD) (Fig. 8). In the cores of Nachvak Fjord neither physical sedimentary structures nor remnants of them are visible. A few cores contain burrows that are open to the sediment surface and can be used to estimate bioturbation depth (i. e. WH0809 BCN1 and WH0809 BCN4). The cores contain IRD ranging from 0.1 cm to 2.5 cm in diameter. Shell fragments are evident (i.e. WH0809 BCN3) but not abundant.

In the cores of Saglek Fjord some remnants of sedimentary layering are visible (WH0808 BC7, Fig. 5a; WH0808 BC11, Fig. 5c; WH0808 BC12, Fig. 5d). Differences in colour and therefore density in core WH0808 BC7 between a depth of 6 and 11 cm suggest remnant cross bedding that seems to be truncated at the base at a depth of 11 cm.

Cores WH0808 BC11 and WH0808 BC12 both show areas of darker colour (thus less dense material) between depths of 7 and 17 cm, suggesting a remnant of a sedimentary bed that contained less dense material (i.e. more mud) than the beds above and below. Cores from the marine basin of Saglek fjord contain IRD in varying abundance. IRD is less abundant in core WH0809 BCS1 and significantly abundant in core WH0808 BC10. The uppermost 8 cm of core WH0808 BC10 consist of about 70% IRD ranging in diameter from 0.01 cm to 3 cm. Shell fragments and polychaetes tubes are more abundant in cores from Saglek fjord compared to cores from Nachvak Fjord (i. e. WH0809 S4).

Inventories of ^{210}Pb

Terrestrial soil inventories of excess of ^{210}Pb were determined for soil cores to estimate atmospheric flux of ^{210}Pb to the land surface in the two fjords:

$$I_t = \sum \frac{A_i \times m_i}{S} \qquad \text{Eq. 8}$$

where I is the inventory, A_i is the activity and m_i is the total dry mass of soil in that depth interval, and S is the surface area of that core.

Inventories of ^{210}Pb in sediment can be calculated as a product of depth-integrated ^{210}Pb activity and dry bulk density by using the following equation (Muhammad et al. 2008):

$$I = \sum \rho_s \, \Delta z \, (1 - \varphi_i) A_i \qquad \text{Eq. 9}$$

where I is the inventory (dpm/cm^2), ρ_s is the mineral density (g/cm^3), Δz is the thickness of the sample interval i (cm), φ is the porosity, and A is the excess activity of ^{210}Pb (dpm/g).

From the inventories we calculated the annual flux of excess ^{210}Pb by (Buesseler et al. 1985):

$$F = \lambda I \qquad \text{Eq. 10}$$

where F is the annual flux (dpm cm^{-2} y^{-1}) required to support the inventory at steady sate and λ is the radioactive decay constant for ^{210}Pb (0.031 y^{-1}). We did the same calculations for soil cores and sediment cores and compared the resulting fluxes.

Table 1 *Inventories and fluxes of ^{210}Pb for box cores from Nachvak Fjord*

^{210}Pb Inventories
Nachvak Fjord

Box Cores			
Core name	210-Pb Inventories (dpm/cm^2)	F (Flux) (dpm/cm^2 y)	R = F/T
BC1	15.27	0.47	0.65
BC2	16.64	0.52	0.71
BC3	16.76	0.52	0.71
BC4	15.89	0.49	0.67
BC5	20.25	0.63	0.86
BCN1	23.32	0.72	0.99
BCN2	24.25	0.75	1.03
BCN3	23.75	0.74	1.01
BCN4	17.87	0.55	0.76
BCN5	19.11	0.59	0.81
Mean	19.31	0.60	0.82
δ	3.24	0.10	0.14
T (Theoretical Flux) based on soil core 2C		0.73	

Table 2 *Inventories and fluxes of ^{210}Pb for box cores from Saglek Fjord*

^{210}Pb Inventories
Saglek Fiord

Box Cores			
Core name	210-Pb Inventories (dpm/cm^2)	F (Flux) (dpm/cm^2 y)	R = F/T
BC7a	22.35	0.69	0.949285
BC10	18.16	0.56	0.771091
BC11	18.26	0.57	0.775531
BC12	28.92	0.90	1.228121
BC13	13.35	0.41	0.56691
BCS1	18.49	0.57	0.785264
BCS2	25.38	0.79	1.077913
BCS3	30.15	0.93	1.280227
BCS4	23.75	0.74	1.008498
BCS5	19.31	0.60	0.819817
Mean	21.81	0.68	0.93
δ	5.02	0.16	0.21
T (Theoretical Flux) based on soil core 2C		0.73	

In Nachvak Fjord ^{210}Pb inventories in sediments range from 15.3 to 24.3 dpm/cm^2, and annual flux required to produce this inventory was 0.47 to 0.75 dpm cm^{-2} y^{-1} (Table 1). In Saglek Fjord ^{210}Pb inventories in sediments range from 13.4 to 30.2 dpm/cm^2, and annual flux of excess ^{210}Pb ranges from 0.41 to 0.93 dpm cm^{-2} y^{-1}(Table 2). The theoretical flux of ^{210}Pb supplied from the atmosphere to the land surface was estimated from ^{210}Pb inventories in soil cores. One of the soil cores appeared to capture the ^{210}Pb

atmospheric fallout efficiently enough to support the global range of annual deposition fluxes of excess ^{210}Pb of 0.3 - 0.9 dpm/cm^{2}y as reported by Appleby and Oldfield (1992). The result for the flux of this soil core is 0.73 dpm/cm^{2}y and will be used in the following discussion as the theoretical flux for the annual deposition of unsupported ^{210}Pb in the study area.

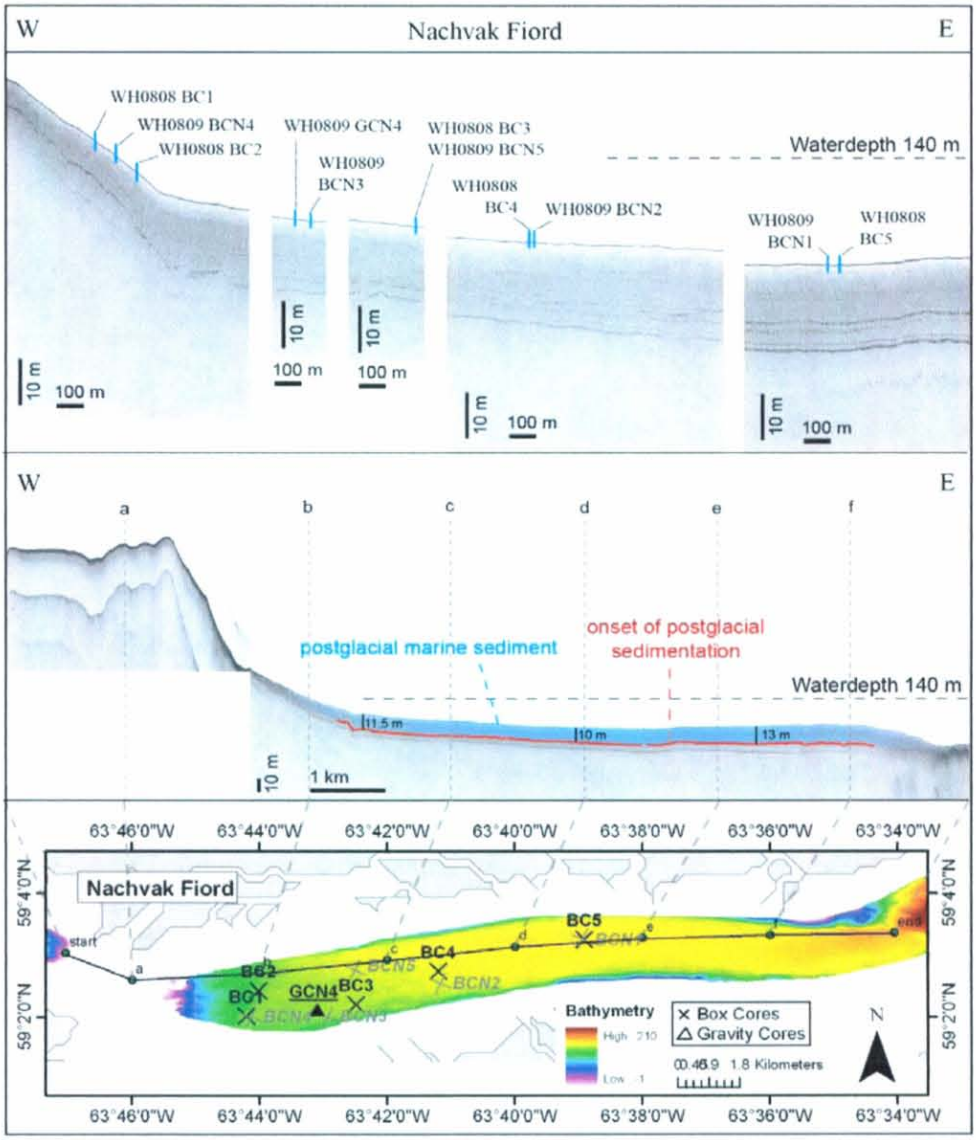

Fig. 9 Compilation of sub-bottom profiles and bathymetry data in Nachvak Fjord. Upper part shows close-ups of profiles with approximate coring locations. Middle part shows a profile line through the entire basin with interpretations about postglacial marine sediment thickness. The geographical location of this line is shown in the lower part.

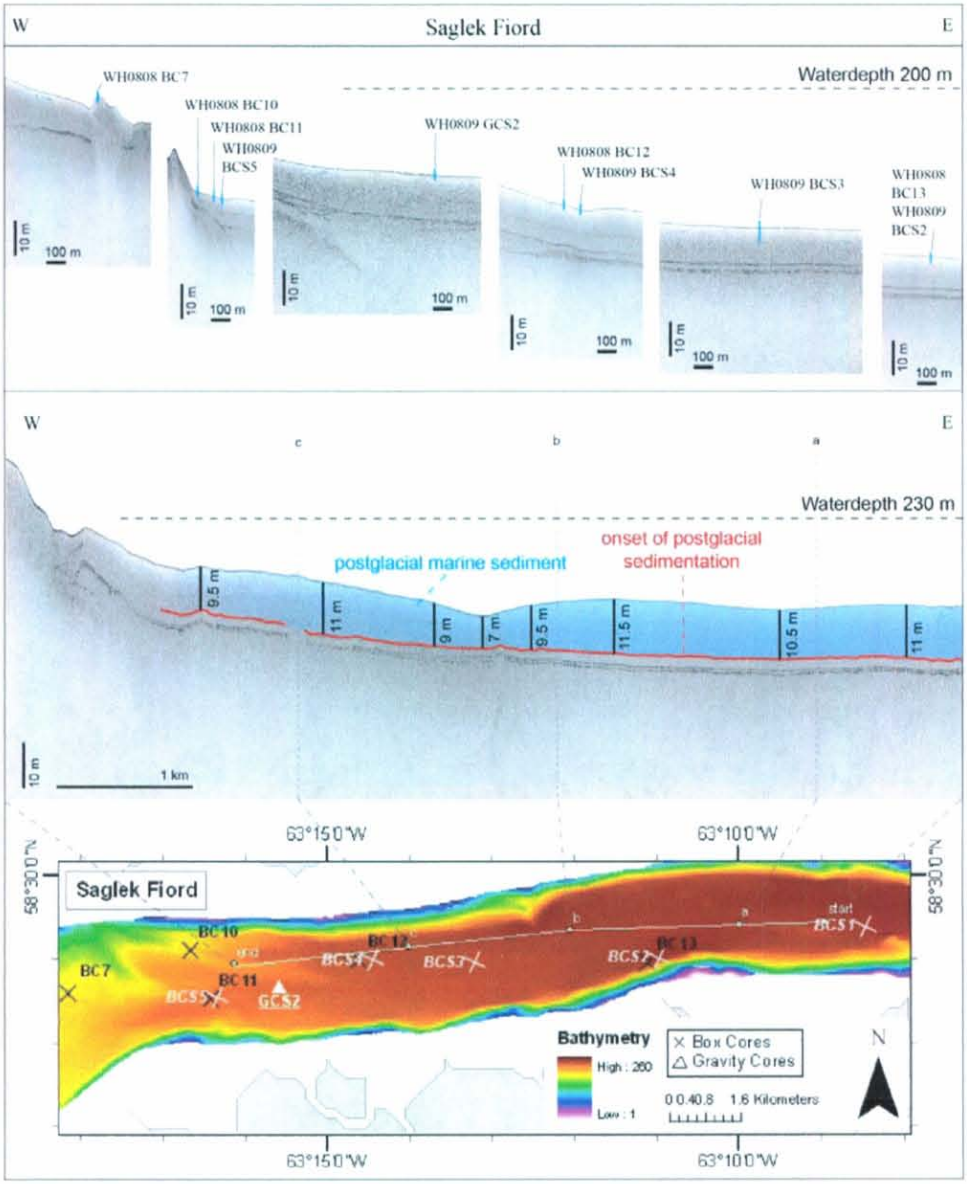

Fig. 10 Compilation of sub-bottom profiles and bathymetry data in Saglek Fjord. Upper part shows close-ups of profiles with approximate coring locations. Middle part shows a profile line through the entire basin with interpretations about postglacial marine sediment thickness. The geographical location of this line is shown in the lower part.

Figures 9 and 10 display cross-sections of the entire basins in each fjord and have been used to map the thickness of postglacial sediment. The first strong reflector in the sub-bottom profiles is interpreted to represent the latest glacial deposits and therefore the onset of postglacial marine sedimentation. Approximate core locations are projected onto each line to display the general sub-bottom conditions in the vicinity of each core (Fig. 9 and 10). In Nachvak Fjord (Fig.9) the profile cuts through the entire basin and across the sill to the West. From as little as 30 meters water depth at the sill in the West the seafloor descends steeply for approximately one kilometer and then with a low gradient for another 1.5 kilometers until the seafloor becomes flat at a water depth of around 164 meters. The sediment evident in Nachvak Fjord data appears as a continuous and homogenous unit throughout the basin. Its thickness ranges from 10 meters in the centre to 13 meters on the eastern side of the profile. In Saglek Fjord (Fig. 10) the profile stretches from close to the mouth of Nakvak Brook in the West to deep in the basin at its eastern end. It shows that the basin is relatively flat at a water depth of around 245 meters except for one depression at the centre which is 250 meters deep. The youngest sedimentary unit in Saglek Fjord seismic data appears homogenous with an average thickness of 9.9 meters.

Stream flow characteristics and seasonal water level changes

Data derived from the HOBO water level loggers show temperature and water level changes for both McCornick River and Nakvak Brook from August 2008 to August 2009.

For the time span where the water temperature falls below 0 °C, water is assumed to be frozen and not flowing.

In McCornick River water temperatures fell below 0 °C in mid-November 2008 and returned to temperatures above 0 °C in late March 2009 (Fig. 11). Highest temperatures appear in late July/early August up to 15 °C and fall and rise in a gradual manner. Because the water level logger was deployed on the river bed, sensor depth can be taken as equivalent to water level. In McCornick River water level peaked as high as 1.4 m with a rapid rise from 0.8 m in late August and a rapid fall in early September back to 0.8 m. A smaller peak can be seen in early November, with a rise from 0.6 m to 0.9 m. The next distinct peak appears in late June up to 1.25 m, with a rise from 0.5 m in beginning of June and a fall in water level to 0.5 m in late July. A small peak can be seen in late July/early August to a water level of 0.7 m.

In Nakvak Brook the highest water temperature of 18.5 °C was measured in early August (Fig. 12). It decreased relatively gradually thereafter and increased relatively gradually from mid-June to early August to 15.5 °C. The time span for water temperatures below 0 °C is longer compared to the time span in McCornick River. Water temperatures in Nakvak Brook were below 0 °C from early November 2008 to early June 2009. Water level peaked in late August to 1.1 m with a rapid increase from 0.3 m in early August and a rapid fall to 0.55 m in early September. Water level remained around 0.3 to 0.5 m until early November. After water temperatures returned to above 0 °C, the water level started to rise in early June from 0.5 m to 1.25 m in late June, and alternated between 0.7m to 1.2 m until a fall to 0.5 m in late July. A smaller peak can be seen in early August at 0.85 m.

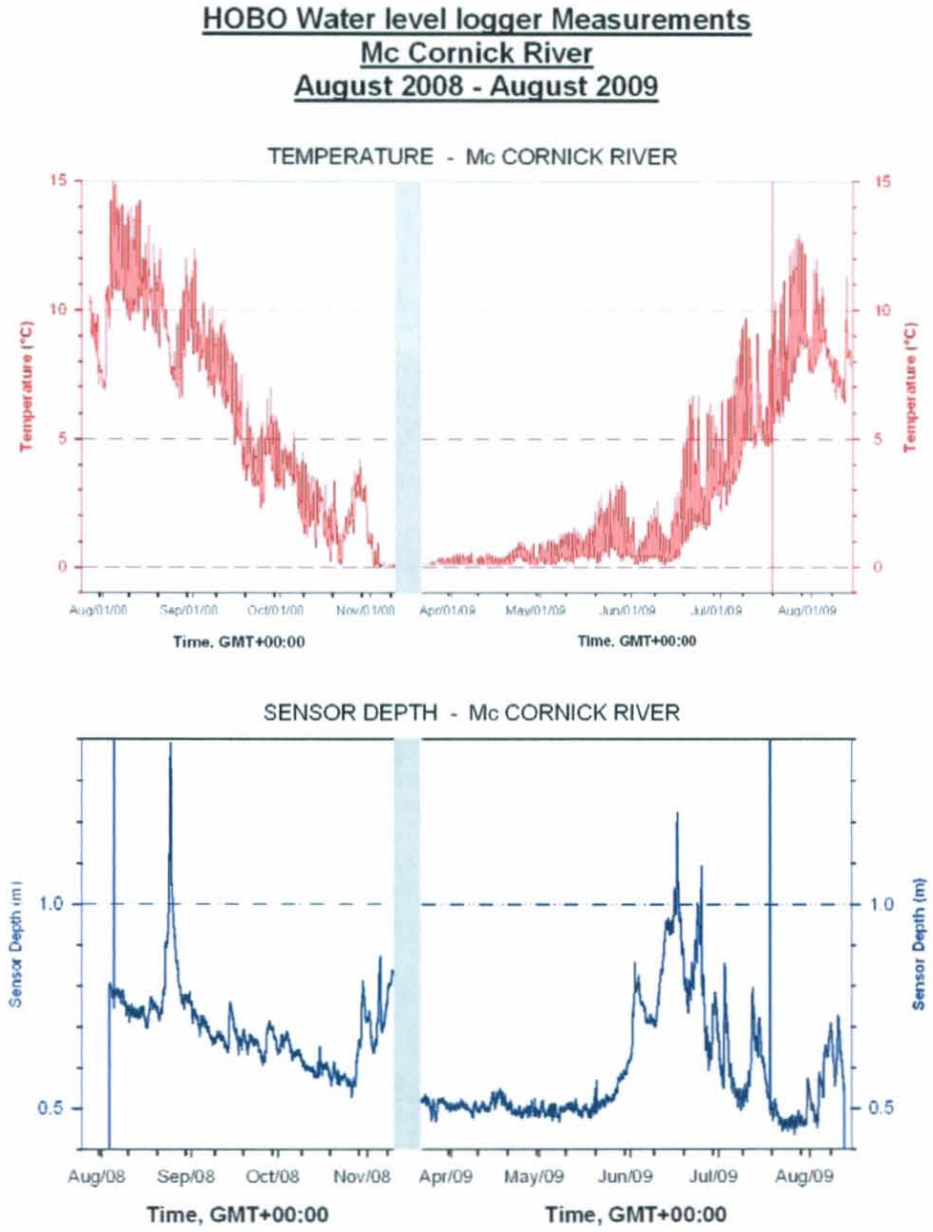

Fig. 11 Temperature and water level data from water level logger in Nakvak Brook from August 2008 to August 2009. Data for the time span where water temperatures fell below zero has been excluded (shaded areas).

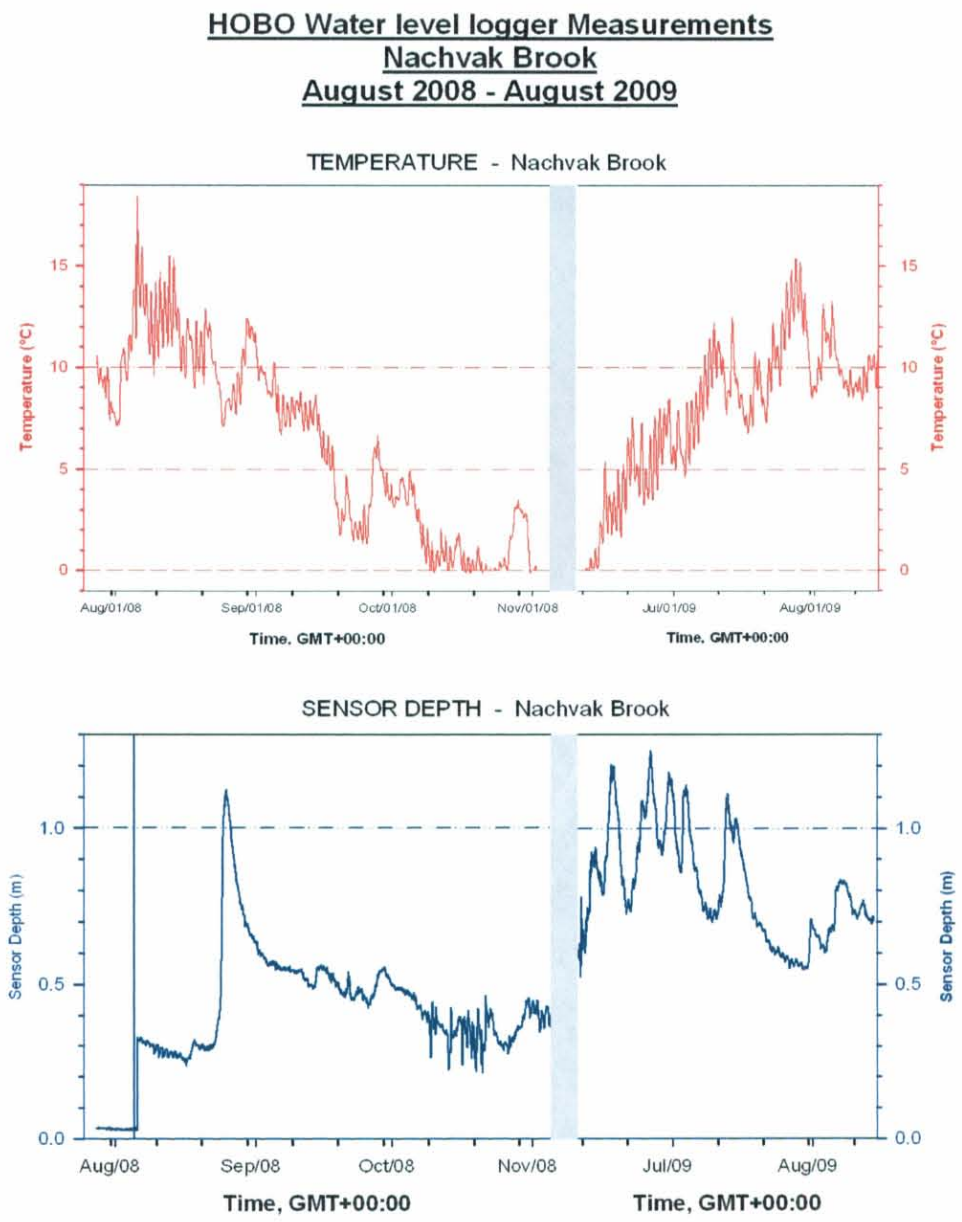

Fig. 12 Temperature and water level data from water level logger in McCornick River from August 2008 to August 2009. Data for the time span where water temperatures fell below zero has been excluded (shaded areas).

Table 3: Accoustic Doppler Velocimeter measurements in McCornick River

Discharge Measurement Summary

Date Generated: Mon Jun 14 2010

File Information

File Name	MC3.WAD
Start Date and Time	2008/08/03 12:40:15

Site Details

Site Name	
Operator(s)	LISI

System Information

Sensor Type	FlowTracker
Serial #	P1296
CPU Firmware Version	3.2
Software Ver	2.30
Mounting Correction	0.0%

Units (Metric Units)

Distance	m
Velocity	m/s
Area	m^2
Discharge	m^3/s

Discharge Uncertainty

Category	ISO	Stats
Accuracy	1.0%	1.0%
Depth	0.2%	5.7%
Velocity	2.5%	11.6%
Width	0.2%	0.2%
Method	2.7%	-
# Stations	4.2%	-
Overall	**5.7%**	**13.0%**

Summary

Averaging Int.	20	# Stations	12
Start Edge	LEW	Total Width	22.000
Mean SNR	16.4 dB	Total Area	8.960
Mean Temp	12.70 °C	Mean Depth	0.407
Disch. Equation	Mid-Section	Mean Velocity	0.4386
		Total Discharge	**3.9296**

Measurement Results

St	Clock	Loc	Method	Depth	%Dep	MeasD	Vel	CorrFact	MeanV	Area	Flow	%Q
0	12:40	0.00	None	0.000	0.0	0.0	0.0000	1.00	0.0000	0.000	0.0000	0.0
1	12:42	2.00	0.6	0.200	0.6	0.080	0.2918	1.00	0.2918	0.400	0.1167	3.0
2	*12:43*	*4.00*	*0.6*	*0.400*	*0.6*	*0.160*	*0.1256*	*1.00*	*0.1256*	*0.800*	*0.1005*	*2.6*
3	*12:45*	*6.00*	*0.6*	*0.500*	*0.6*	*0.200*	*0.5207*	*1.00*	*0.5207*	*1.000*	*0.5207*	*13.3*
4	*12:47*	*8.00*	*0.6*	*0.420*	*0.6*	*0.168*	*0.3195*	*1.00*	*0.3195*	*0.840*	*0.2684*	*6.8*
5	12:49	10.00	0.6	0.500	0.6	0.200	0.5442	1.00	0.5442	1.000	0.5442	13.8
6	12:50	12.00	0.6	0.400	0.6	0.160	0.7737	1.00	0.7737	0.800	0.6190	15.8
7	12:52	14.00	0.6	0.600	0.6	0.240	0.5135	1.00	0.5135	1.200	0.6162	15.7
8	12:54	16.00	0.6	0.590	0.6	0.236	0.5014	1.00	0.5014	1.180	0.5917	15.1
9	12:55	18.00	0.6	0.430	0.6	0.172	0.4303	1.00	0.4303	0.860	0.3701	9.4
10	12:57	20.00	0.6	0.440	0.6	0.176	0.2071	1.00	0.2071	0.880	0.1822	4.6
11	12:57	22.00	None	0.000	0.0	0.0	0.0000	1.00	0.0000	0.000	0.0000	0.0

Rows in italics indicate a QC warning. See the Quality Control page of this report for more information.

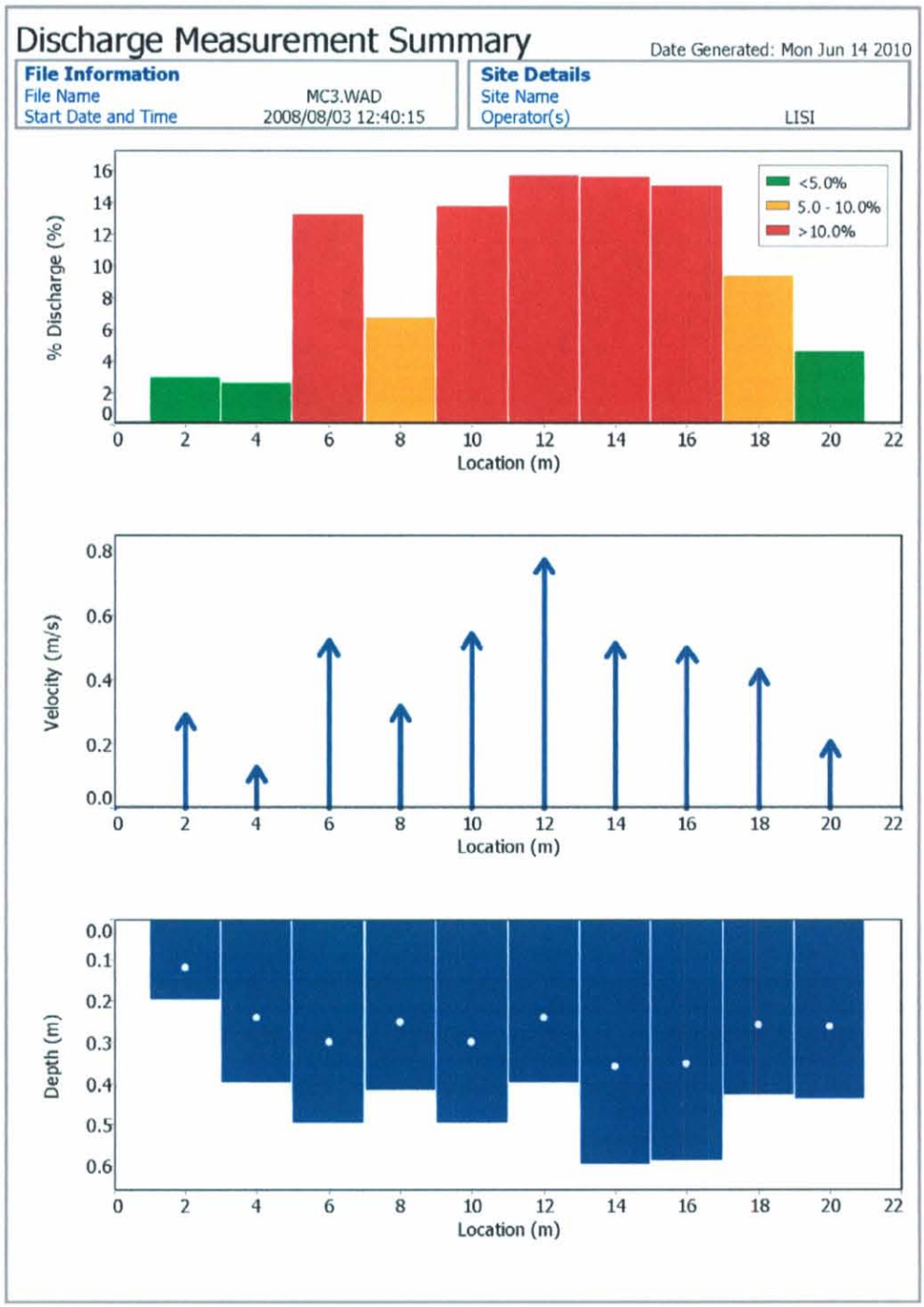

Fig. 13 Water discharge and velocity measurements and depth profile of McCornick River

Table 4: Accoustic Doppler Velocimeter measurements in Nakvak Brook

Discharge Measurement Summary

Date Generated: Mon Jun 14 2010

File Information

File Name	NB1.WAD
Start Date and Time	2008/08/05 16:05:36

Site Details

Site Name	
Operator(s)	LISI

System Information

Sensor Type	FlowTracker
Serial #	P1296
CPU Firmware Version	3.2
Software Ver	2.30
Mounting Correction	0.0%

Units	(Metric Units)
Distance	m
Velocity	m/s
Area	m^2
Discharge	m^3/s

Discharge Uncertainty

Category	ISO	Stats
Accuracy	1.0%	1.0%
Depth	0.1%	2.0%
Velocity	1.1%	4.2%
Width	0.1%	0.1%
Method	1.8%	-
# Stations	2.1%	-
Overall	**3.2%**	**4.8%**

Summary

Averaging Int.	20	# Stations	24
Start Edge	LEW	Total Width	46.000
Mean SNR	9.3 dB	Total Area	29.680
Mean Temp	15.99 °C	Mean Depth	0.645
Disch. Equation	Mid-Section	Mean Velocity	0.3662
		Total Discharge	**10.8676**

Measurement Results

St	Clock	Loc	Method	Depth	%Dep	MeasD	Vel	CorrFact	MeanV	Area	Flow	%Q
0	16:05	0.00	None	0.000	0.0	0.0	0.0000	1.00	0.0000	0.000	0.0000	0.0
1	*16:05*	*2.00*	*0.6*	*0.220*	*0.6*	*0.088*	*0.0523*	*1.00*	*0.0523*	*0.440*	*0.0230*	*0.2*
2	*16:07*	*4.00*	*0.6*	*0.400*	*0.6*	*0.160*	*0.0259*	*1.00*	*0.0259*	*0.800*	*0.0207*	*0.2*
3	16:08	6.00	0.6	0.600	0.6	0.240	0.1707	1.00	0.1707	1.200	0.2048	1.9
4	16:11	8.00	0.6	0.840	0.6	0.336	0.3414	1.00	0.3414	1.680	0.5736	5.3
5	16:13	10.00	0.6	0.710	0.6	0.284	0.3124	1.00	0.3124	1.420	0.4436	4.1
6	16:15	12.00	0.6	0.600	0.6	0.240	0.4140	1.00	0.4140	1.200	0.4968	4.6
7	16:17	14.00	0.6	0.770	0.6	0.308	0.4517	1.00	0.4517	1.540	0.6956	6.4
8	16:19	16.00	0.6	0.830	0.6	0.332	0.4299	1.00	0.4299	1.660	0.7136	6.6
9	16:22	18.00	0.6	0.980	0.6	0.392	0.4583	1.00	0.4583	1.960	0.8983	8.3
10	16:24	20.00	0.6	0.880	0.6	0.352	0.4733	1.00	0.4733	1.760	0.8330	7.7
11	*16:26*	*22.00*	*0.6*	*0.860*	*0.6*	*0.344*	*0.4724*	*1.00*	*0.4724*	*1.720*	*0.8125*	*7.5*
12	16:30	24.00	0.6	0.800	0.6	0.320	0.5373	1.00	0.5373	1.600	0.8597	7.9
13	16:31	26.00	0.6	0.820	0.6	0.328	0.4909	1.00	0.4909	1.640	0.8051	7.4
14	*16:34*	*28.00*	*0.6*	*0.900*	*0.6*	*0.360*	*0.3295*	*1.00*	*0.3295*	*1.800*	*0.5931*	*5.5*
15	16:36	30.00	0.6	0.780	0.6	0.312	0.4569	1.00	0.4569	1.560	0.7128	6.6
16	16:38	32.00	0.6	0.880	0.6	0.352	0.3291	1.00	0.3291	1.760	0.5792	5.3
17	*16:41*	*34.00*	*0.6*	*0.710*	*0.6*	*0.284*	*0.2915*	*1.00*	*0.2915*	*1.420*	*0.4139*	*3.8*
18	16:43	36.00	0.6	0.600	0.6	0.240	0.3211	1.00	0.3211	1.200	0.3853	3.5
19	16:44	38.00	0.6	0.580	0.6	0.232	0.1679	1.00	0.1679	1.160	0.1948	1.8
20	16:45	40.00	0.6	0.500	0.6	0.200	0.3764	1.00	0.3764	1.000	0.3764	3.5
21	16:47	42.00	0.6	0.380	0.6	0.152	0.2844	1.00	0.2844	0.760	0.2161	2.0
22	*16:48*	*44.00*	*0.6*	*0.200*	*0.6*	*0.080*	*0.0390*	*1.00*	*0.0390*	*0.400*	*0.0156*	*0.1*
23	16:48	46.00	None	0.000	0.0	0.0	0.0000	1.00	0.0000	0.000	0.0000	0.0

Rows in italics indicate a QC warning. See the Quality Control page of this report for more information.

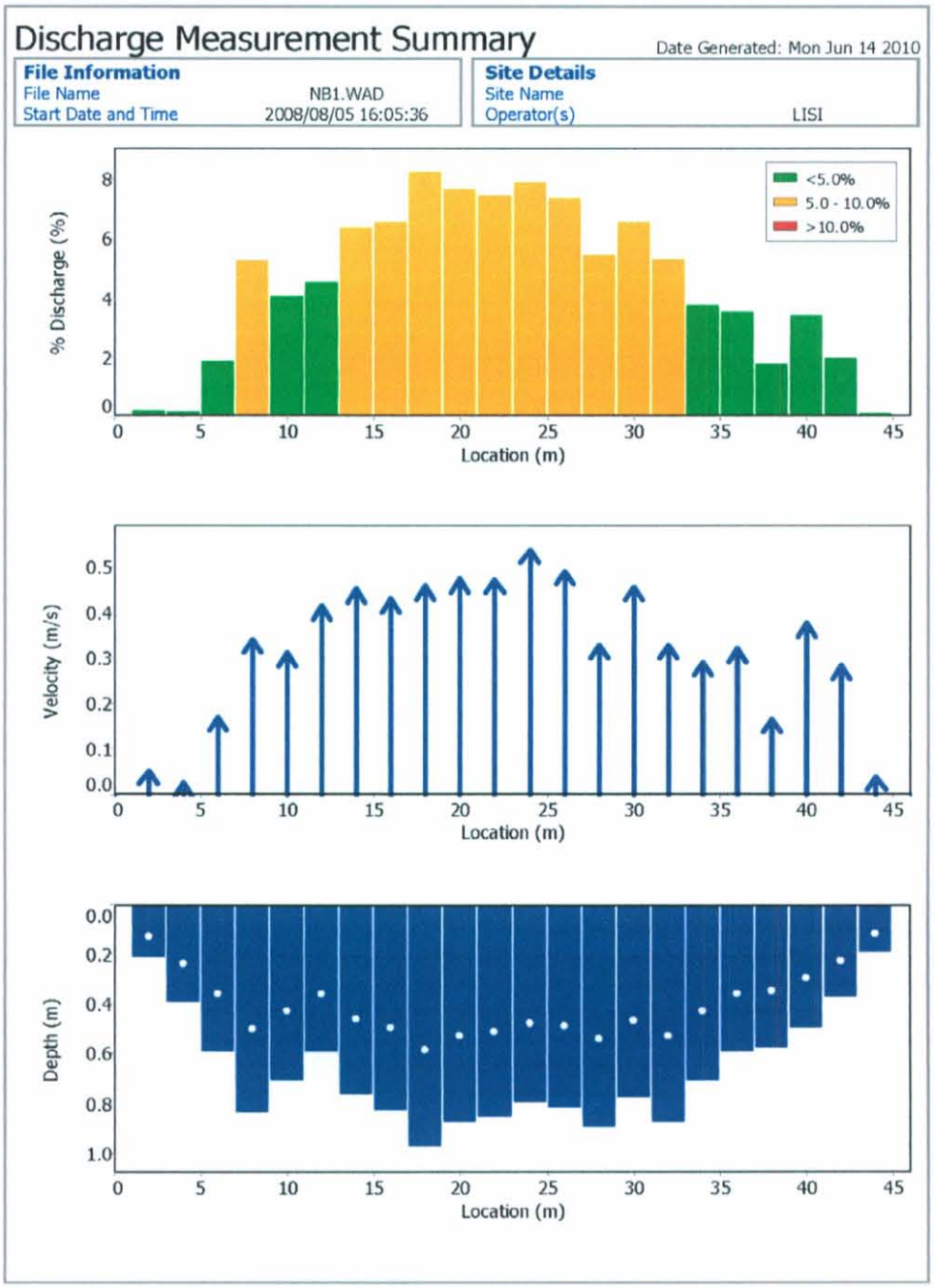

Fig. 14 Water discharge and velocity measurements and depth profile of Nakvak Brook

Results from measurements with the Acoustic Doppler Velocimeter provide a depth profile of the river, as well as stream velocity measurements and discharge measurements along the profile. The results for McCornick River show that the river is about 20 m wide close to the river mouth (Table 3 and Figure 13). Stream velocities range between 0.1 m/s at the outer edges and up to 0.8 m/s at the deepest point of the profile. Total water discharge is around 4 m^3/s. Nakvak Brook is 45 m wide close to the river mouth with stream velocities ranging from 0.03 m/s at the outer edges to 0.54 m/s in the middle of the profile (Table 4 and Figure 14). Total water discharge is 11 m^3/s.

5. Discussion

The sediment accumulation rates compare well with findings in other fjords, such as Effingham Inlet (Vancouver Island, Canada): 0.25cm/y (Dallimore and Jmieff, 2010) and Ameralik Fjord (SW Greenland): 0.2 cm/y (Møller et al., 2006). Fjords such as Inner Barsnesfjord (western Norway): 0.85 cm/y (Paetzel et al., 2010) and Maxwell Bay (West Antarctica): 0.74 cm/y (Hass et al., 2010) show higher sedimentation rates, while fjords such as Nordåsvannet fjord (western Norway): 0.04 cm/y (Paetzel et al., 1994) show lower sedimentation rates. The sediment texture (mainly homogenous with evidence of bioturbation), as well as the fine grain size, and the occurrence of ice rafted debris compare well with sedimentary studies in other fjords. For instance, the sediments of Ameralik Fjord, SW Greenland (Møller et al., 2006 and Seidenkrantz et al., 2007), as well as Maxwell Bay, Antarctica (Hass et al., 2010), and fjords on the mainland of British Columbia, Canada (Dallimore and Jmieff, 2010) contain about 70% fine grained sediment (silt to clay), that is mainly homogenous and with traces of bioturbation. The main difference with other fjord sediments lies not in the grain size but rather in the preservation of physical structures. In fjords where water exchange is restricted and bottom waters are anoxic or dysoxic, sediments often preserve physical structures and annual laminations. This is the case in fjords on Vancouver Island (Dallimore and Jmieff, 2010) and in parts of the sediment cores from Icy Bay, Alaska (Jaeger et al., 1999), as opposed to the homogenized sediments in Nachvak and Saglek Fjord that have been deposited under oxic conditions.

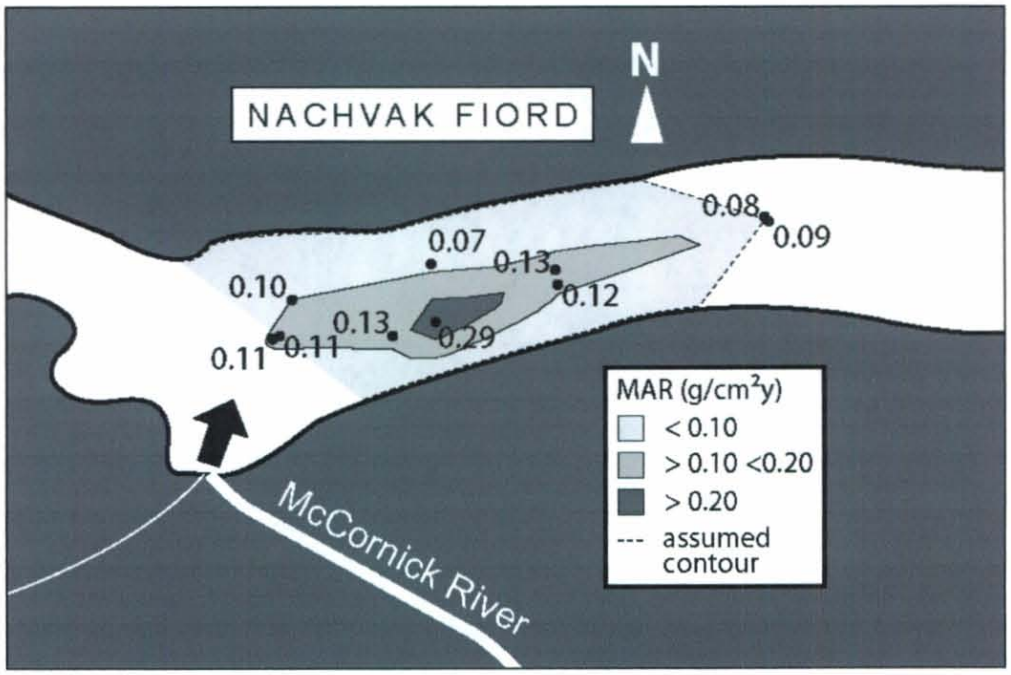

Fig. 15 Sediment budget map in Nachvak fjord using MAR values to show the dispersal of sediment in the marine basin. MAR values are divided in three regions and reflect a depositional centre where sediment accumulation is highest.

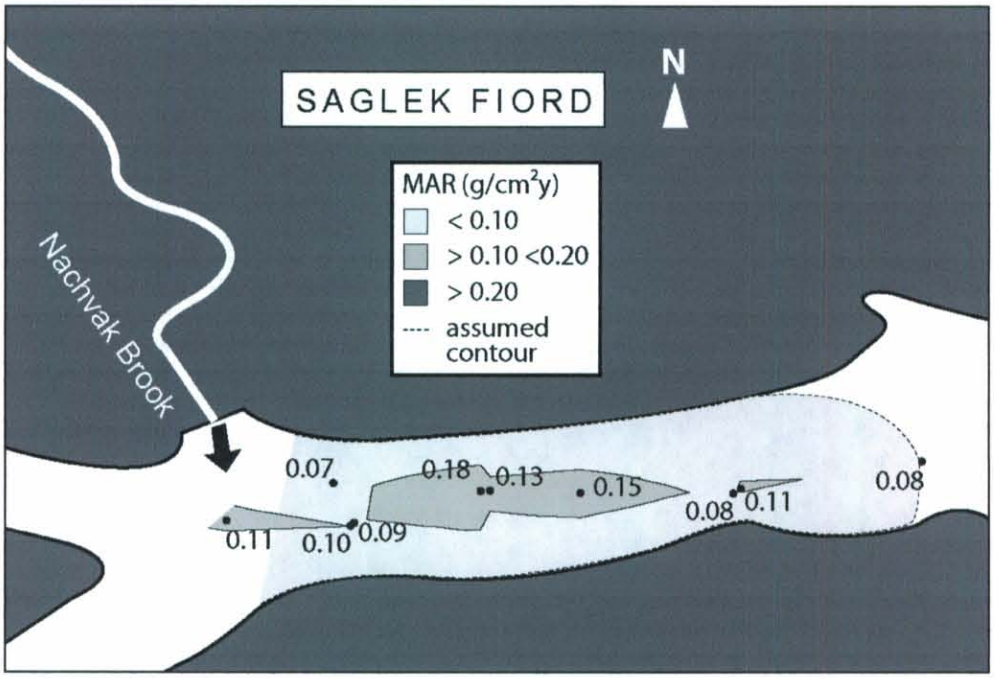

Fig. 16 Sediment budget map in Saglek fjord using MAR values to show the dispersal of sediment in the marine basin. MAR values are divided in three regions and reflect one major depositional centre in the centre of the basin where sediment accumulation is highest.

In order to map the sediment dispersal within the marine basin, mass accumulation rates (MAR) were calculated based on SARs, average core porosity (Φ), and sediment density (ρ_s) assumed to be 2.65 g cm^{-3} (Muhammad et al. 2008):

$$MAR = (1-\Phi)\,\rho_s\,SAR \qquad \text{Eq. 11}$$

MAR values have been divided into three regions and contours have been drawn by extrapolating between the values at each core location and assuming the MAR values at the fjord edges to be 0 (Fig. 15 and 16). In both fjords the sediment is accumulating in depositional centres in the centre of the basin. No obvious relationship between these

depositional centres and bathymetry is evident. In Nachvak Fjord there is one distinct depositional centre with a MAR value as high as 0.29 g/cm^2y (Fig. 15 and Table 5). Whereas, in Saglek Fjord there is one larger depositional centre with MAR values as high as 0.18 g/cm^2y and two smaller regions with MAR values greater than 0.1 g/cm^2y to each side (landward and seaward) (Fig. 16 and Table 5).

Sedimentary processes in fjords often experience down-fjord gradients (Jaeger et al., 1999), which is also the case with the grain-size distribution in Nachvak and Saglek fjords. Generally, the mean sediment grain sizes are coarser close to the river mouth in both fjords; however there is neither a relationship with bathymetry nor with MAR values. Other studies show that a down-fjord trend in the dispersal of sediment is not necessarily true for every fjord, as is the case in Nachvak and Saglek Fjord, where the sediment is focused into depositional centres as opposed to decreasing gradually down-fjord. This compares well with findings by Yoon et al. (1998), who show that the horizontal distribution of suspended sediment in Maxwell Bay (Antarctica) does not show any systematic down-fjord decrease in concentration as might be expected if the dominant source of sediment discharge is at the fjord head. This might suggest that in these areas down-fjord gradients, such as salinity, and related processes, such as flocculation, might not be significantly pronounced.

Table 5: *Results from laboratory analyses and radioisotope geochronology for Nachvak and Saglek Fjord*

Radiochemistry Results - Overview

Nachvak Fjord

Core name	BC1	BC2	BC3	BC4	BC5	BC N1	BC N2	BC N3	BC N4	BC N5
SAR (210-Pb) (cm/y)	0.17	0.16	0.52	0.26	0.18	0.15	0.19	0.19	0.16	0.12
Average Porosity	0.75	0.76	0.79	0.81	0.81	0.8	0.76	0.75	0.75	0.78
MAR (g/cm^2y)	0.11	0.10	0.29	0.13	0.09	0.08	0.12	0.13	0.11	0.07
Average Grainsize (microns)	18.73		16.73	15.19	15.38	16.02	15.27	16.82	18.86	15.75

Saglek Fjord

Core name	BC7a	BC10	BC11	BC12	BC13	BC S1	BC S2	BC S3	BC S4	BC S5
SAR (210-Pb) (cm/y)	0.24	0.08	0.22	0.36	0.27	0.28	0.25	0.33	0.32	0.22
Average Porosity	0.83	0.66	0.83	0.81	0.89	0.89	0.83	0.83	0.85	0.84
MAR (g/cm^2y)	0.11	0.07	0.10	0.18	0.08	0.08	0.11	0.15	0.13	0.09
Average Grainsize (microns)	18.16	22.05	13.01	12.39	14.85	14.58	12.71	15.15	15.96	16.34

In order to put the values of sediment dispersal in a broader spatial and temporal context, a sediment budget was created. This becomes a quantitative statement of the relations between sediment production, transport, storage and permanent burial for a sediment dispersal system (Sommerfield et al., 2007). To do this, the main source and sink terms have to be identified. For quantifying the source term, estimates for the fluvial sediment loads entering the marine basins were generated from Equation 4 (Table 6). In Nachvak Fjord, and in addition to the primary drainage basin of McCornick River (Fig. 2), 14 smaller drainage basins have been taken into consideration (Fig. 2). Maximum relief and area of the drainage basin have been determined by using a digital elevation model in ArcGIS. The drainage basins vary in size from 1.1 km^2 (drainage basin G) to 77

km^2 (drainage basin A), and in maximum relief from 592 m (drainage basins K and N) to 1408 m (drainage basin E) (Fig. 2). For drainage basin A and B, a glacier erosion factor (I) has to be considered as defined by Equation 6. Overall, results for Equation 4 suggest that a long term sediment load of approximately 7,800 t/y is entering the marine basin of Nachvak Fjord (Table 6). In Saglek Fjord eight drainage basins have been taken into consideration as sources for sediment delivered to the marine basin of Saglek Fjord, including the major drainage basin of Nakvak Brook (Fig. 3). Drainage basin areas range from 1.82 km^2 (drainage basin F) to 809 km^2 (drainage basin A), and maximum relief ranges from 865 m (drainage basin C) to 1370 m (drainage basin A). Because there are no glaciers present in the river catchments draining into Saglek Fjord, the glacier erosion factor I is considered to be 1. Overall, Equation 4 model results for Saglek Fjord suggest that a long term sediment load of approximately 19,800 t/y is entering the marine basin of Saglek Fjord (Table 6).

Table 6: *Estimates for supplied and deposited sediment load in Nachvak and Saglek fjords.*

Modeled Sediment Load (supplied by rivers)

based on: BQART model (Syvitski&Milliman 2007)

$$Q_s = 2\,\omega\,B\,Q^{0.31}\,A^{0.5}\,R$$

ω	0.02			L	0.50	average basin-wide lithology factor
A		basin area (km^2)		$(1-T_E)$	0.80	trapping efficiency of lakes and man-made reservoirs
R		maximum relief from sea level to mountain-top (km)		E_h	1.00	human-influenced soil erosion factor
$Q = 0.075 * A^{0.8}$		freshwater discharge (km^3/y)		$I = (1 + 0.09A_g)$		glacier erosion factor
$B = I\,L\,(1-T_E)E_h$		accounts for geological and human factors		A_g		surface area of glaciers as a percentage of the drainage basin area

Nachvak Fjord

Drainage Basin	A (km^2)	R(km)	Q (km^3/y)	A_g	I	B	Q_s (kg/s)
A	76.9500	1.4070	0.0764	2.4548	1.2209	0.4884	0.1086
B	18.7600	1.3050	0.0247	10.1386	1.9125	0.7650	0.0549
C	2.2500	0.7200	0.0045	0.0000	1.0000	0.4000	0.0032
D	11.1100	1.0170	0.0162	0.0000	1.0000	0.4000	0.0151
E	18.7500	1.4080	0.0247	0.0000	1.0000	0.4000	0.0310
F	2.3800	0.8540	0.0047	0.0000	1.0000	0.4000	0.0040
G	1.1000	0.8710	0.0026	0.0000	1.0000	0.4000	0.0023
H	1.5600	0.7660	0.0034	0.0000	1.0000	0.4000	0.0026
I	4.1000	0.9720	0.0073	0.0000	1.0000	0.4000	0.0069
J	1.2800	0.8420	0.0029	0.0000	1.0000	0.4000	0.0025
K	0.5900	0.5920	0.0016	0.0000	1.0000	0.4000	0.0010
L	1.6100	0.9270	0.0035	0.0000	1.0000	0.4000	0.0032
M	1.9400	0.8350	0.0040	0.0000	1.0000	0.4000	0.0034
N	1.2000	0.5920	0.0027	0.0000	1.0000	0.4000	0.0017
O	4.1600	0.9600	0.0074	0.0000	1.0000	0.4000	0.0068
A_{total} (km^2)	147.74						0.2472
Q_s total (kg/s)							
Q_s total (t/y)							**7796.23**

Saglek Fjord

Drainage Basin	A (km^2)	R(km)	Q (km^3/y)	A_g	I	B	Q_s (kg/s)
A	809.3900	1.3700	0.5016	0.0000	1.0000	0.4000	0.5035
B	52.4600	1.2330	0.0562	0.0000	1.0000	0.4000	0.0585
C	6.8500	0.8650	0.0110	0.0000	1.0000	0.4000	0.0090
D	7.6300	1.1590	0.0120	0.0000	1.0000	0.4000	0.0130
E	8.5800	1.1290	0.0132	0.0000	1.0000	0.4000	0.0138
F	1.8200	1.0410	0.0038	0.0000	1.0000	0.4000	0.0040
G	3.9800	1.1220	0.0071	0.0000	1.0000	0.4000	0.0077
H	14.0000	1.0580	0.0195	0.0000	1.0000	0.4000	0.0187
A_{total} (km^2)	904.71						
Q_s total (kg/s)							0.6283
Q_s total (t/y)							**19814.72**

Deposited Sediment Load Estimates		**Deposited Sediment Load as Percentage of Modeled Sediment Load**
based on measurements of sediment mass accumulation rates (burial flux method; Nittrouer, 1978): $M_f = MAR * A$		
Average MAR (t/km^2y)	1200.00	
Area of marine Basin (km^2)	32.40	
M_f (t/y)	**38880.00**	**499**

Sediment yield
$= M_f / A_{total}$
263
(t/km^2y)

Deposited Sediment Load Estimates		**Deposited Sediment Load as Percentage of Modeled Sediment Load**
based on measurements of sediment mass accumulation rates (burial flux method; Nittrouer, 1978): $M_f = MAR * A$		
Average MAR (t/km^2y)	1100.00	
Area of marine Basin (km^2)	39.06	
M_f (t/y)	**42966.00**	**217**

Sediment yield
$= M_f / A_{total}$
47
(t/km^2y)

The sink term for the sediment budget was quantified using the burial flux method by Nittrouer (1978), which is based on MAR and the dispersal over a certain area:

$$M_f = MAR \times A \qquad \text{Eq. 12}$$

where MAR is the average mass accumulation rate for the marine basin, and A is the area of the marine basin. Average MAR values were determined by averaging over MAR values for all box cores in the relevant basin from Table 5. The area of the marine basin is estimated by measuring the dimensions (width and length) of the basin restricted by the coastline in ArcGIS. The average MAR for Nachvak Fjord of 1200 t/km^{2}y and an area of 32 km^2 yield a sediment load of approximately 39,000 t/y that is being deposited in Nachvak Fjord (Table 6). In Saglek Fjord, the average MAR of 1100 t/km^{2}y and an area of 39 km^2 yield a sediment load of approximately 43,000 t/y that is being deposited in Saglek Fjord (Table 6).

Comparing source and sink terms gives information about sediment transport processes. Comparing the modeled sediment load of 7,800 t/y delivered by rivers with the deposited sediment load of 39,000 t/y in Nachvak Fjord shows disagreement between modeled and measured flux (Table 6). In Saglek Fjord a sediment load of 19,800 t/y is modeled to be delivered by rivers and 43,000 t/y of sediment are being deposited, implying that 220% of the modeled sediment is being deposited in the studied marine basin of Saglek Fjord (Table 6). Because the model is accurate within a factor of two, the result for Saglek Fjord suggests that the sediment delivered by rivers is entirely trapped in the marine basin of Saglek Fjord and only minor additional sediment sources may exist.

The results for Nachvak Fjord are beyond the accuracy threshold of the model and may have two implications: a) the catchments of the rivers draining into Nachvak Fjord have a much higher sediment yield than suggested by the model (263 t/km^{2}y in Nachvak Fjord as opposed to sediment yield in Saglek Fjord of 47 t/km^{2}y; Table 6), and/or b) there are major sediment sources additional to the fluvial sediment supply in Nachvak fjord. During fieldwork the presence of glaciomarine terraces has been observed, particularly near the mouth of McCornick River. It is most likely that the river is cutting into these terraces, and is eroding and thus carrying a higher amount of sand and mud than predicted by the model. Moreover, in comparison to the marine basin of Saglek Fjord, which is very well protected from oceanic influences by a relatively shallow sill, the marine basin of Nachvak Fjord lacks any distinct separation from the basin seaward of the basin studied in this paper. This allows for the possibility of sediment transport from the ocean, especially during storm events, and due to tidal exchange. This, however, is contradicted by the relatively high measured sediment yield to Nachvak Fjord, with respect to measured sediment deposition.

Milliman and Syvitski (1992) discuss factors controlling fluvial sediment discharge and emphasize the importance of drainage basin size and topography. Based on sediment load and sediment yield data for 280 rivers they created a baseline for the variations of sediment yield with basin area for seven topographic categories of river basins (high mountain; mountain Asia-Oceania; mountain N/S America, Africa, alpine Europe; mountain non-alpine Europe, high Arctic; upland; lowland; coastal plain). Generally, the greater the drainage basin area the lower is the sediment yield. This is

consistent with our results for McCornick River (sediment yield: 263 t/km^{2}y, drainage basin area: 150 km^2) and Nakvak Brook (sediment yield: 47 t/km^{2}y, drainage basin area: 905 km^2). However, the measured sediment yields for these two rivers are lower than the sediment yields that would be predicted from the baseline after Milliman and Syvitski (1992) for upland rivers (~4000 t/km^{2}y for Nachvak Fjord and ~850 t/km^{2}y for Saglek Fjord).

Comparison of modern sediment accumulation and postglacial sediment thickness

The relationship between modern SARs and postglacial sedimentation can be discussed by comparing SARs to the thickness of the postglacial marine sediment determined in sub-bottom profiles (Fig. 9 and 10). Assuming that sediment accumulation was on average constant during the Holocene with sedimentation rates comparable to modern SARs, one can estimate the thickness of Holocene sediment and compare it with the actual thickness in the profiles. It has to be taken into account that sediments have been compacted during the Holocene. A compaction ratio can be calculated using the following equation:

$$\text{compaction ratio} = (V_{w2}+V_s)/(V_{w1}+V_s) \qquad \text{Eq. 13}$$

where V_s is the volume of sediment, which is assumed to stay constant during compaction, V_{w1} is the volume of water before compaction, and V_{w2} is the volume of water after compaction. In order to determine V_{w2} we used a porosity of postglacial sediment of 0.7 in Nachvak Fjord and 0.79 in Saglek Fjord, derived from long cores taken in the area. We used the following equation:

$$V_{w2} = \frac{\emptyset_{Holocene} * V_s}{1-\emptyset_{Holocene}} \qquad \text{Eq. 14}$$

After applying these equations we were able to estimate the thickness of postglacial sediment by multiplying SARs with the calculated compaction ratio and the time since onset of postglacial sedimentation (8,000 y BP, Clark et al., 1989). Clark et al. (1989) studied a sediment core from Square Lake, which lies within the Nakvak Brook

watershed in the southern Torngat Mountains. They identified a lower unit containing normally graded, distinct couplets, generally uniform laminae thicknesses, and low organic contents, which has been interpreted as classical glacial varves by Ashley (1975), Smith (1978) and Leonard (1986) (cited in: Clark et al., 1989). Moreover, the low pollen concentration, the large number of reworked pollen grains, the low percentage of organic matter, and the absence of diatoms also indicate the presence of nearby ice (Clark et al., 1989). A transition zone from the lower glacial unit to the overlying unit suggests a significant environmental transition, indicated by the rise of pollen concentrations and the first appearance of diatoms. A radiocarbon date of 7950 $\pm$ 100 years BP at the base of the unit overlying the glacial unit provides a minimum age for deglaciation of ca. 8000 years BP (Clark et al. 1989). Josenhans and Zevenhuizen (1989) provide radiocarbon ages from in situ shells in marine sediments, which also suggest an age of 8000 years BP at the base of the postglacial sequence on top of underlying glaciomarine sediments (cited in Clark and Josenhans, 1990).

The average estimated thickness of postglacial sediment in Nachvak Fjord is 12.3 meters and the observed average thickness from sub-bottom profiles is 11.5 meters (Table 7). These values compare well and suggest that average postglacial sedimentation in Nachvak Fjord has been constant or slightly increasing. In Saglek Fjord the average estimated thickness of Holocene sediment is 15.9 meters and the actual thickness seen in sub-bottom profiles is 9.9 meters (Table 7). This suggests that postglacial sedimentation was on average 40 % less than recent sediment accumulation and has been increasing since the onset of postglacial sedimentation. This compares well with other fjord studies.

For example, Paetzel et al. (2010) found a maximum sediment thickness of 100 meters in Inner Barsnesfjord (western Norway), which is 10 times thicker than in Nachvak and Saglek Fjord, but compares well with high sediment accumulation rates of 0.85 cm/y in Inner Barsnesfjord.

Table 7: Estimates for postglacial sediment thickness based on SAR from boxcores

Estimates for postglacial sediment thickness

Nachvak Fiord

Core name	**BC1**	**BC2**	**BC3**	**BC4**	**BC5**	**BC N1**	**BC N2**	**BC N3**	**BC N4**	**BC N5**
SAR (cm/y)	0.17	0.16	0.52	0.26	0.18	0.15	0.19	0.19	0.16	0.12
Porosity	0.75	0.76	0.79	0.81	0.81	0.80	0.76	0.75	0.75	0.78
Vs	0.25	0.24	0.21	0.19	0.19	0.20	0.24	0.25	0.25	0.22
Vw1	0.75	0.76	0.79	0.81	0.81	0.80	0.76	0.75	0.75	0.78
Vw2	0.58	0.56	0.49	0.44	0.44	0.47	0.56	0.58	0.58	0.51
compaction ratio	0.83	0.80	0.70	0.63	0.63	0.67	0.80	0.83	0.83	0.73
estimated Holocene sediment thickness (m)	11.33	10.24	29.12	13.17	9.12	8.00	12.16	12.67	10.67	7.04
Basinwide average estimated postglacial sediment thickness (m)										**12.4**
Average postglacial sediment thickness from sub-bottom profile (m)										**11.5**

Saglek Fiord

Core name	**BC7**	**BC10**	**BC11**	**BC12**	**BC13**	**BC S1**	**BC S2**	**BC S3**	**BC S4**	**BC S5**
SAR (cm/y)	0.24	0.08	0.22	0.36	0.27	0.28	0.25	0.33	0.32	0.22
Porosity	0.83	0.66	0.83	0.81	0.89	0.89	0.83	0.83	0.85	0.84
Vs	0.17	0.34	0.17	0.19	0.11	0.11	0.17	0.17	0.15	0.16
Vw1	0.83	0.66	0.83	0.81	0.89	0.89	0.83	0.83	0.85	0.84
Vw2	0.64	1.28	0.64	0.71	0.41	0.41	0.64	0.64	0.56	0.60
compaction ratio	0.81	1.62	0.81	0.90	0.52	0.52	0.81	0.81	0.71	0.76
estimated Holocene sediment thickness (m)	15.54	10.36	14.25	26.06	11.31	11.73	16.19	21.37	18.29	13.41
Basinwide average estimated postglacial sediment thickness (m)										**15.9**
Average postglacial sediment thickness from sub-bottom profile (m)										**9.9**

^{210}Pb Flux

To discuss the flux of ^{210}Pb in the sediment and the atmospheric source of ^{210}Pb the ratio between the core-calculated flux (F) (required to support the sediment inventory) and the atmospheric flux estimated from soil core 2C (T) (Tables 1 and 2) was calculated according to an equation proposed by Muhammad et al. (2008):

$$R = F/T \qquad \text{Eq.15}$$

If R is 1, an equal amount of ^{210}Pb produced in the atmosphere is deposited in the sediment. A value of R greater than 1 suggests focusing and/or lateral import of ^{210}Pb and a value of R smaller than 1 suggests lateral export of ^{210}Pb. For both Nachvak and Saglek Fjord the values of R are around 1, with mean values of 0.82 and 0.93 (Tables 1 and 2), respectively. This suggests that the amount of ^{210}Pb deposited in the marine sediments of Nachvak and Saglek Fjord is close to the amount of ^{210}Pb supplied from the atmosphere. This implies that the scavenging rate of the sedimentary particles deposited in the marine basins in these areas is efficient enough to support an approximate equilibrium between the atmospheric supply of ^{210}Pb and its uptake and deposition in the marine sediments of Nachvak and Saglek fjords. This compares well with the findings above that have demonstrated that the marine basins examined in this paper are efficient sediment traps.

6. Conclusions

Radiochemical analyses of soft sediment samples have given some insight into the dispersal of sediment within Nachvak and Saglek fjords. The sediments are generally mottled and consist of silt and clay. Sediment accumulation rates are 0.12 – 0.52 cm/y in Nachvak Fjord and 0.08 – 0.36 cm/y in Saglek Fjord with temporal resolutions ranging from 15 – 68 years in Nachvak Fjord and 12 – 49 years in Saglek Fjord. Mass accumulation rate values suggest that the majority of the sediment is accumulating in the centre of the basins. Comparing the sediment load deposited in the basin and the modeled sediment load supplied to the basin by rivers shows that 500 % and 220 % of the modeled sediment load is accumulating in the marine basin of Nachvak and Saglek Fjord, respectively. This implies that both marine basins are excellent natural sediment traps, as hypothesized, and that in Nachvak Fjord sediment sources additional to rivers exist and/or that the river catchments draining into Nachvak Fjord have a much higher sediment yield as compared to Saglek Fjord. Recent sediment accumulation rates in Nachvak Fjord compare well with postglacial sediment thickness observed in sub-bottom profiles, suggesting that postglacial sedimentation was on average constant. In Saglek Fjord recent sediment accumulation rates are higher than average postglacial sedimentation, which implies that average sediment accumulation has been increasing after onset of postglacial sedimentation. Values for ^{210}Pb inventories measured in the marine sediments support an approximate equilibrium between the atmospheric supply of ^{210}Pb and its uptake and deposition in the marine basins of Nachvak and Saglek fjords, which is consistent with the finding that these basins are excellent natural sediment traps.

REFERENCES

Appleby, P.G., Oldfield, F., 1992. Application of lead-210 to sedimentationstudies. In: Ivanovich, M., Harmon, R.S. (Eds.), Uranium-series Disequilibrium: Application to Earth, Marine and Environmental Sciences. Clarendon Press, Oxford, pp. 731–738.

ArcticNet Projects, Phase II (2008-2011), (2008). Understanding and Responding to the Effects of Climate Change and Modernization in Nunatsiavut. Retrieved October 8, 2008, from ArcticNet Web site: http://www.arcticnet.ulaval.ca/index.php?fa=ResearchHome.showThemeProjects&theme=14&project_id=58

ArcticNet home page. Retrieved December 17, 2010, from ArcticNet Web site: http://www.arcticnet.ulaval.ca/index.php

ArcticNet Rational (2008). Retrieved October 8, 2008, from ArcticNet Web site: http://www.arcticnet.ulaval.ca/index.php?fa=ArcticNet.aboutUs

Bell, T., Dellivers, R., Edinger, E., 2009. Application of multibeam sonar technology for benthic habitat mapping in Newfoundland and Labrador. Atlantic Geology, v. 45, p. 83-84.

Bentley, S.J., Nittrouer, C.A., 2003. Emplacement, modification, and preservation of event strata on a flood dominated continental shelf: Eel shelf, northern California. Continental Shelf Research v. 23, p. 1465-1493.

Bentley, S.J., Kahlmeyer, E., 2008. Marine records of sediment flux from glaciated and unglaciated catchments, Torngat Mountains, Canada. Arctic Change 2008, Conference Programme and Abstracts, p. 184-185.

Bøe, R., Rise, L., Blikra, L. H., Longva, O. and Eide, A., 2003. Holocene mass-movement processes in Trondheimsfjorden, Central Norway. Norwegian Journal of Geology, v. 83, p. 3–22.

Buesseler, K. O., Livingston, H.D., Sholkovitz, E.R., (1985). 239,240Pu and excess 210Pb inventories along the shelf and slope of the northeast U.S.A., Earth Planet. Sci. Lett., v. 76, p. 10–22.

Clark, P. U., Short, S. K., Williams, K. M., Andrews, J. T., 1989. Late Quaternary chronology and environments of Square Lake, Torngat Mountains, Labrador. Canadian Journal of Earth Sciences, v. 26, p. 2130 – 2144.

Clark, P.U., Josenhans, H.W., 1990. Reconstructed ice-flow patterns and ice limits using drift pebble lithology, outer Nachvak Fiord, northern Labrador: Discussion. Canadian Journal of Earth Sciences, v. 27, p. 1002-1006.

Clark, P.U., Brook, E.J., Raisbeck, G.M., Yiou, F. Clark, J., 2003. Cosmogenic ^{10}Be ages of the Saglek Moraines, Torngat Mountains, Labrador. Geological Society of America, Geology; v. 31; no. 7; p. 617-620

Cutshall, N.H., Larsen, I.L., Olsen, C.R., 1983. Direct analysis of 210Pb in sediment samples: Self absorption corrections: Nuclear Instruments and Methods. v. 206, p. 1-20.

Dallimore, A., Jmieff, D.G., 2010. Canadian west coast fjords and inlets of the NE Pacific Ocean as depositional archives. Geological Society, London, Special Publications, v. 344, p. 143-162.

Déry, S.J., Stieglitz, M., McKenna, E.C., Wood, E.F., 2005. Characteristics and Trends of River Discharge into Hudson, James, and Ungava Bays, 1964-2000. Journal of Climate, v. 18, p. 2540-2556.

Fawcett, P.J., Agustsdottir, A.M., Alley, R.B., Shuman, C.A., 1997. The Younger Dryas termination and North Atlantic Deep Water formation: Insights from climate model simulations and Greenland ice cores. Paleoceanography, v.12, p.23-38.

Forwick, M. and Vorren, T. O., 2002. Deglaciation History and Postglacial Sedimentation in Balsfjord (North Norway). Polar Research, v. 21, p. 259–266.

Government of Canada, Networks of Centres of Excellence of Canada. Retrieved December 17, 2010, from Web site: http://www.nce-rce.gc.ca/About-APropos/Governance-Gouvernance_eng.asp

Grützner, J. and Meinert, J., 1999. Lateral changes of mass accumulation rates derived from seismic reflection profiles: an example from the Western Atlantic. GeoRes. Forum, v. 5, p. 87–108.

Hall, F.R., Andrews, J.T., Jennings, A., Vilks, G., Moran, K., 1999. Late Quaternary sediments and chronology of the northeast Labrador Shelf (Karlsefni Trough, Saglek Bank): Links to glacial history. GSA Bulletin; v. 111; no. 11; p. 1700-1713.

Hass, H.C., Kuhn, G., Monien, P., Brumsack, H.-J., Forwick, M., 2010. Climate fluctuations during the past two millennia as recorded in sediments from Maxwell Bay, South Shetland Islands, West Antarctica. Geological Society, London, Special Publications, v. 344, p. 243-260.

HORIBA Partica LA-950, Laser Scattering Particle Size Distribution Analyzer, Instruction Manual, 2006.

Hostetler, S.W., Clark, P.U., Bartlein, P.J., Mix, A.C., Pisias, N.J., 1999. Atmospheric transmission of North Atlantic Heinrich events. Journal of Geophysical Research, v. 104, p. 3947-3952.

Howe, J. A., Austin, E. N., Forwick, M., Paetzel, M., Harland, R., Cage, A.G., 2010. Fjord systems and archives: a review. Geological Society, London, Special Publications 2010, v. 344, p. 5-15.

Jaeger, J.M., Nittrouer, C.A., 1999. Sediment Deposition in an Alaskan-Fjord: Controls on the Formation and Preservation of sedimentary structures in Icy Bay. Journal of Sedimentary Research, v. 69, no. 5, p. 1011-1026.

Kahlmeyer, E., Bentley, S. J., 2009. Comparison of the sedimentary record in three sub-arctic fjord systems in northern Labrador. BSc Thesis, Memorial University of Newfoundland, St. John's, NL, Canada, 79 pp.

Milliman, J.D., Syvitski, J.P.M., 1992. Geomorphic/Tectonic Control of Sediment Discharge to the Ocean: The Importance of Small Mountainous Rivers. The Journal of Geology, v. 100, p. 525-544.

Møller, H.S., Jensen, K.G., Kuijpers, A., Aagaard-Sørensen, S., Seidenkrantz, M.-S., Prins, M., Endler, R., Mikkelsen, N., 2006. Late-Holocene environment and climatic changes in Ameralik Fjord, southwest Greenland: evidence from the sedimentary record. The Holocene, v. 16, no. 5, p. 685-695.

Muhammad, Z., Bentley, S. J., Febo, L. A., Droxler, A. W., Dickens, G. R., Peteson, C., Opdyke, B. N., 2008. Excess ^{210}Pb inventories and fluxes along the continental slope and basins of the Gulf of Papua. Journal of Geophysical Research, v. 113.

National Climate Data and Information Archive. (2011). Climate Data Online. Retrieved February 7, 2011, from Environment Canada Web site: http://climate.weatheroffice.gc.ca/climate_normals/results_e.html

Natural Resources Canada. (2011). Geological Survey of Canada, Permafrost. Retrieved February 7, 2011, from Web site: http://gsc.nrcan.gc.ca/permafrost/wheredoes_e.php

Nittrouer, C.A., 1978. The process of detrital sediment accumulation in a continental shelf environment: example from the Washington shelf. Thesis, Univeristy of Washington, Seattle, WA, 243 pp.

Nittrouer, C.A., Sternberg, R.W., Carpenter, R., Bennett, J.T., 1979. The use of ^{210}Pb geochronology as a sedimentological tool: application to the Washington continental shelf. Marine Geology v. 31, p. 297-316.

Nittrouer, C.A., Sternberg, R.W., 1981. The formation of sedimentary strata in an allochthonous shelf environment: the Washington continental shelf. Marine Geology, v. 42, p. 201-232.

Nittrouer, C.A., DeMaster, D.J., McKee, B.A., Cutshall, N.H., Larsen, I.L., 1984. The effect of sediment mixing on ^{210}Pb accumulation rates for the Washington Continental shelf. Marine Geology v. 54, p. 201-221.

Paetzel, M., Schrader, H., Croudace, I., 1994. Sewage history in the anoxic sediments of the fjord Nordåsvannet, western Norway: (I) dating and trace-metal accumulation. The Holocene, v. 4, no. 3, p. 290-298.

Paetzel, M., Dale, T., 2010. Climate proxies for recent fjord sediments in the inner Sognefjord region, western Norway. Geological Society, London, Special Publications, v. 344, p. 271-288.

Reimer, K.J., Sheldon, T.A., Brown T.M., Luque, S.P., Biasutti-Brown, M., Burgess, N.M., 2008. Strengthening partnerships in Labrador: The true legacy of a local source of contamination in Nunatsiavut. Arctic Change 2008, Conference Programme and Abstracts, p. 298.

Relling, O. and Nordseth, K., 1979. Sedimentation of a river suspension into a fjord basin. Gaupnefjord in western Norway. Norsk geogr. Tidsskr., v. 33, p. 187–203.

Richerol, T., Pienitz, R., Rochon, A., 2007. Paleoceanographic studies of the impacts of natural and anthropogenic perturbations in three Labrador fjord ecosystems

(Nachvak, Saglek and Anaktalak): Preliminary results. ArcticNet 2007 Annual Scientific Meeting, p. 80-81.

Seidenkrantz, M.-S., Aagaard-Sørensen, S., Sulsbrück, H., Kuijpers, A., Jensen, K.G., Kunzendorf, H., 2007. Hydrography and climate of the last 4400 years in a SW Greenland fjord: implications for Labrador Sea palaeoceanography. The Holocene, v. 17, no. 3, p. 387-401.

Sommerfield, C. K., Ogston, A. S., Mullenbach, B. L., Drake, D.E., Alexander, C. R., Nittrouer, C. A., Borgeld, J. C., Wheatcroft, R. A., Leithold, E. L., 2007. Oceanic dispersal and accumulation of river sediment. Continental-Margin Sedimentation: Transport to Sequence. Blackwell Publishing.

SonTek/YSI FlowTracker Handheld ADV, Technical Manual, Firmware Version 3.7, Software Version 2.30, 2009.

Syvitski, J. P. M., Burrell, D. C. and Skei, J. M. 1987. Fjords – Processes and Products. Springer, New York.

Syvitski, J.P.M., Shaw, J., 1995. Sedimentology and Geomorphology of Fjords. Geomorphology and Sedimentology of Esutaries. Developments in Sedimentology v. 53, p. 113-178.

Syvitski, J.P.M, Lee, H.J., 1997. Postglacial sequence stratigraphy of Lake Melville, Labrador. Marine Geology v. 143, p. 55-79.

Syvitski, J.P.M, Peckham, S.D., Hilberman, R., Mulder, T., 2003. Predicting the terrestrial flux of sediment to the global ocean: a planetary perspective. Sedimentary Geology v. 162, p. 5-24.

Syvitski, J.P.M, Milliman, J.D., 2007. Geology, Geography, and Humans Battle for Dominance over the Delivery of Fluvial Sediment to the Coastal Ocean. The Journal of Geology, v. 115, p. 1–19.

Wardle, R. J. 1983. Nain-Churchill province cross section, Nachvak Fjord, northern Labrador. Government of Newfoundland and Labrador, Department of Mines and Energy, Report v. 83-1, p. 68-90.

Wheatcroft, R.A., Wiberg, P.L., Alexander, C.R., Bentley, S.J., Drake, D.E., Harris, C.K., Ogston, A.S., 2006. Post-depositional alteration and preservation of sedimentary strata. Continental Margin Sedimentation. Blackwell Publishing, p. 101-155.

Wilton, D.H.C., 1996. Metallogenic overview of the Nain Province, northern Labrador. CIM Bulletin, v. 89, p. 43-52.

Yoon, H.I., Park, B.-K., Domack, E.W., Kim, Y., 1998. Distribution and dispersal pattern of suspended particulate matter in Maxwell Bay and its tributary, Marian Cove, in the South Shetland Islands, West Antarctica. Marine Geology, v. 152, p. 261-275.

Chapter 3

Summary

As part of a baseline ecosystem study of the Torngat Mountains National Park, the objectives of this thesis were to map the dispersal of fluvial sediment in one major basin in Nachvak and in Saglek fjord, to study the mode of sediment delivery from land to ocean, and to acquire a temporal resolution for palaeoenvironmental marine records in this area.

Methods used to achieve the objectives included:

- Collection of soft-sediment samples (box cores) in the fjords, and subsequent analysis for X-radiography, grainsize, and radiochemical analysis (based on ^{210}Pb and ^{137}Cs) to date the sediment, estimate sediment accumulation rates and to study the mode of sediment deposition.
- Conducting and analyzing sub-bottom profiles and bathymetry data to estimate sediment thickness and extent.
- Measuring stream flow in summer by using a hand held accoustic doppler velocimeter, and stream stage by using a HOBO water level logger deployed in each stream (Nachvak Brook and McCornick River) for one year.
- Collection of soil cores near river banks by using a hand auger to determine the long-term average supply of the radioisotope ^{210}Pb to the land surface.

Results show:

- that sediment accumulation rates are on average 0.21 cm/y in Nachvak fjord and 0.26 cm/y in Saglek Fjord with temporal resolutions ranging from 15 – 68 years in Nachvak Fjord and 12 – 49 years in Saglek Fjord. The sediments are mottled and fine grained (mainly silt). Putting values for sedimentation rates in a spatial context suggests that the bulk of the fluvial sediment is accumulating in the centre of each marine basin.
- that postglacial strata deposited in the basins of Nachvak and Saglek fjords are a generally homogenous with a thickness of around 10 meters. Observations from sub-bottom profiles suggest that in Nachvak Fjord recent sediment accumulation compares well with postglacial sediment thickness; while in Saglek Fjord average sediment accumulation has been more rapid for the past ~100 years as compared to sedimentation averaged over post-glacial time.
- that water levels of McCornick River and Nakvak Brook peak in late August and in June/July; and McCornick River and Nakvak Brook discharge 4 m^3/s and 11 m^3/s, respectively, in the summer.

This thesis provides baseline data on sediment properties, sedimentation rates, possible sources for the sediments and marine depocentres in Nachvak and Saglek Fjord, and will be useful in studying changes in the marine ecosystem. Information on grainsize is important, because a high percentage of clay minerals increases the adsorptive capacity, resulting in sediments with large quantities of adsorbed nutrients, trace elements, or

pollutants. Information on freshwater and sediment discharge from land to the ocean is important, because changes in salinity or sediment supply (i. e. through changes in fresh water inflow) can disturb the regime to which the marine organisms are adapted. Moreover, information on marine sedimentary depocentres is important, because the high sediment trapping efficiency of silled basins also results in excellent pollution sinks.

This thesis will contribute to ongoing studies in the Torngat Mountains National Park. The results on sediment properties and sources will contribute to the benthic habitat mapping in the fjords, and help as a baseline for monitoring the marine ecological integrity in the fjords. Information on fluvial sediment delivery and its dispersal in the marine basin will help to assess where potentially hazardous material from land will accumulate. The dispersal of sediment and burial rate will contribute to studies on the dispersal and fate of PCBs buried in fjord basins.

This thesis can also be used as a baseline for future sedimentological studies in the fjords. These might include palaeoenvironmental studies using long cores. Bathymetry, sub-bottom profiles, information on recent sediment accumulation and dispersal presented in this thesis can be helpful in choosing adequate coring locations and as a reference point for recent sedimentological conditions in comparison with palaeoenvironmental findings.

Appendix A

Radiochemistry Data for Box cores 2008

Explanation

Appendix A contains the extended results of $^{210}Pb_{xs}$ and ^{137}Cs analyses performed on box cores collected in 2008 from Saglek and Nachvak Fjord, northern Labrador. The tables list the activities of $^{210}Pb_{total}$ (dpm/g), $^{210}Pb_{excess}$ (dpm/g), and ^{137}Cs (dpm/g) and associated errors for each depth interval. Total ^{210}Pb was determined by measurement of the 46.5 keV gamma peak. Supported ^{210}Pb (from decay of ^{226}Ra within the seabed) was determined by measurement of the granddaughters of ^{226}Ra: ^{214}Pb (295 and 352 keV) and ^{214}Bi (609 keV). The unsupported ^{210}Pb (excess ^{210}Pb) was determined by subtracting the supported ^{210}Pb from the total ^{210}Pb. ^{137}Cs activities were determined by measuring the 662 keV peak directly.

Radiochemistry Data

Core name: WH0808 BC1

Depth (cm)	$^{210}Pb_{total}$ Activity (dpm/g)	$^{210}Pb_{excess}$ Activity (dpm/g)	$^{210}Pb_{excess}$ Error (dpm/g)	^{137}Cs Activity (dpm/g)	^{137}Cs Error (dpm/g)
0.5	6.88	5.84	0.31	0.41	0.07
1.5	6.76	5.86	0.30	0.55	0.06
2.5	6.76	5.80	0.28	0.56	0.06
3.5	6.42	5.54	0.26	0.48	0.06
4.5	6.40	5.62	0.29	0.49	0.06
5.5	5.50	4.69	0.32	0.38	0.07
6.5	5.17	4.46	0.27	0.40	0.06
7.5	3.94	3.12	0.26	0.52	0.06
8.5	3.19	2.47	0.25	0.42	0.07
9.5	3.35	2.67	0.25	0.39	0.06

Radiochemistry Data

Core name: WH0808 BC2

Depth (cm)	$^{210}Pb_{total}$ Activity (dpm/g)	$^{210}Pb_{excess}$ Activity (dpm/g)	$^{210}Pb_{excess}$ Error (dpm/g)	^{137}Cs Activity (dpm/g)	^{137}Cs Error (dpm/g)
0.5	6.43	5.64	0.30	0.36	0.06
1.5	6.02	5.23	0.31	0.42	0.06
2.5	6.07	5.08	0.32	0.41	0.07
3.5	6.02	5.21	0.29	0.36	0.06
4.5	6.12	5.16	0.30	0.48	0.07
5.5	5.27	4.50	0.29	0.41	0.06
6.5	5.79	5.01	0.33	0.28	0.07
7.5	5.34	4.63	0.29	0.44	0.06
8.5	4.33	3.60	0.27	0.43	0.07
9.5	3.53	2.87	0.25	0.50	0.06
11.0	2.52	1.75	0.21	0.31	0.06
13.0	1.80	0.95	0.15	0.00	0.00
15.0	2.57	1.79	0.21	0.00	0.00

Radiochemistry Data

Core name: WH0808 BC3

Depth (cm)	$^{210}Pb_{total}$ Activity (dpm/g)	$^{210}Pb_{excess}$ Activity (dpm/g)	$^{210}Pb_{excess}$ Error (dpm/g)	^{137}Cs Activity (dpm/g)	^{137}Cs Error (dpm/g)
0.5	6.98	6.05	0.34	0.59	0.07
1.5	6.99	6.11	0.32	0.49	0.07
2.5	5.93	5.00	0.32	0.47	0.07
3.5	6.20	5.18	0.30	0.58	0.07
4.5	6.51	5.37	0.30	0.38	0.07
5.5	5.52	4.71	0.30	0.42	0.07
6.5	5.68	4.84	0.28	0.68	0.06
7.5	4.68	3.70	0.26	0.51	0.06
8.5	5.05	4.17	0.26	0.47	0.06
9.5	4.80	4.09	0.28	0.61	0.06
11.0	3.23	2.59	0.24	0.34	0.05
13.0	3.62	2.92	0.25	0.30	0.06

Radiochemistry Data

Core name: WH0808 BC4

Depth (cm)	$^{210}Pb_{total}$ Activity (dpm/g)	$^{210}Pb_{excess}$ Activity (dpm/g)	$^{210}Pb_{excess}$ Error (dpm/g)	^{137}Cs Activity (dpm/g)	^{137}Cs Error (dpm/g)
0.5	7.45	6.60	0.35	0.53	0.08
1.5	7.76	6.92	0.35	0.53	0.07
2.5	7.26	6.22	0.32	0.57	0.07
3.5	8.06	6.97	0.33	0.61	0.07
4.5	7.40	6.38	0.32	0.70	0.07
5.5	7.03	6.15	0.32	0.63	0.07
6.5	6.60	5.65	0.31	0.62	0.07
7.5	5.93	4.96	0.28	0.65	0.07
8.5	5.43	4.58	0.27	0.61	0.07
9.5	4.77	3.90	0.28	0.55	0.07
11.0	3.26	2.40	0.22	0.39	0.05

Radiochemistry Data

Core name: WH0808 BC5

Depth (cm)	$^{210}Pb_{total}$ Activity (dpm/g)	$^{210}Pb_{excess}$ Activity (dpm/g)	$^{210}Pb_{excess}$ Error (dpm/g)	^{137}Cs Activity (dpm/g)	^{137}Cs Error (dpm/g)
0.5	7.47	6.40	0.34	0.63	0.07
1.5	8.09	7.09	0.32	0.65	0.07
2.5	7.51	6.30	0.32	0.53	0.07
3.5	7.58	6.35	0.30	0.58	0.07
4.5	6.98	5.69	0.31	0.70	0.08
5.5	7.64	6.31	0.30	0.62	0.07
6.5	7.16	5.96	0.30	0.63	0.07
7.5	7.90	6.64	0.31	0.70	0.07
8.5	6.97	5.80	0.30	0.67	0.07
9.5	6.42	5.25	0.30	0.73	0.07
11.0	5.42	4.46	0.27	0.61	0.07
13.0	3.28	2.20	0.20	0.47	0.07
15.0	2.73	1.74	0.17	0.18	0.06
17.0	1.93	0.91	0.13	0.15	0.05

Radiochemistry Data

Core name: WH0808 BC7a

Depth (cm)	$^{210}Pb_{total}$ Activity (dpm/g)	$^{210}Pb_{excess}$ Activity (dpm/g)	$^{210}Pb_{excess}$ Error (dpm/g)	^{137}Cs Activity (dpm/g)	^{137}Cs Error (dpm/g)
0.5	9.54	8.60	0.39	0.79	0.08
1.5	8.93	8.11	0.39	0.77	0.09
2.5	8.31	7.40	0.36	0.74	0.08
3.5	8.54	7.60	0.35	0.86	0.08
4.5	8.61	7.74	0.36	0.92	0.08
5.5	7.93	7.18	0.35	0.84	0.08
6.5	7.57	6.72	0.36	0.93	0.08
7.5	7.08	6.25	0.33	0.97	0.08
8.5	6.18	5.19	0.30	0.97	0.08
9.5	5.48	4.58	0.29	0.90	0.07
11.0	4.51	3.67	0.30	0.93	0.09
13.0	4.31	3.25	0.26	0.86	0.08
15.0	2.92	1.96	0.23	0.57	0.08
17.0	3.16	2.17	0.23	0.26	0.07
19.0	2.08	0.99	0.16	0.00	0.00
21.0	2.43	1.41	0.20	0.00	0.00
23.0	1.42	0.40	0.09	0.00	0.00
25.0	0.87	-0.21	-0.07	0.00	0.00
27.0	0.94	0.00	0.00	0.00	0.00
29.0	1.90	1.09	0.17	0.13	0.06

Radiochemistry Data

Core name: WH0808 BC10

Depth (cm)	$^{210}Pb_{total}$ Activity (dpm/g)	$^{210}Pb_{excess}$ Activity (dpm/g)	$^{210}Pb_{excess}$ Error (dpm/g)	^{137}Cs Activity (dpm/g)	^{137}Cs Error (dpm/g)
0.5	7.50	6.62	0.31	0.67	0.07
1.5	7.43	6.68	0.29	0.80	0.06
2.5	6.60	5.80	0.30	0.53	0.06
3.5	6.78	5.87	0.30	0.76	0.06
4.5	5.21	4.29	0.26	0.61	0.06
5.5	4.70	3.71	0.25	0.57	0.07
6.5	2.66	1.92	0.23	0.53	0.07
7.5	1.73	0.93	0.15	0.30	0.06
8.5	1.68	0.81	0.14	0.25	0.06
9.5	1.62	0.78	0.13	0.00	0.00
11.0	1.30	0.44	0.08	0.00	0.00
13.0	1.58	0.76	0.12	0.00	0.00
15.0	1.29	0.24	0.50	0.00	0.00

Radiochemistry Data

Core name: WH0808 BC11

Depth (cm)	$^{210}Pb_{total}$ Activity (dpm/g)	$^{210}Pb_{excess}$ Activity (dpm/g)	$^{210}Pb_{excess}$ Error (dpm/g)	^{137}Cs Activity (dpm/g)	^{137}Cs Error (dpm/g)
0.5	9.94	8.99	0.43	1.01	0.09
1.5	10.87	9.93	0.40	0.98	0.08
2.5	8.83	7.82	0.36	0.87	0.08
3.5	9.57	8.68	0.37	1.04	0.09
4.5	6.69	5.83	0.33	0.88	0.08
5.5	7.07	6.15	0.34	1.09	0.08
6.5	6.20	5.09	0.32	1.15	0.09
7.5	5.67	4.55	0.29	1.25	0.09
8.5	5.43	4.41	0.29	1.41	0.09
9.5	4.20	3.20	0.26	1.15	0.08
11.0	3.63	2.56	0.23	0.90	0.08
13.0	3.00	1.83	0.22	0.48	0.07
15.0	2.48	1.25	0.17	0.00	0.00
17.0	2.50	1.34	0.17	0.00	0.00
19.0	1.61	0.41	0.08	0.00	0.00
21.0	1.90	0.56	0.09	0.00	0.00
23.0	1.16	-0.21	-0.06	0.00	0.00
25.0	1.54	0.38	0.07	0.00	0.00
27.0	0.71	-0.23	-0.08	0.00	0.00

Radiochemistry Data

Core name: WH0808 BC12

Depth (cm)	$^{210}Pb_{total}$ Activity (dpm/g)	$^{210}Pb_{excess}$ Activity (dpm/g)	$^{210}Pb_{excess}$ Error (dpm/g)	^{137}Cs Activity (dpm/g)	^{137}Cs Error (dpm/g)
0.5	10.15	9.27	0.42	0.01	0.00
1.5	10.22	9.32	0.41	0.01	0.00
2.5	9.76	8.87	0.40	0.00	0.00
3.5	9.55	8.56	0.37	0.00	0.00
4.5	9.02	8.19	0.38	0.00	0.00
5.5	8.66	7.67	0.36	0.00	0.00
6.5	7.52	6.65	0.36	0.00	0.00
7.5	7.11	6.24	0.34	0.00	0.00
8.5					
9.5	5.99	4.86	0.31	0.00	0.00
11.0	5.06	4.10	0.31	0.00	0.00
13.0	4.32	3.14	0.26	0.00	0.00
15.0	4.04	2.91	0.27	0.00	0.00
17.0	3.29	2.32	0.23	0.00	0.00
19.0	2.18	1.02	0.17	0.00	0.00
21.0	2.25	1.21	0.17	0.00	0.00
23.0	1.87	0.82	0.14	0.00	0.00
25.0	1.89	0.88	0.15	0.00	0.00
27.0	1.37	0.30	0.07	0.00	0.00
29.0	1.88	0.76	0.13	0.00	0.00
31.0	1.40	0.42	0.08	0.00	0.00

Radiochemistry Data

Core name: WH0808 BC13

Depth (cm)	$^{210}Pb_{total}$ Activity (dpm/g)	$^{210}Pb_{excess}$ Activity (dpm/g)	$^{210}Pb_{excess}$ Error (dpm/g)	^{137}Cs Activity (dpm/g)	^{137}Cs Error (dpm/g)
0.5	9.56	8.47	0.38	0.65	0.08
1.5	9.75	8.80	0.38	0.89	0.08
2.5	9.21	8.09	0.36	0.94	0.08
3.5	9.27	8.18	0.35	0.82	0.07
4.5	8.99	7.98	0.36	0.74	0.08
5.5	8.85	7.81	0.36	0.85	0.08
6.5	8.01	7.02	0.36	0.87	0.09
7.5					
8.5	7.31	6.20	0.34	0.99	0.08
9.5	6.97	5.92	0.32	0.92	0.09
11.0	4.87	3.96	0.29	0.76	0.08
13.0	3.54	2.44	0.24	0.33	0.07
15.0	2.54	1.45	0.18	0.28	0.06
17.0	2.88	1.82	0.21	0.00	0.00
19.0	2.45	1.35	0.19	0.00	0.00
21.0	1.58	0.52	0.10	0.00	0.00
23.0	1.37	0.03	0.01	0.00	0.00

Appendix B

Radiochemistry Data for Box cores 2009

Explanation

Appendix **B** contains the extended results of $^{210}Pb_{xs}$ and ^{137}Cs analyses performed on box cores collected in 2009 from Saglek and Nachvak Fjord, northern Labrador. The tables list the activities of $^{210}Pb_{total}$ (dpm/g), $^{210}Pb_{excess}$ (dpm/g), and ^{137}Cs (dpm/g) and associated errors for each depth interval. Total ^{210}Pb was determined by measurement of the 46.5 keV gamma peak. Supported ^{210}Pb (from decay of ^{226}Ra within the seabed) was determined by measurement of the granddaughters of ^{226}Ra: ^{214}Pb (295 and 352 keV) and ^{214}Bi (609 keV). The unsupported ^{210}Pb (excess ^{210}Pb) was determined by subtracting the supported ^{210}Pb from the total ^{210}Pb. ^{137}Cs activities were determined by measuring the 662 keV peak directly.

Radiochemistry Data

Core name: WH0809 BCN1

Depth (cm)	$^{210}Pb_{total}$ Activity (dpm/g)	$^{210}Pb_{excess}$ Activity (dpm/g)	$^{210}Pb_{excess}$ Error (dpm/g)	^{137}Cs Activity (dpm/g)	^{137}Cs Error (dpm/g)
0.5	9.85	8.66	0.42	0.45	0.08
1.5	10.02	8.73	0.38	0.55	0.08
2.5	9.73	8.48	0.39	0.78	0.08
3.5	8.35	6.98	0.36	0.63	0.08
4.5	8.20	6.89	0.34	0.48	0.09
5.5	7.80	6.50	0.37	0.60	0.09
6.5	7.29	6.11	0.35	0.53	0.08
7.5	7.38	5.94	0.33	0.70	0.08
8.5	7.30	6.14	0.34	0.58	0.08
9.5	5.74	4.65	0.30	0.67	0.08
10.5	5.68	4.62	0.32	0.59	0.09
11.5	4.76	3.63	0.29	0.65	0.08
12.5	3.85	2.83	0.25	0.54	0.08
13.5	3.32	2.20	0.22	0.28	0.07
14.5	3.18	2.03	0.22	0.25	0.08
15.5	2.45	1.45	0.18	0.25	0.07
16.5	1.91	0.89	0.15	0.00	0.00
17.5	1.87	0.82	0.15	0.00	0.00
18.5	1.43	0.45	0.10	0.00	0.00

Radiochemistry Data

Core name: WH0809 BCN2

Depth (cm)	$^{210}Pb_{total}$ Activity (dpm/g)	$^{210}Pb_{excess}$ Activity (dpm/g)	$^{210}Pb_{excess}$ Error (dpm/g)	^{137}Cs Activity (dpm/g)	^{137}Cs Error (dpm/g)
0.5	8.97	7.71	0.38	0.62	0.08
1.5	8.18	6.90	0.35	0.57	0.08
2.5	8.28	7.11	0.36	0.55	0.08
3.5	8.53	7.28	0.34	0.59	0.07
4.5	7.71	6.55	0.35	0.56	0.08
5.5	6.97	5.76	0.31	0.56	0.07
6.5	7.27	6.03	0.33	0.55	0.08
7.5	6.36	5.17	0.31	0.64	0.08
8.5	6.24	5.18	0.31	0.63	0.08
9.5	4.77	3.61	0.26	0.60	0.08
10.5	4.39	3.47	0.27	0.40	0.07
11.5	3.73	2.73	0.24	0.36	0.07
12.5	3.26	2.31	0.24	0.41	0.08
13.5	2.12	1.08	0.17	0.41	0.07
14.5	2.28	1.36	0.19	0.33	0.07
15.5	2.51	1.56	0.21	0.27	0.07
16.5	1.34	0.39	0.09	0.00	0.00
17.5	1.11	0.31	0.08	0.00	0.00
18.5	1.61	0.77	0.14	0.00	0.00
19.5	1.40	0.62	0.13	0.00	0.00
20.5	1.18	0.36	0.08	0.00	0.00

Radiochemistry Data

Core name: WH0809 BCN3

Depth (cm)	$^{210}Pb_{total}$ Activity (dpm/g)	$^{210}Pb_{excess}$ Activity (dpm/g)	$^{210}Pb_{excess}$ Error (dpm/g)	^{137}Cs Activity (dpm/g)	^{137}Cs Error (dpm/g)
0.5	8.57	7.59	0.36	0.58	0.07
1.5	8.37	7.19	0.33	0.54	0.07
2.5	7.70	6.61	0.33	0.47	0.07
3.5	7.12	6.10	0.34	0.54	0.08
4.5	6.66	5.62	0.32	0.55	0.07
5.5	6.00	4.90	0.30	0.43	0.07
6.5	5.68	4.64	0.28	0.59	0.07
7.5	6.21	5.22	0.28	0.43	0.07
8.5	5.03	4.14	0.27	0.73	0.07
9.5	5.22	4.30	0.26	0.54	0.06
10.5	3.90	2.96	0.25	0.48	0.07
11.5	4.53	3.79	0.27	0.59	0.07
12.5	1.86	0.91	0.17	0.27	0.07
13.5	2.93	1.88	0.19	0.36	0.06
14.5	1.55	0.58	0.10	0.17	0.06
15.5	2.00	1.12	0.18	0.21	0.06
16.5	2.27	1.29	0.16	0.21	0.06
17.5	1.42	0.41	0.09	0.00	0.00
18.5	1.76	0.81	0.14	0.00	0.00
19.5	1.51	0.52	0.10	0.12	0.06
20.5	1.96	1.14	0.17	0.00	0.00

Radiochemistry Data

Core name: WH0809 BCN4

Depth (cm)	$^{210}Pb_{total}$ Activity (dpm/g)	$^{210}Pb_{excess}$ Activity (dpm/g)	$^{210}Pb_{excess}$ Error (dpm/g)	^{137}Cs Activity (dpm/g)	^{137}Cs Error (dpm/g)
0.5	7.76	6.72	0.44	0.42	0.10
1.5	6.94	5.78	0.30	0.48	0.07
2.5	6.96	5.96	0.34	0.51	0.07
3.5	6.58	5.54	0.33	0.45	0.08
4.5	6.21	5.07	0.27	0.48	0.07
5.5	5.42	4.44	0.25	0.37	0.06
6.5	5.04	4.05	0.25	0.63	0.06
7.5	4.37	3.54	0.24	0.42	0.06
8.5	4.47	3.62	0.25	0.46	0.06
9.5	3.17	2.48	0.21	0.43	0.06
10.5	3.02	2.21	0.23	0.25	0.06
11.5	2.40	1.51	0.18	0.00	0.00
12.5	2.43	1.39	0.18	0.00	0.00
13.5	1.71	0.76	0.13	0.00	0.00
14.5	1.74	0.85	0.14	0.00	0.00

Radiochemistry Data

Core name: WH0809 BCN5

Depth (cm)	$^{210}Pb_{total}$ Activity (dpm/g)	$^{210}Pb_{excess}$ Activity (dpm/g)	$^{210}Pb_{excess}$ Error (dpm/g)	^{137}Cs Activity (dpm/g)	^{137}Cs Error (dpm/g)
0.5	6.20	5.05	0.36	0.43	0.08
1.5	7.07	5.95	0.36	0.45	0.08
2.5	7.07	5.95	0.32	0.44	0.07
3.5	6.14	5.09	0.29	0.44	0.06
4.5	6.91	5.86	0.34	0.42	0.07
5.5	6.42	5.27	0.31	0.49	0.07
6.5	6.27	5.24	0.29	0.50	0.06
7.5	5.59	4.63	0.28	0.53	0.06
8.5	6.29	5.15	0.73	0.00	0.00
9.5	5.64	4.65	0.28	0.41	0.06
10.5	4.58	3.70	0.29	0.37	0.07
11.5	3.39	2.54	0.26	0.49	0.08
12.5	2.49	1.67	0.22	0.31	0.06
13.5	2.00	1.10	0.17	0.17	0.06
14.5	1.90	1.06	0.17	0.11	0.06
15.5	1.45	0.71	0.15	0.00	0.00
16.5	1.93	1.12	0.16	0.00	0.00
17.5	1.37	0.52	0.12	0.00	0.00
18.5	1.10	0.32	0.08	0.00	0.00

Radiochemistry Data

Core name: WH0809 BCS1

Depth (cm)	$^{210}Pb_{total}$ Activity (dpm/g)	$^{210}Pb_{excess}$ Activity (dpm/g)	$^{210}Pb_{excess}$ Error (dpm/g)	^{137}Cs Activity (dpm/g)	^{137}Cs Error (dpm/g)
0.5	10.30	9.11	0.45	0.69	0.09
1.5	10.20	9.07	0.41	0.82	0.08
2.5	10.26	9.30	0.43	0.77	0.09
3.5	9.89	8.49	0.38	0.75	0.08
4.5	9.36	8.08	0.38	0.85	0.08
5.5	10.18	8.93	0.39	0.79	0.08
6.5	8.57	7.37	0.36	0.80	0.08
7.5	8.55	7.51	0.37	0.85	0.08
8.5	8.19	7.11	0.36	0.98	0.08
9.5	6.35	5.20	0.33	0.90	0.08
10.5	6.58	5.50	0.35	0.88	0.10
11.5	6.45	5.35	0.32	0.81	0.08
12.5	5.18	4.17	0.32	0.83	0.09
13.5	5.22	4.19	0.32	0.85	0.09
14.5	5.78	4.77	0.34	0.92	0.09
15.5	5.17	4.13	0.30	0.87	0.08
16.5	4.07	2.92	0.28	0.93	0.09
17.5	4.01	3.08	0.30	0.66	0.08
18.5	3.73	2.86	0.29	0.57	0.08
19.5	3.02	2.02	0.25	0.37	0.08
20.5	2.68	1.41	0.19	0.00	0.00
21.5	2.48	1.33	0.20	0.00	0.00
22.5	1.81	0.62	0.13	0.00	0.00
23.5	2.35	1.14	0.16	0.00	0.00
24.5	1.49	0.33	0.08	0.00	0.00
25.5	1.59	0.31	0.06	0.00	0.00
26.5	1.04	-0.14	-0.05	0.00	0.00
27.5	0.96	-0.11	-0.04	0.00	0.00
28.5	1.87	0.73	0.12	0.00	0.00
29.5	1.74	0.65	0.10	0.00	0.00
30.5	1.79	0.79	0.16	0.00	0.00
31.5	1.62	0.40	0.08	0.00	0.00
32.5	0.82	-0.24	-0.09	0.00	0.00

Radiochemistry Data

Core name: WH0809 BCS2

Depth (cm)	$^{210}Pb_{total}$ Activity (dpm/g)	$^{210}Pb_{excess}$ Activity (dpm/g)	$^{210}Pb_{excess}$ Error (dpm/g)	^{137}Cs Activity (dpm/g)	^{137}Cs Error (dpm/g)
0.5	11.07	9.93	0.53	0.73	0.13
1.5	11.60	10.42	0.41	0.86	0.09
2.5	10.89	9.83	0.41	1.11	0.09
3.5	10.39	9.20	0.36	0.71	0.08
4.5	10.03	8.92	0.38	0.86	0.08
5.5	9.26	8.12	0.36	0.79	0.08
6.5	8.91	7.81	0.37	0.98	0.09
7.5	8.15	7.17	0.38	1.06	0.09
8.5	7.40	6.17	0.32	0.84	0.08
9.5	6.54	5.28	0.29	0.81	0.08
10.5	5.62	4.66	0.32	0.94	0.09
11.5	5.36	4.30	0.27	0.85	0.08
12.5	5.49	4.43	0.30	0.86	0.08
13.5	4.60	3.47	0.28	0.65	0.09
14.5	2.93	1.68	0.20	0.41	0.08
15.5	2.76	1.64	0.20	0.19	0.07
16.5	2.56	1.28	0.16	0.18	0.07
17.5	2.69	1.42	0.18	0.00	0.00
18.5	2.61	1.38	0.17	0.00	0.00
19.5	2.46	1.27	0.18	0.00	0.00
20.5	1.48	0.33	0.08	0.00	0.00
21.5	2.34	1.27	0.16	0.00	0.00
22.5	1.79	0.69	0.12	0.00	0.00
23.5	1.71	0.55	0.09	0.00	0.00
24.5	1.88	0.70	0.11	0.00	0.00
25.5	1.33	0.13	0.03	0.00	0.00
26.5	1.78	0.64	0.10	0.00	0.00

Radiochemistry Data

Core name: WH0809 BCS3

Depth (cm)	$^{210}Pb_{total}$ Activity (dpm/g)	$^{210}Pb_{excess}$ Activity (dpm/g)	$^{210}Pb_{excess}$ Error (dpm/g)	^{137}Cs Activity (dpm/g)	^{137}Cs Error (dpm/g)
0.5	11.78	10.74	0.42	0.82	0.09
1.5	10.99	9.81	0.42	0.96	0.09
2.5	10.53	9.62	0.40	0.97	0.08
3.5	11.06	9.80	0.41	0.87	0.09
4.5	9.65	8.37	0.41	0.79	0.09
5.5	9.62	8.37	0.35	0.86	0.09
6.5	8.50	7.34	0.33	1.12	0.08
7.5	7.29	6.00	0.32	0.98	0.09
8.5	7.80	6.65	0.32	1.14	0.08
9.5	6.74	5.46	0.31	1.03	0.09
10.5	6.51	5.44	0.33	0.99	0.09
11.5	6.05	5.09	0.33	1.13	0.09
12.5	5.96	4.78	0.32	1.04	0.10
13.5	5.69	4.55	0.31	1.12	0.09
14.5	4.70	3.41	0.28	1.16	0.09
15.5	4.36	3.22	0.26	1.18	0.09
16.5	4.52	3.34	0.25	1.06	0.09
17.5	4.02	2.65	0.23	0.75	0.08
18.5	3.94	2.67	0.25	0.69	0.09
19.5	3.44	2.15	0.20	0.44	0.07
20.5	3.46	2.10	0.22	0.00	0.00
21.5	3.46	2.14	0.22	0.00	0.00
22.5	3.17	1.80	0.19	0.00	0.00
23.5	3.19	1.75	0.19	0.00	0.00
24.5	2.29	0.96	0.14	0.00	0.00
25.5	2.38	1.02	0.14	0.00	0.00
26.5	1.73	0.33	0.06	0.00	0.00
27.5	2.16	0.90	0.15	0.00	0.00
28.5	2.26	0.95	0.13	0.00	0.00
29.5	1.73	0.44	0.08	0.00	0.00
30.5	1.63	0.31	0.06	0.00	0.00
31.5	0.98	-0.23	-0.08	0.00	0.00
32.5	1.84	0.59	0.10	0.00	0.00
33.5	1.85	0.66	0.12	0.00	0.00
34.5	1.23	-0.07	-0.02	0.00	0.00
35.5	1.69	0.44	0.08	0.00	0.00

Radiochemistry Data

Core name: WH0809 BCS4

Depth (cm)	$^{210}Pb_{total}$ Activity (dpm/g)	$^{210}Pb_{excess}$ Activity (dpm/g)	$^{210}Pb_{excess}$ Error (dpm/g)	^{137}Cs Activity (dpm/g)	^{137}Cs Error (dpm/g)
0.5	10.56	9.57	0.42	0.85	0.08
1.5	9.95	9.05	0.41	0.72	0.08
2.5	9.30	8.43	0.43	0.90	0.09
3.5	8.43	7.34	0.36	0.75	0.08
4.5	9.24	8.19	0.38	0.89	0.08
5.5	8.31	7.29	0.37	0.82	0.08
6.5	7.41	6.51	0.34	0.82	0.08
7.5	6.83	5.94	0.34	0.94	0.08
8.5	7.72	6.83	0.34	0.99	0.08
9.5	6.43	5.40	0.31	1.03	0.08
10.5	6.62	5.84	0.34	0.85	0.09
11.5	5.90	4.92	0.33	0.83	0.08
12.5	5.23	4.24	0.31	0.87	0.09
13.5	4.53	3.64	0.30	1.02	0.08
14.5	4.30	3.39	0.28	0.87	0.08
15.5	3.83	2.93	0.27	0.93	0.08
16.5	3.57	2.43	0.24	0.74	0.08
17.5	3.74	2.72	0.28	0.49	0.08
18.5	3.59	2.39	0.25	0.34	0.07
19.5	2.34	1.21	0.18	0.19	0.06
20.5	3.39	2.22	0.24	0.00	0.00
21.5	2.46	1.29	0.18	0.00	0.00
22.5	2.10	1.04	0.17	0.00	0.00
23.5	2.89	1.67	0.19	0.00	0.00
24.5	2.73	1.63	0.22	0.00	0.00
25.5	1.89	0.72	0.13	0.00	0.00
26.5	1.89	0.70	0.12	0.00	0.00
27.5	1.90	0.74	0.13	0.00	0.00
28.5	1.47	0.41	0.09	0.00	0.00
29.5	1.47	0.38	0.09	0.00	0.00
30.5	1.40	0.36	0.08	0.00	0.00
31.5	1.32	0.08	0.02	0.00	0.00

Radiochemistry Data

Core name: WH0809 BCS5

Depth (cm)	$^{210}Pb_{total}$ Activity (dpm/g)	$^{210}Pb_{excess}$ Activity (dpm/g)	$^{210}Pb_{excess}$ Error (dpm/g)	^{137}Cs Activity (dpm/g)	^{137}Cs Error (dpm/g)
0.5	8.51	7.61	0.50	0.65	0.12
1.5	9.03	8.21	0.40	0.80	0.09
2.5	9.76	8.83	0.38	0.99	0.08
3.5	9.82	8.71	0.36	0.86	0.09
4.5	8.79	7.77	0.38	1.04	0.08
5.5	8.71	7.80	0.37	0.84	0.08
6.5	7.21	6.38	0.33	0.81	0.08
7.5	6.46	5.59	0.31	0.98	0.08
8.5	5.17	4.38	0.29	0.75	0.07
9.5	4.99	4.23	0.29	0.90	0.08
10.5	4.95	3.96	0.28	0.88	0.08
11.5	4.02	2.91	0.26	0.57	0.08
12.5	3.60	2.37	0.24	0.42	0.08
13.5	3.53	2.35	0.25	0.27	0.08
14.5	3.21	2.27	0.25	0.21	0.07
15.5	3.08	1.92	0.22	0.10	0.07
16.5	2.66	1.50	0.21	0.00	0.00
17.5	1.99	0.89	0.15	0.00	0.00
18.5	1.91	0.71	0.12	0.00	0.00
19.5	2.02	0.84	0.14	0.00	0.00
20.5	1.78	0.83	0.15	0.00	0.00
21.5	1.02	0.02	0.01	0.00	0.00
22.5	2.17	0.98	0.18	0.00	0.00
23.5	0.87	0.04	0.01	0.00	0.00

Appendix C

Grain Size Data for Box cores 2008

Explanation

Appendix C contains the extended results of grain size analyses performed on box cores collected in 2008 from Saglek and Nachvak Fjord, northern Labrador. The tables list the mean grain size (microns), median grain size (microns), and the cumulative percentile for sand, silt and clay for each depth interval. Granulometric measurements were done with a HORIBA Partica LA-950, using a laser scattering method.

Grain size Data

Core name: WH0808 BC1

Depth (cm)	Mean (microns)	Median (microns)	Sand %	Silt %	Clay %
0.5	18.46	13.40	2.90	97.10	0.00
1.5	18.25	13.03	3.18	96.70	0.12
2.5	17.10	12.41	2.71	96.92	0.37
3.5	16.28	12.07	2.34	97.13	0.53
4.5	17.23	12.85	2.27	97.60	0.13
5.5	19.18	13.11	3.64	96.23	0.13
6.5	15.06	11.66	1.81	95.79	2.39
7.5	22.90	12.00	6.93	90.82	2.25
8.5	26.32	13.04	5.83	94.03	0.14
9.5	17.55	13.20	2.37	97.49	0.14
11	17.75	13.24	2.44	97.45	0.11

Grain size Data

Core name: WH0808 BC2

Depth (cm)	Mean (microns)	Median (microns)	Sand %	Silt %	Clay %
0.5	15.74	12.64	1.40	98.26	0.34
1.5	14.62	12.89	0.20	99.65	0.14
2.5	13.90	12.16	0.23	98.23	1.53
3.5	13.23	11.52	0.06	92.48	7.46
4.5	18.33	14.16	2.16	97.84	0.00
5.5	13.44	11.40	0.51	89.41	10.08
6.5	15.90	13.31	1.04	98.84	0.12
7.5	15.43	13.20	0.73	99.15	0.11
8.5	17.41	12.57	2.82	96.33	0.86
9.5	13.79	11.87	0.57	97.89	1.54
11	18.48	13.28	2.95	96.90	0.15
13	27.89	14.09	5.58	94.32	0.11
15	16.52	12.59	2.04	97.57	0.39

Grain size Data

Core name: WH0808 BC3

Depth (cm)	Mean (microns)	Median (microns)	Sand %	Silt %	Clay %
0.5	13.22	11.46	0.53	99.02	0.46
1.5	13.66	12.11	0.45	99.39	0.16
2.5	16.73	11.72	2.77	96.80	0.44
3.5	14.95	11.85	1.32	98.49	0.19
4.5	15.61	11.59	2.03	97.49	0.48
5.5	16.41	11.76	2.51	96.97	0.52
6.5	16.12	12.28	1.93	97.91	0.17
7.5	14.27	12.70	0.34	99.66	0.00
8.5	14.24	12.54	0.52	99.37	0.12
9.5	34.59	12.34	5.31	94.55	0.14
11	20.75	12.54	4.66	95.16	0.19
13	10.21	8.98	0.22	78.24	21.54

Grain size Data

Core name: WH0808 BC4

Depth (cm)	Mean (microns)	Median (microns)	Sand %	Silt %	Clay %
0.5	9.09	8.29	0.00	74.93	25.07
1.5	12.35	10.06	0.97	81.95	17.08
2.5	16.31	12.73	1.77	98.10	0.14
3.5	16.66	12.29	2.30	97.52	0.18
4.5	17.91	11.88	3.33	96.28	0.39
5.5	13.74	10.10	1.90	93.91	4.19
6.5	18.15	12.33	3.46	95.63	0.92
7.5	19.24	12.98	3.82	95.47	0.71
8.5	17.56	11.37	3.47	95.68	0.85
9.5	14.08	11.21	1.37	98.05	0.58
11	12.01	9.69	0.87	89.62	9.51

Grain size Data

Core name: WH0808 BC5

Depth (cm)	Mean (microns)	Median (microns)	Sand %	Silt %	Clay %
0.5	16.57	12.03	2.43	97.38	0.19
1.5	11.07	9.88	0.00	94.36	5.65
2.5	15.59	11.42	2.46	95.52	2.01
3.5	16.86	12.47	2.29	97.56	0.15
4.5	16.99	12.33	2.70	96.69	0.60
5.5	16.34	11.08	3.04	94.14	2.82
6.5	16.86	13.08	1.89	98.11	0.00
7.5	13.95	9.45	2.52	84.44	13.04
8.5	19.17	11.93	4.36	94.59	1.05
9.5	12.99	10.27	1.23	89.77	9.00
11	16.37	12.39	2.02	97.81	0.16
13	11.93	9.99	0.60	90.55	8.86
15	11.35	9.75	0.45	79.64	19.92
17	19.26	12.42	4.06	95.77	0.17

Grain size Data

Core name: WH0808 BC7a

Depth (cm)	Mean (microns)	Median (microns)	Sand %	Silt %	Clay %
0.5	14.20	13.08	0.00	100.00	0.00
1.5	11.41	9.62	0.49	84.26	15.25
2.5	15.64	12.12	1.65	97.90	0.45
3.5	19.93	13.15	1.74	98.26	0.00
4.5	25.47	12.52	5.30	94.59	0.11
5.5	10.08	8.50	0.42	73.91	25.67
6.5	23.51	13.99	5.28	94.72	0.00
7.5	17.97	12.64	2.98	97.02	0.00
8.5	24.73	13.95	6.29	93.71	0.00
9.5	20.03	12.13	3.44	96.44	0.13
11	16.58	13.26	1.55	98.45	0.00
13	17.46	13.15	2.32	97.68	0.00
15	20.84	14.02	4.22	95.78	0.00
17	11.35	9.12	0.85	82.57	16.58
19	21.22	12.37	5.83	88.29	5.87
21	17.96	13.61	2.31	97.69	0.00
23	18.89	12.67	3.72	96.11	0.18
25	22.71	13.10	5.86	94.14	0.00
27	14.35	12.33	0.87	99.02	0.11
28.5	18.87	10.76	5.25	87.96	6.79

Grain size Data

Core name: WH0808 BC10

Depth (cm)	Mean (microns)	Median (microns)	Sand %	Silt %	Clay %
0.5	20.46	11.42	6.67	74.21	19.12
1.5	20.34	12.41	5.50	93.69	0.82
2.5	32.75	13.22	13.65	83.40	2.96
3.5	25.84	13.67	8.38	91.62	0.00
4.5	23.41	11.96	8.91	75.89	15.20
5.5	157.91	16.00	28.43	58.71	12.86
6.5	22.68	11.23	7.95	69.47	22.58
7.5	19.52	9.35	7.14	64.77	28.09
8.5	31.86	11.94	9.13	87.91	2.96
9.5	14.50	9.23	3.37	66.85	29.78
11	14.49	9.77	3.11	77.09	19.80
13	18.36	11.35	4.67	83.17	12.17
15	20.36	12.83	5.09	94.58	0.33

Grain size Data

Core name: WH0808 BC11

Depth (cm)	Mean (microns)	Median (microns)	Sand %	Silt %	Clay %
0.5	13.03	12.20	0.00	100.00	0.00
1.5	13.99	12.24	0.39	99.49	0.12
2.5	13.70	12.51	0.11	99.89	0.00
3.5	8.55	7.20	0.20	68.65	31.15
4.5	18.44	10.42	4.43	90.38	5.19
5.5	9.08	8.11	0.07	77.22	22.71
6.5	8.72	7.70	0.07	73.75	26.19
7.5	8.47	7.54	0.00	72.36	27.64
8.5	14.11	8.54	3.06	75.27	21.67
9.5	11.70	10.84	0.00	99.45	0.55
11	12.66	11.82	0.00	99.89	0.11
13	28.32	12.14	4.23	95.64	0.14
15	8.43	7.69	0.00	71.65	28.35
17	14.27	12.46	0.52	99.38	0.11
19	16.95	12.12	2.55	97.27	0.19
21	12.43	10.40	0.64	97.70	1.67
23	8.79	7.57	0.07	73.63	26.31
25	14.11	9.17	2.61	82.76	14.62
27	11.48	10.55	0.00	98.67	1.34

Grain size Data

Core name: WH0808 BC12

Depth (cm)	Mean (microns)	Median (microns)	Sand %	Silt %	Clay %
0.5	12.35	11.63	0.00	99.88	0.12
1.5	8.34	7.54	0.00	71.76	28.24
2.5	12.06	10.02	0.55	96.38	3.07
3.5	11.51	10.80	0.00	99.46	0.55
4.5	9.84	8.72	0.00	90.15	9.85
5.5	11.97	11.15	0.00	99.64	0.36
6.5	8.77	7.79	0.06	74.64	25.30
7.5	8.91	7.77	0.00	74.10	25.90
8.5					
9.5	13.63	11.70	0.51	99.35	0.15
11	19.68	11.41	4.28	95.37	0.35
13	7.36	6.29	0.00	64.77	35.23
15	31.26	12.53	4.25	95.75	0.00
17	12.91	11.74	0.11	99.77	0.12
19	11.64	8.68	1.27	79.91	18.82
21	11.86	10.93	0.00	99.33	0.67
23	16.48	13.14	1.58	98.42	0.00
25	14.89	11.70	1.57	98.23	0.20
27	13.10	11.98	0.06	99.81	0.13
29	12.62	11.33	0.19	99.21	0.60
31	9.30	7.99	0.07	74.82	25.11
33	14.06	11.39	1.06	98.71	0.23

Grain size Data

Core name: WH0808 BC13

Depth (cm)	Mean (microns)	Median (microns)	Sand %	Silt %	Clay %
0.5	18.98	11.55	1.48	98.41	0.11
1.5	11.54	10.97	0.00	99.86	0.15
2.5	12.74	11.86	0.00	100.00	0.00
3.5	12.87	10.87	0.64	98.92	0.44
4.5	15.51	11.78	1.37	98.51	0.12
5.5	16.44	11.70	2.58	97.27	0.15
6.5	9.00	8.08	0.06	78.36	21.58
7.5					
8.5	11.28	10.46	0.00	98.77	1.23
9.5	17.48	10.47	3.73	94.98	1.28
11	21.90	10.53	6.69	89.45	3.87
13	9.36	8.34	0.00	83.55	16.45
15	17.56	11.10	3.96	94.34	1.71
17	20.57	11.96	2.22	97.65	0.12
19	17.12	11.80	2.96	96.56	0.49
21	18.75	10.52	4.63	91.42	3.94
23	12.66	11.33	0.20	99.24	0.55
25	8.62	8.08	0.00	78.15	21.85

Appendix D

Grain Size Data for Box cores 2009

Explanation

Appendix C contains the extended results of grain size analyses performed on box cores collected in 2009 from Saglek and Nachvak Fjord, northern Labrador. The tables list the mean grain size (microns), median grain size (microns), and the cumulative percentile for sand, silt and clay for each depth interval. Granulometric measurements were done with a HORIBA Partica LA-950, using a laser scattering method.

Grain size Data

Core name: WH0809 BN1

Depth (cm)	Mean (microns)	Median (microns)	Sand %	Silt %	Clay %
0.5	10.58	9.15	0.21	82.74	17.06
1.5	15.83	12.17	1.80	98.05	0.15
2.5	15.80	11.94	2.03	97.78	0.19
3.5	16.32	12.69	1.87	98.13	0.00
4.5	16.45	12.12	2.28	97.56	0.16
5.5	12.48	10.77	0.39	98.40	1.20
6.5	11.66	10.39	0.19	97.79	2.02
7.5	22.89	12.37	3.96	95.90	0.15
8.5	19.01	12.17	3.49	96.35	0.15
9.5	19.47	12.14	2.92	97.08	0.00
10.5	20.48	13.43	4.21	95.68	0.11
11.5	17.04	12.50	2.42	97.40	0.18
12.5	18.33	13.40	2.70	97.30	0.00
13.5	15.46	11.53	2.19	93.80	4.01
14.5	19.84	13.19	4.03	94.97	1.00
15.5	15.62	12.75	1.35	98.50	0.15
16.5	17.20	12.58	2.58	97.08	0.34
17.5	9.31	8.32	0.00	72.10	27.90
18.5	10.67	9.21	0.27	77.32	22.42

Grain size Data

Core name: WH0809 BCN2

Depth (cm)	Mean (microns)	Median (microns)	Sand %	Silt %	Clay %
0.5	12.37	11.29	0.00	99.44	0.56
1.5	14.80	12.53	0.69	99.30	0.00
2.5	18.35	11.76	3.42	95.26	1.31
3.5	19.78	12.17	3.19	96.60	0.21
4.5	16.09	12.49	1.79	98.05	0.16
5.5	12.83	11.38	0.33	98.89	0.78
6.5	8.83	7.91	0.00	70.61	29.39
7.5	18.67	12.19	2.59	97.25	0.16
8.5	19.89	12.37	1.92	97.90	0.18
9.5	45.77	12.45	10.99	88.82	0.19
10.5	14.53	12.69	0.54	99.34	0.12
11.5	9.43	8.89	0.00	92.96	7.04
12.5	10.80	10.17	0.00	97.93	2.07
13.5	11.83	11.16	0.00	99.47	0.53
14.5	18.77	13.33	3.41	96.44	0.15
15.5	9.44	9.04	0.00	83.63	16.37
16.5	13.04	12.20	0.00	99.82	0.18
17.5	9.09	8.71	0.00	85.76	14.24
18.5	13.07	12.27	0.00	99.85	0.16
19.5	13.52	12.33	0.00	99.67	0.33
20.5	9.69	9.16	0.00	89.79	10.21

Grain size Data

Core name: WH0809 BCN3

Depth (cm)	Mean (microns)	Median (microns)	Sand %	Silt %	Clay %
0.5	12.75	12.10	0.00	100.00	0.00
1.5	12.78	12.00	0.00	99.85	0.15
2.5	10.94	10.33	0.00	97.27	2.73
3.5	9.88	9.46	0.00	80.22	19.78
4.5	11.14	10.40	0.00	96.44	3.56
5.5	10.57	9.88	0.00	94.72	5.28
6.5	12.89	12.16	0.00	99.85	0.15
7.5	46.74	13.46	9.01	90.88	0.11
8.5	37.11	12.81	4.39	95.61	0.00
9.5	14.14	12.85	0.00	99.88	0.12
10.5	36.04	13.23	4.41	95.59	0.00
11.5	13.22	12.08	0.00	99.65	0.35
12.5	13.17	12.04	0.00	99.66	0.34
13.5	13.29	12.30	0.00	99.86	0.14
14.5	14.61	13.13	0.00	99.89	0.11
15.5	12.91	11.98	0.00	99.82	0.18
16.5	14.34	12.99	0.00	100.00	0.00
17.5	13.18	12.29	0.00	99.88	0.12
18.5	13.47	12.35	0.00	99.85	0.15
19.5	16.34	12.50	1.09	98.70	0.21
20.5	13.76	11.51	0.55	96.03	3.42

Grain size Data

Core name: WH0809 BCN4

Depth (cm)	Mean (microns)	Median (microns)	Sand %	Silt %	Clay %
0.5	14.85	13.43	0.07	99.93	0.00
1.5	14.98	13.24	0.40	99.60	0.00
2.5	16.24	12.91	1.55	98.45	0.00
3.5	16.59	12.89	1.95	97.94	0.11
4.5	14.20	12.57	0.36	99.53	0.11
5.5	17.21	12.92	2.22	97.67	0.12
6.5	14.77	12.84	0.60	99.28	0.11
7.5	529.12	554.88	68.75	30.92	0.00
8.5	33.72	13.70	7.57	92.43	0.00
9.5	17.27	13.27	2.01	97.86	0.12
10.5	18.26	13.72	2.43	97.46	0.12
11.5	32.00	14.16	5.01	94.82	0.17
12.5	12.83	12.01	0.41	99.06	0.53
13.5	15.74	12.92	1.19	98.60	0.20
14.5	20.91	15.52	3.37	96.63	0.00
15.5	23.36	14.95	5.42	94.44	0.14

Grain size Data

Core name: WH0809 BCN5

Depth (cm)	Mean (microns)	Median (microns)	Sand %	Silt %	Clay %
0.5	17.43	13.25	2.01	97.81	0.17
1.5	12.57	11.09	0.19	98.02	1.79
2.5	23.78	12.86	4.15	95.85	0.00
3.5	25.73	12.50	3.62	96.24	0.14
4.5	13.76	12.45	0.08	99.79	0.13
5.5	13.60	11.92	0.39	99.15	0.45
6.5	14.97	12.64	0.73	99.14	0.13
7.5	13.84	12.34	0.22	99.59	0.19
8.5					
9.5	12.16	10.78	0.06	96.74	3.20
10.5	14.39	12.32	0.80	98.16	1.04
11.5	18.85	13.95	2.82	97.05	0.13
12.5	14.09	12.53	0.23	99.64	0.13
13.5	11.18	9.67	0.07	85.58	14.35
14.5	16.40	11.88	2.43	95.77	1.80
15.5	16.68	12.45	2.15	97.41	0.44
16.5	13.97	12.16	0.53	99.26	0.22
17.5	18.95	13.41	3.21	96.62	0.17
18.5	11.13	9.96	0.00	83.90	16.10

Grain size Data

Core name: WH0809 BCS1

Depth (cm)	Mean (microns)	Median (microns)	Sand %	Silt %	Clay %
0.5	6.86	6.67	0.00	70.17	29.83
1.5	13.66	12.68	0.00	100.00	0.00
2.5	14.19	13.16	0.00	100.00	0.00
3.5	12.86	12.13	0.00	99.90	0.10
4.5	12.98	12.21	0.00	100.00	0.00
5.5	8.53	7.99	0.00	89.45	10.55
6.5	11.62	10.68	0.00	97.28	2.72
7.5	12.84	12.03	0.00	99.89	0.11
8.5	12.57	11.84	0.00	100.00	0.00
9.5	11.78	11.09	0.00	99.76	0.24
10.5	27.14	14.09	5.53	94.47	0.00
11.5	10.37	9.67	0.00	96.07	3.93
12.5	28.22	15.34	7.29	92.71	0.00
13.5	11.31	10.10	0.00	93.05	6.95
14.5	15.20	13.46	0.37	99.63	0.00
15.5	19.00	14.27	2.47	97.53	0.00
16.5	18.20	13.35	2.58	97.25	0.17
17.5	8.66	7.95	0.00	86.10	13.90
18.5	13.80	12.71	0.00	99.87	0.13
19.5	13.36	12.41	0.00	99.89	0.12
20.5	12.51	11.73	0.00	99.52	0.48
21.5	13.47	12.67	0.00	100.00	0.00
22.5	11.40	10.40	0.00	95.96	4.05
23.5	21.25	11.86	4.03	94.97	1.00
24.5	12.64	11.68	0.00	99.84	0.16
25.5	7.79	7.37	0.00	74.18	25.82
26.5	11.50	10.40	0.00	97.34	2.66
27.5	32.94	13.59	8.22	91.67	0.11
28.5	20.47	13.32	4.27	95.63	0.11
29.5	15.18	13.23	0.30	99.70	0.00
30.5	9.79	9.00	0.00	86.93	13.07
31.5	12.04	11.26	0.00	99.47	0.53
32.5	16.87	12.86	2.40	97.38	0.22

Grain size Data

Core name: WH0809 BCS2

Depth (cm)	Mean (microns)	Median (microns)	Sand %	Silt %	Clay %
0.5	12.61	11.94	0.00	100.00	0.00
1.5	8.88	8.41	0.00	89.23	10.77
2.5	10.22	9.58	0.00	97.47	2.53
3.5	8.12	7.76	0.00	94.97	5.03
4.5	9.40	8.99	0.00	97.19	2.81
5.5	9.69	9.24	0.00	97.01	2.99
6.5	7.69	7.18	0.00	73.81	26.20
7.5	12.19	11.55	0.00	99.86	0.14
8.5	9.14	8.64	0.00	89.17	10.84
9.5	8.28	7.81	0.00	87.94	12.06
10.5	18.88	13.67	3.09	96.81	0.11
11.5	12.32	11.09	0.00	98.49	1.51
12.5	8.74	8.42	0.00	88.78	11.22
13.5	12.96	12.10	0.00	99.86	0.14
14.5	11.09	10.36	0.00	98.63	1.37
15.5	20.61	13.00	4.61	95.29	0.10
16.5	15.56	13.30	0.74	99.26	0.00
17.5	9.28	8.61	0.00	89.02	10.98
18.5	11.79	10.75	0.00	95.76	4.24
19.5	16.82	14.30	0.78	99.22	0.00
20.5	14.89	12.78	0.67	99.21	0.12
21.5	20.23	13.67	2.02	97.98	0.00
22.5	15.29	12.81	0.38	97.27	2.35
23.5	19.89	13.65	2.36	97.53	0.11
24.5	15.20	13.31	0.24	99.66	0.10
25.5	11.11	10.58	0.00	99.13	0.87
26.5	12.28	10.97	0.06	98.52	1.42

Grain size Data

Core name: WH0809 BCS3

Depth (cm)	Mean (microns)	Median (microns)	Sand %	Silt %	Clay %
0.5	10.99	10.70	0.00	100.00	0.00
1.5	10.31	9.80	0.00	98.69	1.31
2.5	11.90	11.28	0.00	99.79	0.21
3.5	8.16	7.68	0.00	77.96	22.04
4.5	10.07	9.28	0.00	93.94	6.06
5.5	11.79	11.01	0.00	99.47	0.53
6.5	26.73	12.70	3.73	96.27	0.00
7.5	10.99	10.37	0.00	98.94	1.06
8.5	11.21	10.40	0.00	98.42	1.58
9.5	10.20	9.51	0.00	95.98	4.02
10.5	17.45	12.41	2.72	97.13	0.15
11.5	9.83	9.01	0.00	93.78	6.22
12.5	8.63	7.93	0.00	85.44	14.56
13.5	32.79	13.46	6.10	93.90	0.00
14.5	13.54	12.44	0.00	100.00	0.00
15.5	10.08	9.11	0.00	90.64	9.36
16.5	11.34	10.47	0.00	98.36	1.64
17.5	13.43	11.44	0.52	99.29	0.20
18.5	16.58	12.20	2.25	97.63	0.12
19.5	17.23	13.04	2.18	97.82	0.00
20.5	11.36	10.29	0.00	97.32	2.68
21.5	12.41	10.94	0.21	99.19	0.60
22.5	16.73	12.97	1.83	98.17	0.00
23.5	19.78	12.69	3.66	96.22	0.12
24.5	28.23	13.25	5.76	94.24	0.00
25.5	17.50	13.64	2.29	97.61	0.10
26.5	19.67	12.92	4.30	95.58	0.13
27.5	21.70	12.67	3.74	96.14	0.13
28.5	11.42	10.58	0.00	98.89	1.11
29.5	9.12	8.32	0.00	79.67	20.33
30.5	16.45	11.79	2.61	96.91	0.48
31.5	30.53	12.50	5.79	94.05	0.16
32.5	9.21	8.34	0.00	81.58	18.42
33.5	10.62	9.27	0.18	93.75	6.07
34.5	14.90	11.53	1.64	98.00	0.36
35.5	22.54	13.04	6.57	93.29	0.14

Grain size Data

Core name: WH0809 BCS4

Depth (cm)	Mean (microns)	Median (microns)	Sand %	Silt %	Clay %
0.5	11.87	11.21	0.00	99.83	0.18
1.5	12.08	11.41	0.00	99.87	0.13
2.5	11.51	10.82	0.00	99.02	0.99
3.5	12.87	12.12	0.00	100.00	0.00
4.5	12.36	11.67	0.00	99.87	0.13
5.5	12.99	11.86	0.13	99.87	0.00
6.5	14.66	12.52	0.60	99.40	0.00
7.5	17.51	12.13	2.87	97.13	0.00
8.5	11.41	10.60	0.00	98.93	1.07
9.5	11.51	10.50	0.00	98.47	1.53
10.5	23.93	13.41	6.03	93.97	0.00
11.5	18.43	12.22	3.12	96.74	0.14
12.5	15.85	12.24	1.82	98.01	0.17
13.5	26.90	12.59	4.55	95.45	0.00
14.5	23.54	12.58	4.17	95.69	0.14
15.5	18.37	13.06	3.06	96.94	0.00
16.5	10.37	9.86	0.00	98.39	1.61
17.5	9.56	8.98	0.00	95.34	4.66
18.5	24.74	12.29	4.80	95.03	0.18
19.5	14.47	12.82	0.38	99.62	0.00
20.5	10.87	10.22	0.00	98.39	1.61
21.5	15.69	12.08	1.78	97.60	0.62
22.5	12.00	11.12	0.00	99.39	0.61
23.5	15.94	13.17	1.26	98.64	0.10
24.5	18.47	14.30	2.30	97.70	0.00
25.5	10.61	9.83	0.00	96.08	3.92
26.5	21.35	12.94	4.03	95.97	0.00
27.5	16.55	13.62	1.41	98.59	0.00
28.5	9.15	8.21	0.00	79.44	20.56
29.5	25.48	13.73	7.73	92.27	0.00
30.5	23.75	13.09	5.44	94.56	0.00
31.5	16.00	11.36	2.68	96.89	0.43

Grain size Data

Core name: WH0809 BCS5

Depth (cm)	Mean (microns)	Median (microns)	Sand %	Silt %	Clay %
0.5	13.23	12.45	0.00	100.00	0.00
1.5	13.77	12.58	0.11	99.89	0.00
2.5	13.29	12.47	0.00	100.00	0.00
3.5	13.43	12.59	0.00	100.00	0.00
4.5	15.26	13.57	0.31	99.69	0.00
5.5	14.59	13.19	0.21	99.79	0.00
6.5	23.33	12.15	4.35	95.65	0.00
7.5	11.66	9.74	0.44	95.96	3.60
8.5	10.05	9.10	0.00	90.08	9.92
9.5	13.58	11.37	0.68	99.13	0.19
10.5	19.87	13.16	4.18	95.72	0.10
11.5	19.48	13.30	3.62	96.27	0.11
12.5	22.28	14.94	4.57	95.43	0.00
13.5	12.58	11.21	0.07	98.19	1.74
14.5	28.35	14.29	8.72	91.28	0.00
15.5	25.29	14.50	6.87	93.13	0.00
16.5	9.06	8.18	0.00	79.74	20.26
17.5	9.58	8.66	0.00	82.49	17.51
18.5	19.50	13.31	3.49	96.40	0.10
19.5	28.90	13.60	5.69	94.31	0.00
20.5	17.62	12.27	2.89	96.78	0.33
21.5	14.74	13.22	0.08	99.91	0.00
22.5	18.34	12.31	3.44	96.39	0.17
23.5	11.54	10.72	0.00	99.14	0.86

Appendix E

Sub-bottom profiles in Nachvak Fjord

Explanation

Appendix E contains all sub-bottom profiles recorded during fieldwork in 2008 and their location on a map. Sub-bottom profiles and sidescan sonar data were collected by using a 2-16 kHz Chirp system (Edgetech 3200XS). The profiles and lines in the map showing the geographic location of each profile are labelled with corresponding numbers.

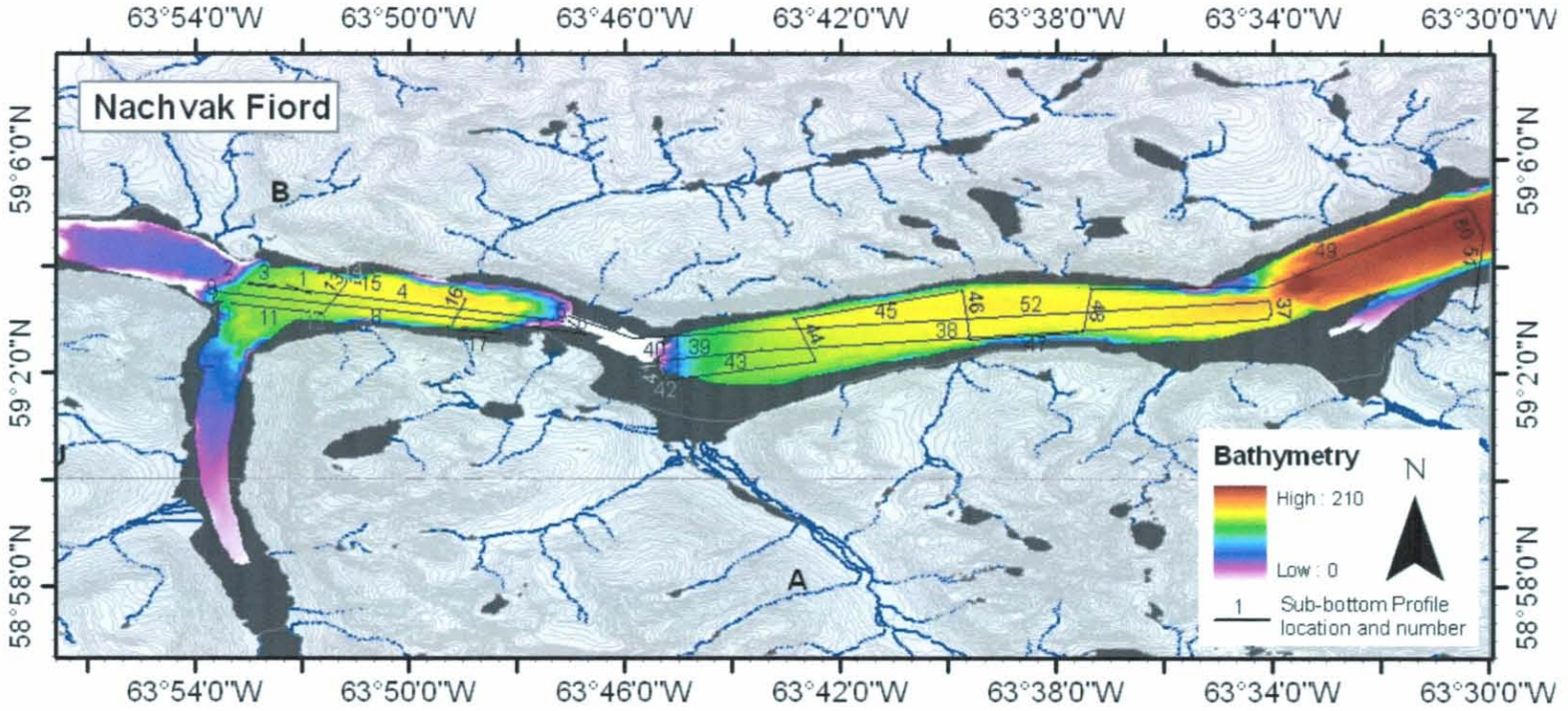
Nachvak Fiord
63°54'0"W
63°50'0"W
63°46'0"W
63°42'0"W
63°38'0"W
63°34'0"W
63°30'0"W
59°6'0"N
59°2'0"N
58°58'0"N
B
A
Bathymetry
High : 210
Low : 0
N
1
Sub-bottom Profile
location and number

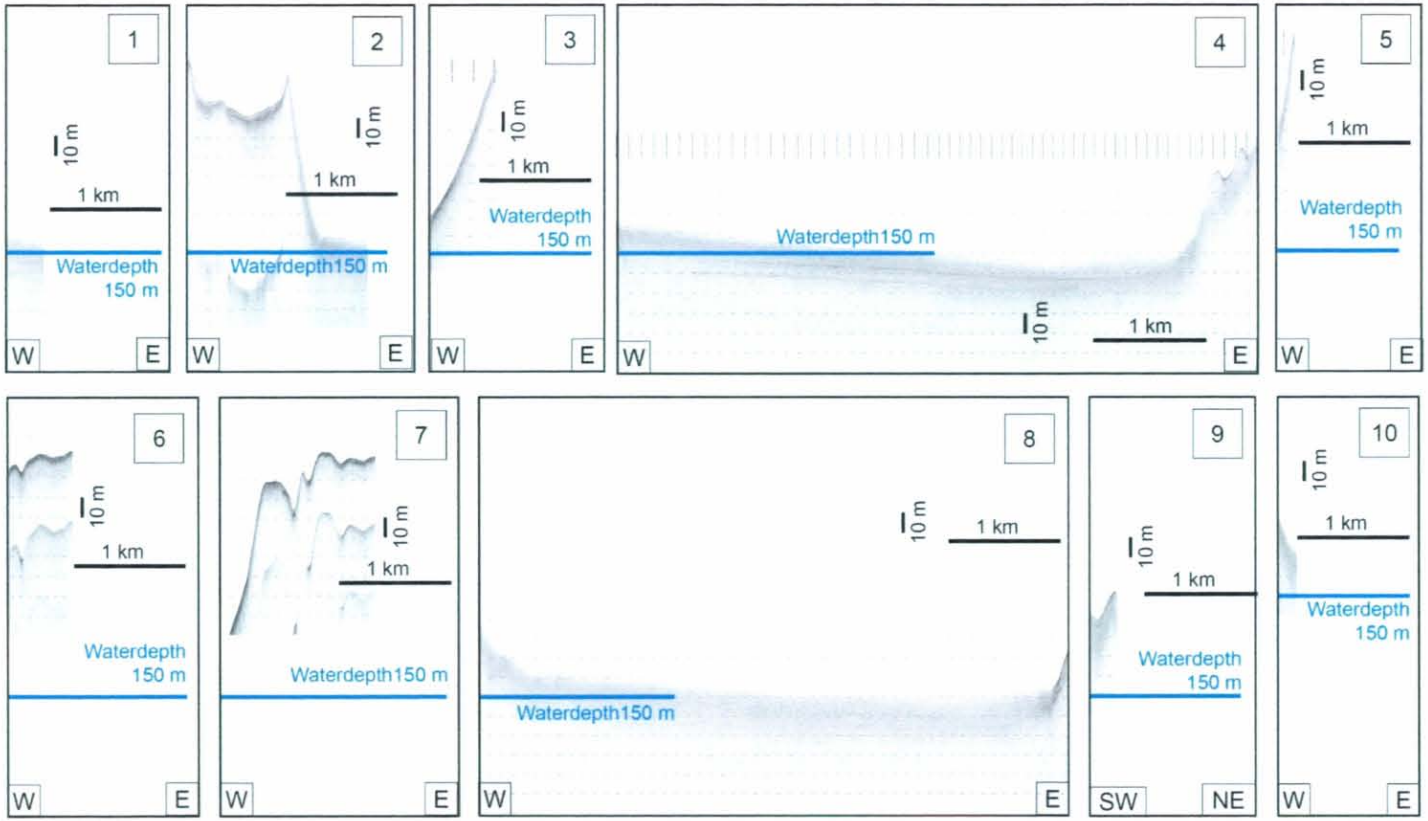
1
10 m
1 km
Waterdepth
150 m
W
E
2
10 m
1 km
Waterdepth150 m
W
E
3
10 m
1 km
Waterdepth
150 m
W
E
4
Waterdepth150 m
10 m
1 km
W
E
5
10 m
1 km
Waterdepth
150 m
W
E
6
10 m
1 km
Waterdepth
150 m
W
E
7
10 m
1 km
Waterdepth150 m
W
E
8
10 m
1 km
Waterdepth150 m
W
E
9
10 m
1 km
Waterdepth
150 m
SW
NE
10
10 m
1 km
Waterdepth
150 m
W
E


11
Waterdepth
150 m
10 m
1 km
W
E
12
Waterdepth
150 m
10 m
1 km
W
E
13
Waterdepth150 m
1 km
10 m
SW
NE
16
1 km
Waterdepth150 m
10 m
SW
NE
17
10 m
Waterdepth150 m
1 km
W
E
37
1 km
Waterdepth
150 m
10 m
S
N
38
1 km
10 m
Waterdepth150 m
W
E
39
1 km
10 m
Waterdepth150 m
W
E
41
10 m
1 km
Waterdepth
150 m
S
N
42
10 m
1 km
Waterdepth
150 m
W
E
43
1 km
10 m
Waterdepth
150 m
W
E
44
1 km
10 m
Waterdepth
150 m
N
S

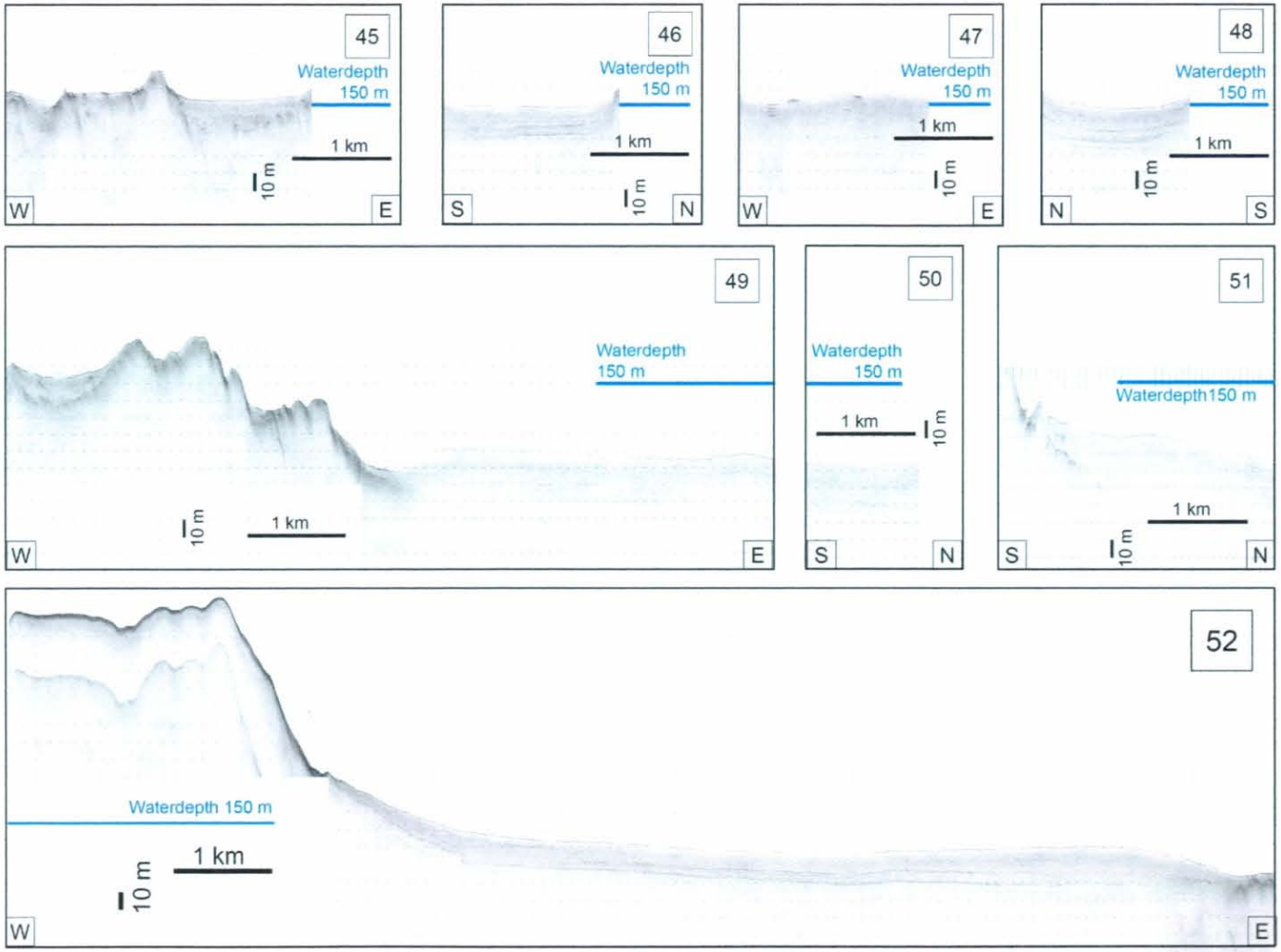
45
Waterdepth
150 m
1 km
10 m
W
E
46
Waterdepth
150 m
1 km
10 m
S
N
47
Waterdepth
150 m
1 km
10 m
W
E
48
Waterdepth
150 m
1 km
10 m
N
S
49
Waterdepth
150 m
1 km
10 m
W
E
50
Waterdepth
150 m
1 km
10 m
S
N
51
Waterdepth150 m
1 km
10 m
S
N
52
Waterdepth 150 m
1 km
10 m
W
E

Appendix F

Sub-bottom profiles in Saglek Fjord

Explanation

Appendix F contains all sub-bottom profiles recorded during fieldwork in 2008 and their location on a map. Sub-bottom profiles and sidescan sonar data were collected by using a 2-16 kHz Chirp system (Edgetech 3200XS). The profiles and lines in the map showing the geographic location of each profile are labelled with corresponding numbers.

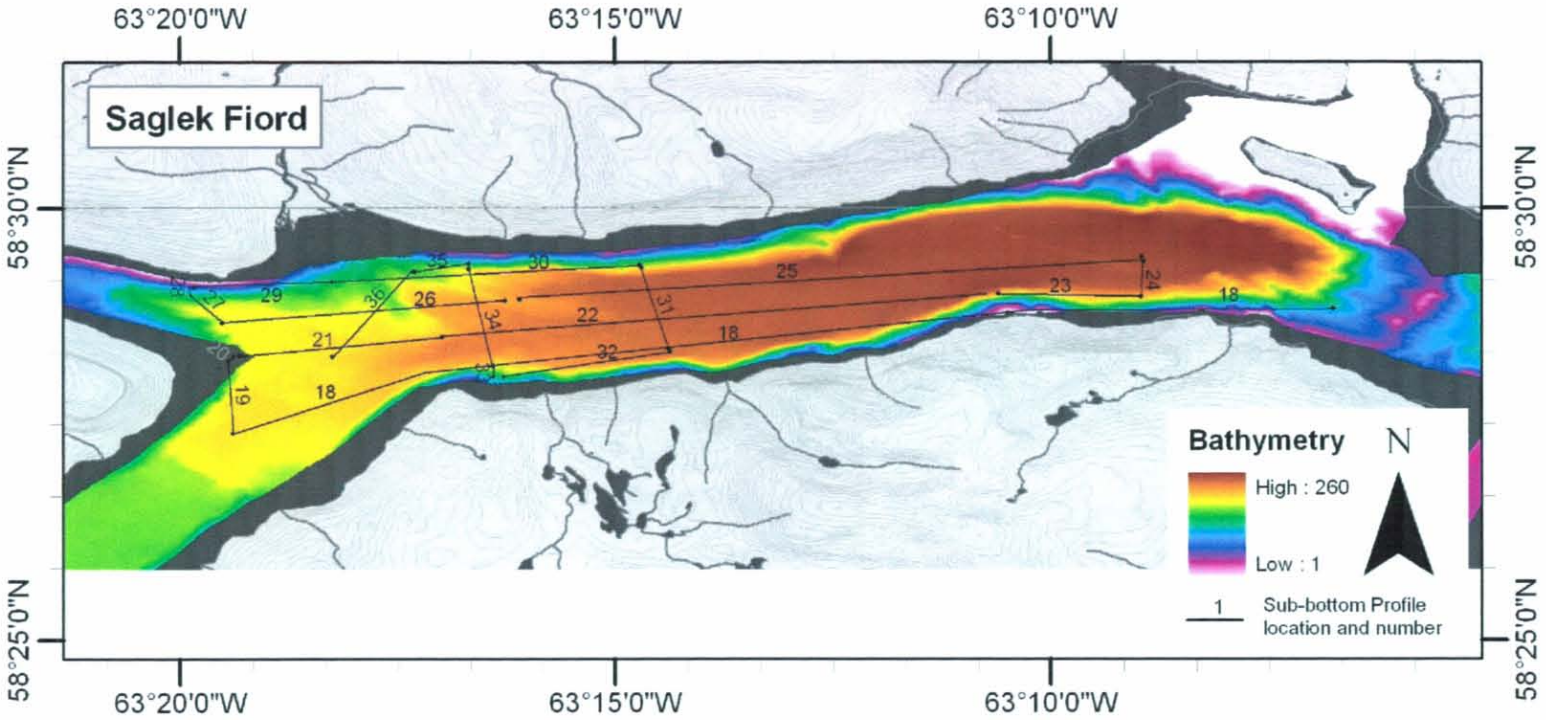
Saglek Fiord
63°20'0"W
63°15'0"W
63°10'0"W
58°30'0"N
58°25'0"N
Bathymetry
High : 260
Low : 1
N
1
Sub-bottom Profile location and number

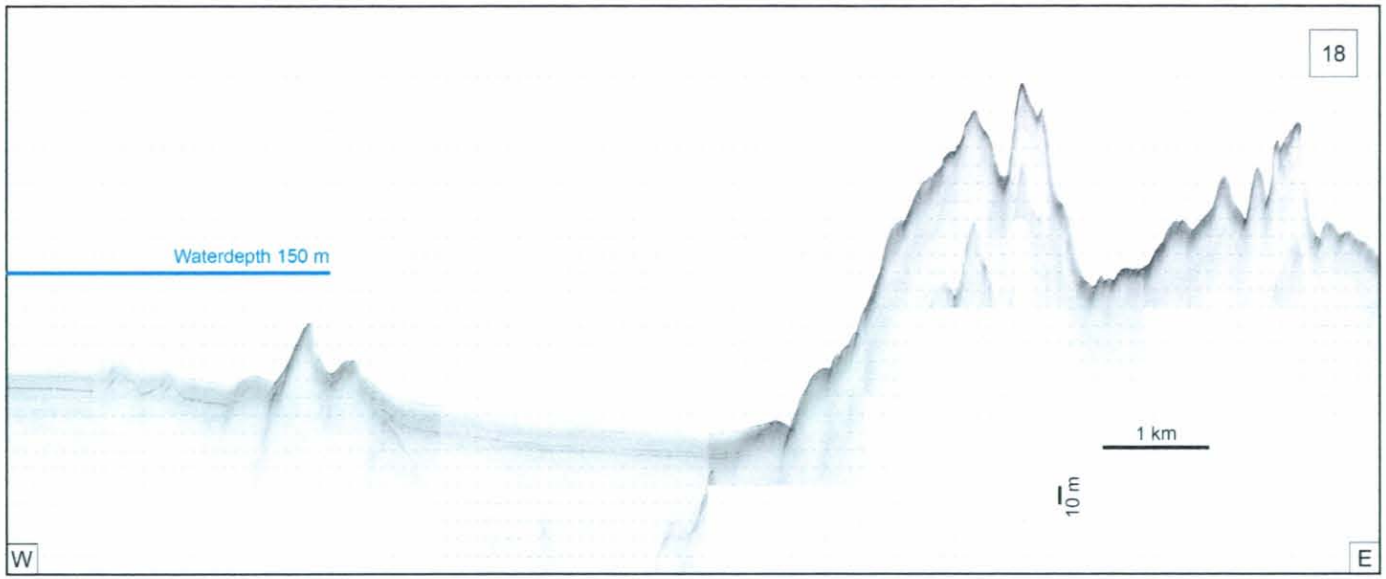
18
Waterdepth 150 m
1 km
10 m
W
E

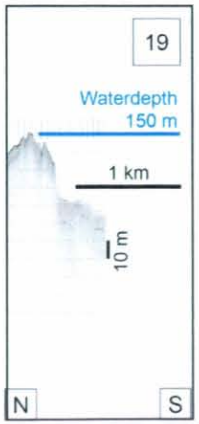
19
Waterdepth
150 m
1 km
10 m
N
S


20
Waterdepth
150 m
1 km
10 m
W
E

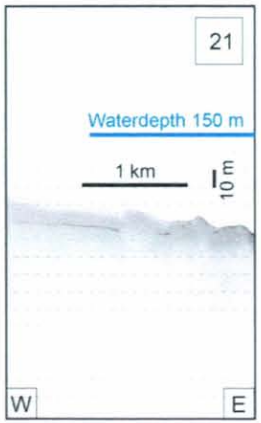
21
Waterdepth 150 m
1 km
10 m
W
E

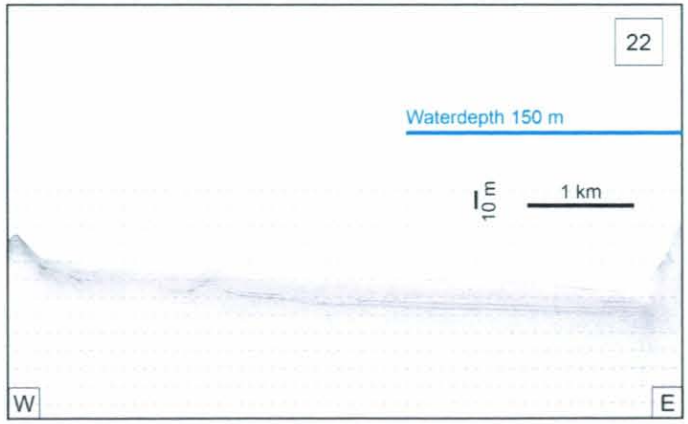
22
Waterdepth 150 m
10 m
1 km
W
E

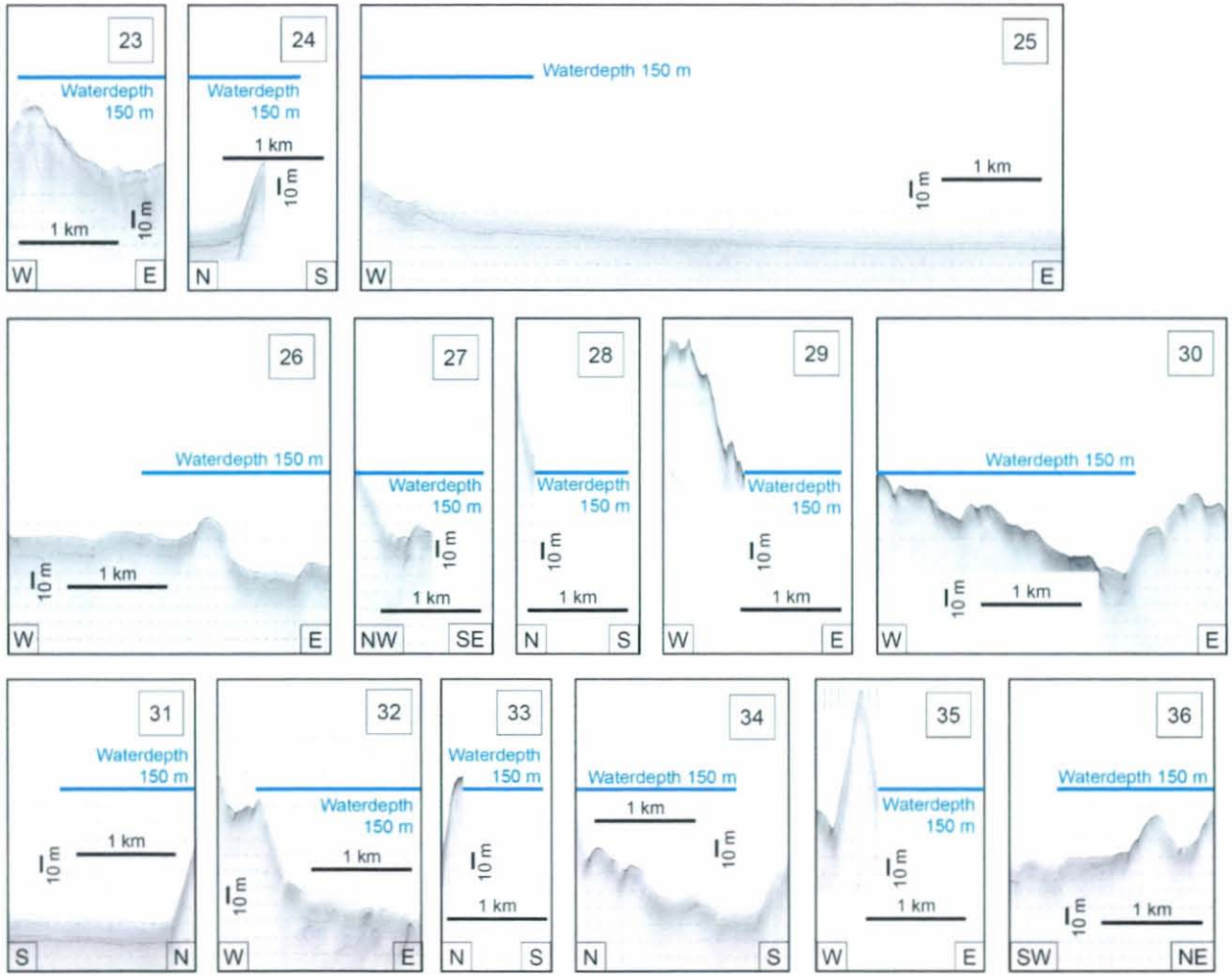
23
Waterdepth 150 m
1 km
10 m
W
E
24
Waterdepth 150 m
1 km
10 m
N
S
25
Waterdepth 150 m
10 m
1 km
W
E
26
Waterdepth 150 m
10 m
1 km
W
E
27
Waterdepth 150 m
10 m
1 km
NW
SE
28
Waterdepth 150 m
10 m
1 km
N
S
29
Waterdepth 150 m
10 m
1 km
W
E
30
Waterdepth 150 m
10 m
1 km
W
E
31
Waterdepth 150 m
10 m
1 km
S
N
32
Waterdepth 150 m
10 m
1 km
W
E
33
Waterdepth 150 m
10 m
1 km
N
S
34
Waterdepth 150 m
1 km
10 m
N
S
35
Waterdepth 150 m
10 m
1 km
W
E
36
Waterdepth 150 m
10 m
1 km
SW
NE

Appendix G

Inventories of ^{210}Pb in Soil cores

Explanation

Appendix G contains the extended results of ^{210}Pb inventories and flux for soil cores collected in 2008 in Nachvak and Saglek Fjord. The table lists ^{210}Pb inventories (dpm/cm^2) and flux (dpm/cm^{2}y) for every soil core. Total ^{210}Pb was determined by measurement of the 46.5 keV gamma peak. Supported ^{210}Pb (from decay of ^{226}Ra within the seabed) was determined by measurement of the granddaughters of ^{226}Ra: ^{214}Pb (295 and 352 keV) and ^{214}Bi (609 keV). The unsupported ^{210}Pb (excess ^{210}Pb) was determined by subtracting the supported ^{210}Pb from the total ^{210}Pb.

Inventories of excess of ^{210}Pb were determined by the following equation:

$$I_t = \sum \frac{A_i \times m_i}{S}$$

where I is the inventory, A_i is the activity and m_i is the total dry mass of soil in that depth interval, and S is the surface area of that core.

Flux was determined by the following equation:

$$F = \lambda I$$

where F is the annual flux (dpm cm^{-2} y^{-1}) required to support the inventory at steady sate and λ is the radioactive decay constant for ^{210}Pb (0.031 y^{-1}).

^{210}Pb Inventories

Soil Cores

Core name	210-Pb Inventories (dpm/cm^2)	F (Flux) ($dpm/cm^2\ y$)
	Nachvak Fjord	
2A	3.24	0.10
2C	23.45	0.73
MCSC1	1.34	0.04
	Saglek Fjord	
NVBK1	0.82	0.03
NVBK2	0.71	0.02
NVBK3	1.52	0.05